Sustained Epigenetic Programming of

POMC by Early Life Stress

Dissertation
der Fakultät für Biologie
der Ludwig-Maximilians-Universität
München

Vorgelegt von
YONGHE WU

2011

Erstgutachter: Prof. Dr. Rainer Landgraf

Zweitgutachter: Prof. Dr. Elisabeth Weiβ

Tag der mündlichen Prüfung: 17-04-2012

TABLE OF CONTENTS

1 Introduction

1.1 Early life stress model

1.1.1 Early life stress as a risk factor

Early life events can have a life-long impact on physical and mental health. There is increasing evidence that childhood trauma and neglect can profoundly influence behavior and increase risk for depression, anxiety disorders and substance abuse (de Wilde et al., 1992; Dube et al., 2001) (Kendler et al., 1995; Johnson et al., 2002). The quality of mother-infant interactions is of crucial importance during early development. Abundant evidence shows that postnatal disruption of the normal mother-infant interaction can lead to critical changes in the developing neuroendocrine response to stress in rodents. In fact, numerous studies have shown that early life stress can alter behavioral and neuroendocrine responsiveness and brain morphology. Subsequent dysregulation of the hypothalamic-pituitary-adrenal (HPA) axis can increase the vulnerability to psychiatric diseases (Arborelius et al., 1999; Jaffee et al., 2002; Newport et al., 2002; Iversen et al., 2007; Rikhye et al., 2008). Such findings have raised the question of whether similar processes take place in the human infant and, if so, through which mechanism early life adversity programs the infant HPA axis. To address these questions, I will first briefly describe the anatomy and regulation of the HPA axis and focus on critical time windows for programming by adverse events. A rodent model of early life stress will be introduced to show how early experiences modulate behavioral, cognitive and physiological development.

1.1.2 Hypothalamic-pituitary-adrenal (HPA) axis

Hyperactivity of the HPA axis is one of the key findings described in major depression (Holsboer, 2000). Secretion of hypothalamic corticotrophin-releasing hormone (CRH) from nerve terminals in the median eminence into the hypophysial portal circulation stimulates the synthesis of the precursor protein proopiomelanocortin (POMC), its cleavage and release as adrenocorticotrophic hormone (ACTH) from the anterior pituitary. Although CRH is the primary ACTH secretagogue, other neuroactive peptides, in particular arginine vasopressin (AVP),

are coexpressed in parvocellular neurons of the hypothalamic paraventricular nucleus (PVN); these act synergistically with CRH to stimulate ACTH release under sustained stress (Plotsky et al., 1991; Sawchenko et al., 1993). When released into the systemic circulation, ACTH stimulates adrenocortical synthesis and release of cortisol (human) or corticosterone (rodents) from the adrenal gland, which in turn, inhibits CRH and AVP production via a negative feedback loop (Figure 1).
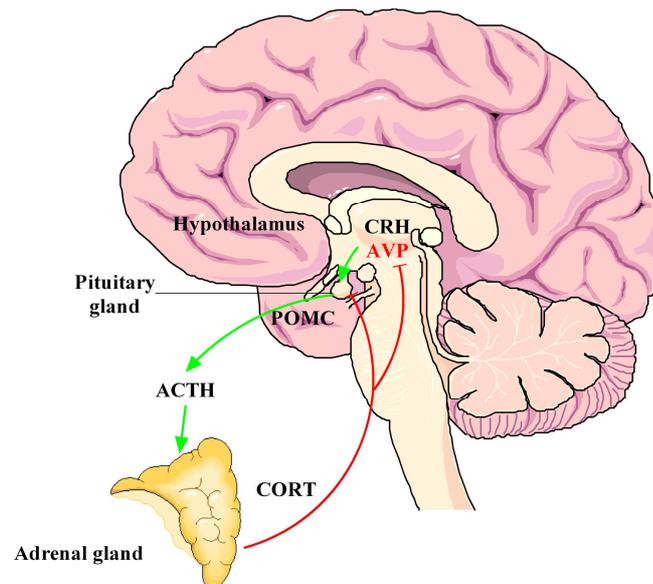
Figure1. The hypothalamic-pituitary-adrenal (HPA) axis. The neuropeptides corticotrophin-releasing hormone (CRH) and arginine vasopressin (AVP) are expressed in the parvocelluar neurons of the hypothalamic nucleus paraventricularis. The co-release of CRH and AVP into the portal blood vessels leads to potent stimulation of anterior pituitary ACTH secretion and POMC transcription. ACTH is derived from the POMC precursor mRNA and in turn stimulates secretion and synthesis of stress hormones (corticosteroids; CORT) by the adrenal glands. The activational effects of the HPA axis are counteracted by the inhibitory effects of CORT on the hypothalamus and pituitary and serve to attenuate and determinate the stress response. Adopted from (Murgatroyd et al., 2010)

1.1.3 Stress hypo-responsive period (SHRP)

Rodents undergo a period in early postnatal development during which they exhibit a reduced response to stress (stress hypo-responsive period, SHRP). This period has been suggested to last from approximately postnatal day (PND) 4 to PND 14 (Schapiro et al., 1962; Sapolsky and Meaney, 1986; Walker et al., 1986; Levine, 1994, 2001) in rats and from PND 1-12 in mice (Cirulli et al., 1994; Schmidt et al., 2002; Schmidt et al., 2003). This period is characterized by lower baseline plasma corticosterone concentrations than those measured at later stages of development and

in mature mice, and by blunted CRH and ACTH responses to acute stressors. During the SHRP, the adrenal gland is relatively insensitive to ACTH stimulation, resulting in only a minimal amount of corticosterone release upon stress (Stanton et al., 1988; Rosenfeld et al., 1991). The HPA axis is a dynamic system which undergoes postnatal maturation. During the first two weeks of life, the rodent brain passes through a number of critical developmental processes including dendritic outgrowth, synaptogenesis, and the formation of neural circuits. As a consequence, adverse events during the SHRP can lead to long term behavioral and physiological changes later in life. For example, during the SHRP, neonatal rat pups displayed increased cell death of neurons and glia in several cortical regions when subjected to a single (24 hour) bout. However, the same paradigm is less harmful when applied outside the SHRP (Zhang et al., 2002). The quality of maternal behaviors, such as licking/grooming and feeding received during the early weaning period have significant impact on anxiety- and depression-like behaviour and HPA activity and these effects can persist into adulthood (Liu et al., 1997). Based on these observations, several animal models have been developed building up on the manipulation of the interaction between mother and pups during the critical period; one of these is maternal separation.

1.1.4 Maternal separation (MS) of newborn mice

Neonatal maternal separation (MS) has been used as a model of adverse early life events to induce long-term changes in behaviour and neuroendocrine regulation (Anisman et al., 1998; Slotten et al., 2006). This model is based on the observation that dams often leave their pups for foraging for 15-30 minutes, while a mother living in a harsh environment (e.g. drought) may have to forage for up to 2-3 hours, exposing the pups to increased separation stress. In the MS model, pups are separated for 3 hours daily from their mother during the first 10 days of life. These manipulations are normally performed in the morning with the pups removed to an incubator or heating pad to maintain body temperature. From postnatal day 11, pups are reared by their mother, undisturbed in the home cage until PND 21 when they are weaned and housed in sex-matched groups (3-5 mice per cage).

Maternal separation performed in this time window (PND 1-10) can confer detrimental effects to the neonatal pups when they reach adulthood. Until weaning,

pups are almost entirely dependent on their mother for the maintenance of body temperature, nutrition, and protection from predators, and in addition, their brains are undergoing significant development (the rodent brain at birth is thought to correspond to that of a human infant's at gestational age 23-24 weeks). In this respect, early trauma can impose severe changes to the offspring. In general, many early-life stress paradigms induce persistent increases in anxiety- and depression-like behaviours, as well as hyperactivation of the HPA axis.

As adults, animals that have experienced maternal separation stress show several behavioural alterations. They spend more time in the closed arm of the elevated plus maze when compared with control animals, suggesting an anxiety-like phenotype (Romeo et al., 2003). Slotten and colleagues (Slotten et al., 2006) pointed out that adult rats previously exposed to 3 hours of daily separation (PND 3-15) preferentially stayed in the closed protected arm of the T-maze compared with the control rats. In addition, MS animals also exhibit depression-like behaviour. For example, rodents exposed to 3 hours of daily separation during the first two weeks of life spend more time floating in the force swim test when compared with control animals; this is thought to reflect depression-like behaviour. Maternal separation can also produce other depression-like syndromes, including increased consumption of ethanol (Pohorecky, 1981, 2006) and signs of anhedonia (the inability to perceive or respond appropriately to pleasurable stimuli) (Matthews and Robbins, 2003).

Maternal separation can lead to long-lasting alterations of neuroendocrine regulation. When compared with control animals, adult MS offspring displays higher levels of basal corticosterone (CORT) and adrenocorticotropic hormone (ACTH), and increased level of hypothalamic CRH and AVP in the PVN. The adult MS animals exhibit resistance to glucocorticoid-mediated feedback, as evident from a failure of the dexamethasone suppression test (Murgatroyd et al., 2009). Furthermore, MS treated animals show decreased levels of gama amino butyric acid A ($GABA_A$) receptor expression in the medial prefrontal cortex, noradrenergic (NA) cell body regions of the nucleus tractus solitarius and the locus coeruleus (Caldji et al., 2000). Moreover, reduced levels of brain-derived neurotropic factor (BDNF) and synaptophysin mRNA densities were detected (Lippmann et al., 2007; Aisa et al., 2009). Maternal separation can also inhibit neurogenesis in the hippocampus , which

consequently impairs memory formation. Aisa and colleagues (Aisa et al., 2009) found that MS treated animals showed spatial learning deficits when tested in the Morris Water Maze compared with non-handled controls.

1.1.5 Early life environment and the epigenome

A critical question concerns the mechanisms coupling early social environment to long-term alterations of behaviour and stress responses later in life. Recent findings from rodent models implied that epigenetic mechanisms, especially DNA methylation, are mediating the gene X environment dialogue by laying down stable marks in the genome, thus affecting the phenotype later in life. In the rat, different levels of maternal care early in life can lead to DNA methylation changes that persist, along with altered behavioral and neuroendocrine phenotypes in adulthood. Meaney and coworkers (Weaver et al., 2004) showed that pups reared under high maternal care, including licking/grooming and arch-back nursing (LG-ABN), have increased glucocorticoid receptor (GR) expression in the hippocampus when compared with pups reared by low LG-ABN dams. This higher glucocorticoid receptor (NR3C1, GR) mRNA expression is associated with lower DNA methylation in the promoter region of the GR, thereby facilitating the binding of the transcription factor nerve growth factor-induced protein A (NGFI-A). The authors further performed a series of experiments to show that the impact of early experience can be reversed by later interventions in adulthood, e.g. environmental enrichment, cross-fostering or treatment with histone deacetylase (HDAC) inhibitors. This example demonstrated that changes in the epigenome established by the environment during early development can be reversed in adulthood, indicating the plasticity of DNA methylation processes in the adult brain.

In humans, adverse events such as childhood abuse can also lead to epigenetic programming in the adult brain. McGowan and coworkers (McGowan et al., 2009) found that DNA methylation at a neuron-specific GR promoter was significantly higher in the hippocampus of suicide victims who had suffered from childhood abuse than in controls or non-abused suicide victims. The increased DNA methylation in suicide victims who underwent childhood abuse is associated with decreased levels of GR mRNA as well as the GR 1F splice variant, suggesting a functional correlation between DNA methylation and GR mRNA expression. Thus, the findings in rodent

models implicating early environmental exposure in programming the epigenome also appears to apply to humans. In sum, results both from animal models and humans indicate the plasticity of the epigenome when exposed to environmental stimuli, opening the possibility of developing approaches for early diagnosis, prevention, and treatment of disease.

1.2 DNA methylation and MeCP2

1.2.1 Epigenetics

The term "*epigenetics*" was first introduced by the developmental biologist Conrad Waddington in 1940 to describe the gene-environment interactions that result in specific phenotypes (Waddington, 1942; Van Speybroeck, 2002). While Waddington originally used this concept in a developmental context, the term's current use has extended to describe the study of heritable changes (both mitotic and meiotic) in gene expression that are not due to changes in DNA sequence (Russo, 1996). The concept of *epigenetics* was recently revised by the British scientist Adrian Bird who proposed that epigenetic events are the structural adaptation of chromosomal regions (genes) to register, signal or perpetuate altered activity states (Bird, 2007). In this new definition of *epigenetics*, both chromatin marks and DNA modifications, regardless of their heritability, are considered as epigenetic events. DNA methylation and histone modifications are the two main mechanisms of epigenetic regulation. Whereas histone modifications are often transient events, DNA methylation is thought of as a stable modification of DNA. In our studies, we focused on DNA methylation.

1.2.2 DNA methylation

DNA methylation is a covalent chemical modification involving the addition of a methyl group to the fifth position of the pyrimidine ring in the nucleotide cytosine. This modification can be inherited through cell division. DNA methylation is normally removed during zygote formation and reestablished by *de novo* methylation. In mammals, DNA methylation mostly occurs in the context of CpG dinucleotides, which consist of a cytosine immediately followed by a guanine (Richards, 2006). In

addition, recent research revealed that DNA methylation can also appear in a non-CpG manner, although the function of this is still not very clear (Barres et al., 2009). It has been suggested that about 25% of all methylation in embryonic stem (ES) cells occurs in a non-CpG context. Non-CpG methylation disappears during differentiation, but is restored in induced pluripotent stem cells, suggesting that non-CpG methylation might play a role in the establishment and maintenance of pluripotency (Lister et al., 2009).

About 70% of all CpG dinucleotides are methylated across the genome (Ehrlich et al., 1982), except for the high CpG density regions called CpG islands (Bird, 1986; Gardiner-Garden and Frommer, 1987). The common formal definition of a CpG island is a region spanning at least 200 bp in length and containing a GC percentage greater than 50% with an observed/expected CpG ratio of more than 60%. Another recent study revised the rules for CpG island prediction in order to exclude other GC-rich genomic sequences such as Alu repeats. Accordingly, CpG islands are defined as DNA regions of >500 bp with a GC content >55% and observed CpG/expected CpG ratio of 0.65 (Takai and Jones, 2002). CpG islands are normally present within or close to the promoter region responsible for regulating the transcription rate of a gene. Typically, CpG islands are free of methylation. New studies by Weber and coworkers (Weber et al., 2007) have pointed out that DNA methylation at a given CpG island is dependent on the CpG density of the promoter. High CpG promoters are unmethylated and promoters with low CpG contents tend to be hypermethylated.

DNA methylation has been shown to play important roles in mammalian development. For example, DNA methylation is essential for establishing tissue-specific gene expression patterns. In addition, DNA methylation is also associated with a number of key processes such as X-chromosome inactivation, parental imprinting, suppression of repetitive elements and carcinogenesis (Bird, 2002).

1.2.3 DNA methyltransferases

In mammalian cells, DNA methylation occurs mainly at the 5 position of CpG dinucleotides and is catalyzed by DNA methyltransferases (DNMTs). There are four known DNMTs which can be subcategorized into two groups by their functions: *de novo* and maintenance DNA methylation.

The addition of methyl groups to previously unmethylated DNA, the so called *de novo* methylation, is catalyzed by two enzymes: DNMT3a and DNMT3b. Compared with DNMT3a, DNMT3b shows relatively low expression in most tissues except for the testis, suggesting a crucial function for DNMT3b in spermatogenesis (Okano et al., 1998a; Robertson et al., 1999; Xie et al., 1999). DNMT3a and DNMT3b are essential for normal development (Okano et al., 1999). *Dnmt3a* homozygous knockout mice appear normal at birth but die after 4 weeks of age; while *Dnmt3b* homozygous knockout mice show various embryonic defects and die before E15.5. Combined knock-out of *Dnmt3a* and *Dnmt3b* produces more severe symptoms than those of *Dnmt3a* and *Dnmt3b* alone. This indicates that Dnmt3a and Dnmt3b have at least partially overlapping functions in the establishment of cellular DNA methylation patterns during development.

Maintenance DNA methylation activity is essential for preserving DNA methylation patterns in each cellular DNA replication cycle. DNMT1 functions as a maintenance DNA methyltransferase, and specifically recognizes hemi-methylated CpGs following DNA replication of the daughter strand. DNMT1 is responsible for transmitting DNA methylation patterns to the daughter strand. Dnmt1 is essential for mammalian development, because null mutants show widespread demethylation in the embryo and die at E9.5 (Li et al., 1992). Dnmt1 mRNA expression is also observed in low-proliferation tissues such as the adult heart and brain. These unexpected results suggest a new role of Dnmt1 in addition to its known role to maintain DNA methylation levels during cell division. Recent finding suggests that DNMT1 can interact with methyl-CpG binding proteins as well as with HDACs and histone methyltransferases to exert transcriptional repression (Tatematsu et al., 2000; Fuks et al., 2003a; Kimura and Shiota, 2003).

In 1998, scientists seeking to identify a putative *de novo* DNA methyltransferase discovered the DNMT2 gene (Okano et al., 1998b). DNMT2 contains the well-conserved catalytic domain. However, only traceable methyltransferase activity of the DNMT2 gene was found using *in vitro* systems (Hermann et al., 2003). Moreover, *Dnmt2* knockout ES cells show normal *de novo* or maintenance methyltransferase function (Okano et al., 1998b). Consistent with this finding, *Dnmt2* knockout mice fail to display an abnormal phenotype. Recent research showed that human DNMT2 can work as a tRNA methyltransferase which specifically methylates cytosine 38 in

the anticodon loop (Goll et al., 2006). However, it is not known how many RNA species can be methylated by Dnmt2. Thus the functions of DNMT2 still need to be determined in the future.

DNMT3L is highly expressed in the testis and embryos, and is likely to play a role in the setting of imprints in oocytes (Bourc'his et al., 2001; Margot et al., 2003). Unlike the other DNMTs, no functionally relevant catalytic motif was mapped in the DNMT3L protein sequence and DNMT3L has not been associated with intrinsic enzymatic activity until now.

1.2.4 Readers of DNA methylation

The best documented function of DNA methylation is gene silencing. DNA methylation may affect gene expression in two ways. Firstly, if the DNA sequence is methylated, the methylation of DNA itself might impede the binding of a specific transcriptional factor to its recognition site and suppress gene expression. For example, a methylated DNA sequence can interfere with the binding of transcription factors such as E2F, NGFI-A or CREB (Iguchi-Ariga and Schaffner, 1989; Campanero et al., 2000; Weaver et al., 2004), thereby preventing transcriptional activation. While the consequence of DNA methylation is generally thought of as transcriptional silencing, methylation of repressor protein-binding sites can lead to increased gene expression. For example, the imprinted gene insulin-like growth factor 2 (*Igf2*) can be activated if the upstream repressor sites are differentially methylated in the paternal allele (Eden et al., 2001).

Secondly, methylated DNA might recruit proteins known as methyl-CpG-binding domain proteins (MBDs). These can recruit additional proteins, such as histone deacetylases (HDACs) and other chromatin remodeling complexes known to promote the formation of a condensed chromatin structure that is inaccessible to transcription regulators (Jones et al., 1998; Nan et al., 1998; Wade et al., 1999; Fuks et al., 2003b). These methyl-CpG-binding domain proteins serve as readers and writers of epigenetic marks/signatures and provide a platform on which DNA methylation and chromatin modifications are carried out. There are 5 MBDs in mammals, namely, MeCP2, MBD1, MBD2, MBD3 and MBD4. Among these, MeCP2, MBD1, MBD4 bind to methylated DNA sequences through a conserved

methyl-CpG binding domain (MBD). MBD3, which contains amino acid substitutions in the well-conserved methyl-CpG-binding domain, is involved in transcriptional repression as a component of a co-repressor complex irrespective of the DNA methylation status (Saito and Ishikawa, 2002).

Besides the MBD family proteins, other proteins such as Kaiso, ZBTB4, and ZBTB38 are able to preferentially bind to methylated DNA in a sequence-specific manner through their zinc finger binding domains (Prokhortchouk et al., 2001; Filion et al., 2006).

1.2.5 MeCP2

1.2.5.1   Rett syndrome and MeCP2

MeCP2 is the founding member of the methyl-CpG-binding protein family. MeCP2 was firstly purified by Adrian Bird's group from rat brain in 1992 (Lewis et al., 1992). It has been extensively studied since 1999 because patients with the neurodevelopmental disorder Rett syndrome harbor mutations in the *MECP2* gene (Amir et al., 1999). It is estimated that one out of 10,000-20,000 females develops Rett syndrome (Percy, 2002). Newer reports suggest that Rett syndrome can also occur in males with much more severe symptoms (Hardwick et al., 2007). Rett syndrome is a progressive disease characterized by normal early development followed by mental retardation, loss of speech, stereotype hand movements and other neurological symptoms (Hagberg et al., 1983). It is thought that mutations in MECP2 account for up to 96% of classic Rett syndrome cases (Shahbazian and Zoghbi, 2001).

MeCP2 is also essential in mice: *Mecp2*-null animals exhibit phenotypic similarities of Rett syndrome; they show a period of normal postnatal development followed by hindlimb clasping, breath difficulties, reduced mobility, brain size and body weight, and death at around 8 weeks of age (Chen et al., 2001; Guy et al., 2001). Moreover, conditional deletion of the *Mecp2* gene in cells of the neuronal lineage results in the same phenotype, indicating that the absence of normal MeCP2 function in neurons may be sufficient to cause disease. In addition, mice expressing a truncated MeCP2 protein (*Mecp2*[308]) that retains partial function display a less severe phenotype than that displayed by *Mecp2*-null mice (Shahbazian et al., 2002a). Furthermore, *Mecp2* deletion in post-mitotic neurons leads to milder defects of RTT-

like phenotypes, suggesting that mature neurons require continuous expression of MeCP2 to function properly (Chen et al., 2001).

The mammalian central nervous system requires tightly adjusted MeCP2 levels for its proper function. MECP2 duplications in human have been found to cause a progressive postnatal neurological disorder with features of Rett syndrome. MECP2 duplication in a girl produced effects with features of Rett syndrome in the presence of preserved speech (Ariani et al., 2004), while MECP2 duplication in a boy led to mental retardation and typical clinical features of Rett syndrome (Meins et al., 2005; Van Esch et al., 2005). Consistent with these findings, Mecp2 overexpression in transgenic mice results in severe neural defects in postnatal life (Collins et al., 2004). Mecp2-depleted neurons do not suffer severe irreversible damage since the restoration of Mecp2 can largely reverse the Rett syndrome phenotypes in mice (Luikenhuis et al., 2004).

1.2.5.2 MeCP2 gene structure

MeCP2, located at Xq28 in the human genome (Quaderi et al., 1994), comprises 4 exons spanning a region of more than 75 kb in length. In mammals, MeCP2 is an 84 kDa protein which is composed of three functional domains (Figure 2): the methyl-CpG binding domain (MBD) (amino acids 78-160) which is responsible for recognizing and binding to methylated CpGs, the transcriptional repression domain (TRD) (amino acids 207-310) which recruits a corepressor complex including Sin3A and histone deacetylases, and a C-terminal region which contains a proline-rich protein interaction surface capable of binding to group II WW domains. MeCP2 contains a nuclear localization signal (NLS: amino acid 255-271) which resides in the middle of the transcriptional repression domain and is responsible for transport of the protein into the nucleus (Chandler et al., 1999).

MeCP2 encodes two splice variants (Kriaucionis and Bird, 2004; Mnatzakanian et al., 2004). MeCP2α, which contains a distinct N-terminus is more abundant than another isoform (MeCP2β) in mouse tissues and human brain. In addition, MeCP2β mRNA has an upstream open reading frame that inhibits its translation, leading to lower translational efficiency. As a consequence, > 90% of the MeCP2 in mouse brain

corresponds to MeCP2α. Both protein isoforms are nuclear and colocalize with densely methylated heterochromatic foci in mouse cells (Kriaucionis and Bird, 2004).

MeCP2 is ubiquitously expressed in normal tissues. Although MeCP2 shows low levels of expression during early stages of development, MeCP2 is widely expressed in embryonic and adult tissues, with high concentrations in brain, lung, pituitary and spleen, moderate in kidney and heart, and very low expression levels in liver, stomach and small intestine (Shahbazian et al., 2002b).
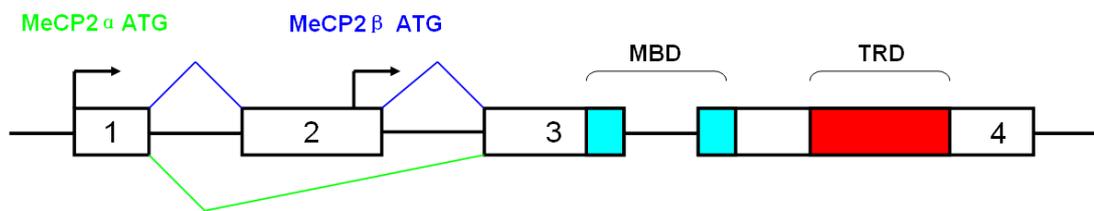
Figure 2. Structure of the MeCP2 gene and mRNA. Alternative splicing for the MeCP2α isoform is shown in green and for the MeCP2β isoform in blue. The region encoding the MBD (Methyl-CpG Binding Domain) is depicted in cyan. The TRD (Transcription Repression Domain) is shown in red (Adopted from Kriaucionis and Bird, 2004).

Generally, the affinity of MBD proteins for methylated DNA is 3-10-fold higher than for unmethylated DNA and may depend on sequence context (Fraga et al., 2003). *In vitro* binding assays revealed that MeCP2 is bound with high affinity to DNA containing AT sequences (AT≥4) adjacent to methylated CpGs (Klose et al., 2005).

1.2.5.3   MeCP2 function

Several diverse functions have been reported for MeCP2, including transcriptional repression, activation of transcription, nuclear organization, and splicing. MeCP2 was initially thought of as a global repressor since it can bind to regulatory DNA sequences and exert strong transcriptional repression (Jones et al., 1998; Kokura et al., 2001). However, transcriptional profiling of brains derived from *Mecp2*-null mice showed only subtle changes in gene expression compared with wild type mice (Tudor et al., 2002). Moreover, when RNA was isolated from the cerebellum of *Mecp2* mutant mice, similar expression profiles were obtained by microarray analysis (Jordan et al., 2007). At this step, the lack of obvious changes in gene expression indicated that the transcriptional changes in *Mecp2* mutant mice might only occur in some subsets of cells and might not be detected when whole cortex or hippocampus are processed.

MeCP2 also confers gene activation. Recent studies of *Mecp2*-null mice showed that MeCP2 rather activates than represses hypothalamic gene expression (Chahrour et al., 2008). Although there remains the possibility that some genes are affected by one or more indirect interactions, chromatin immunoprecipitation (ChIP) assay proved the binding of MeCP2 to the promoter region of some activated genes (Chahrour et al., 2008).

Because DNA methylation is important in the regulation of imprinted gene expression, it has been proposed that *Mecp2*-deficient mice might show dys-regulation of imprinted gene expression due to altered chromatin configuration. Several imprinted genes, including Dlx5, Dlx6 and Ube3A, have been reported to show abnormal expression levels in the brain of *Mecp2*-null mice (Horike et al., 2005; Makedonski et al., 2005; Samaco et al., 2005). The reason for such dysregulation might be the loss of MeCP2-dependent chromatin looping on the imprinted allele.

MeCP2 has also been ascribed a role as regulator of splicing. In the brain, MeCP2 works as a modulator of alternative splicing via an interaction with the RNA-binding protein YB-1 (Young et al., 2005). The MeCP2-YB-1 complex is very sensitive to RNAse treatment, suggesting that this interaction requires RNA for its formation and stability. Microarray analysis of mRNA from cerebral cortex of RTT mutant mice (*Mecp2$^{308/Y}$*) revealed altered splicing of some genes following loss of functional MeCP2.

1.2.5.4 Post-translational modifications of MeCP2

Using a candidate gene approach, brain-derived neurotrophic factor (*Bdnf*) was first identified as a direct target for MeCP2 in cultured neurons. It was found that MeCP2, together with the co-repressor molecule Sin3a, forms a complex to maintain the repressed state of the *Bdnf* gene (Chen et al., 2003; Martinowich et al., 2003). Treatment of cultured neurons with potassium chloride (KCl), which induces membrane depolarization and calcium influx through opening of L-type voltage-sensitive calcium channels, leads to MeCP2 phosphorylation at serine 421 in the rat (Zhou et al., 2006). Phosphorylation of this residue promotes MeCP2's dissociation from DNA, as demonstrated by southwestern assays (Chen et al., 2003). Zhou and coworkers (Zhou et al., 2006) demonstrated that Calmodulin-dependent Protein

Kinase II (CaMKII) mediates the phosphorylation of MeCP2 at serine 421 and underpins activity-dependent BDNF transcription. Moreover, it was reported that MeCP2 phosphorylation at serine 80 in the rat is critical for the association of MeCP2 with chromatin (Tao et al., 2009). Calcium influx in neurons elicits dephosphorylation at S80 and probably contributes to the dissociation of MeCP2 from the chromatin. All these data support the concept that phosphorylation may be part of a reversible mechanism for adjustable, neuronal-activity controlled, gene repression by MeCP2.

1.3 The pituitary gland

The pituitary gland, or hypophysis, is a small endocrine gland (pea-sized in the adult human male) located at the base of the brain. It is functionally connected to the hypothalamus by the median eminence via the pituitary stalk. Anatomically, the pituitary gland is composed of two lobes: the larger anterior pituitary (adenohypophysis) and the smaller posterior pituitary (neurohypophysis). In rodents, there is a third component, the intermediate lobe (pars intermedia) that is located between the adeno- and neurohypophses; in humans, the intermediate lobe is only a small rudimentary structure. The anterior pituitary receives neurohormonal signals (hypothalamic releasing factors/hormones via the median eminence), whereas the posterior pituitary is directly innervated by the hypothalamus, with nerve endings that release the so-called neurohypophysial hormones oxytocin and arginine vasopressin from cell bodies in the magnocellular division of the paraventricular nucleus. Whereas the hypothalamic hormones that reach the anterior pituitary do not enter the general blood stream, neurohypophysial oxytocin and vasopressin are secreted into the general blood stream and act at distal peripheral organs such as the uterus and mammary glands (oxytocin-targets) and kidneys, liver, and heart (vasopressin-targets).

The anterior pituitary is derived from ectodermal cells in Rathke's pouch to generate morphologically-distinct cell types: corticotropes, thyrotropes, gonadotropes, somatotropes, and lactotropes. There is also a sixth cell type which is non-hormone producing, the folliculostellate cells. During development, under the control of

14

various pituitary specific transcriptional factors and growth factors, these endocrine cells arise in the following sequence: corticotropes, thyrotropes, gonadotropes, somatotropes, and lastly, lactotropes. Somatotropes constitute approximately 50% of the cell population, lactotropes (10-25%), corticotropes (10-20%), thyrotropes (10%), and gonadotropes (10%) (Horvath and Kovacs, 1988). Of particular interest in the context of this study is the corticotropes which produce pro-opiomelanocortin (POMC), which is then proteolytically cleaved to adrenocorticotrophic (ACTH), β-endorphin and αMSH, as well as other small peptides whose function is still incompletely understood.
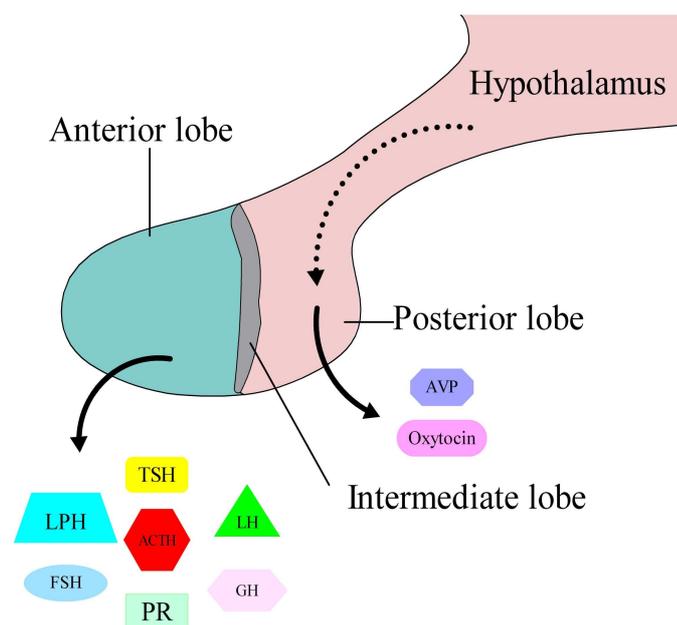
Figure 3. Schematic diagram of the human pituitary. The pituitary gland is located at the base of the skull between the optic nerves. The anterior pituitary comprises 5 main cell types that synthesize and release (into the blood stream) the adenohypophyseal hormones adrenocorticotrophic (ACTH) (target: adrenal cortex), luteinizing hormone (LH) and follicle-stimulating hormone (FSH) (gonads), growth hormone (GH) (skeletal and metabolic tissues), prolactin (PRL) (mammary glands), and thyroid-stimulating hormone (TSH) (thyroid). AVP and oxytocin are released from hypothalamic nerve terminals contacting the posterior lobe and then into the general circulation.

Rodent anterior pituitary (from now on, referred to simply as pituitary) cells, including corticotropes, proliferate and differentiate during postnatal development. Friend (Friend, 1979) showed that the weight of the rat pituitary increases more than 3-fold during the first 10 days of life and doubles over the next 15 days. Pituitaries from adult rats weigh 5 times more than those of 25-day-old animals. Interestingly, the different pituitary cell types proliferate at different rates; they are first detectable in fetuses aged 15.5 days. While embryonic corticotropes arise from undifferentiated

cells, those produced postnatally derive from pre-existing corticotropes (Taniguchi et al., 2000; Taniguchi et al., 2002).

1.4 *Pomc* gene

1.4.1 *Pomc* gene structure and function

The pro-opiomelanocortin (*Pomc*) gene, localized at chromosome 12 in mouse, encodes a cDNA comprising 1007 nucleotides spanning 3 exons and 2 introns. Computational analysis (CpGPlot, EMBOSS) and previous literature (Gardiner-Garden and Frommer, 1994) revealed 2 CpG islands within the mouse *Pomc* gene locus: CpG island 1 (CGI 1), flanking the *Pomc* transcription start site and CpG island 2 (CGI 2), approximately 5 kb downstream, encompassing the third exon of the *Pomc* gene. The *Pomc* gene is predominantly expressed in the anterior and intermediate lobes of the pituitary. *Pomc* mRNA is also detected in the hypothalamus (Gee et al., 1983), amygdala, cortex, testes (Chen et al., 1984), lymphoid cells (Lolait et al., 1986), adrenal medulla (Evans et al., 1983), ovaries, placenta (Chen et al., 1986) and some tumor tissues (Lacaze-Masmonteil et al., 1987; DeBold et al., 1988). The size of the mature POMC transcript in the pituitary is about 1200 nucleotides, while in the hypothalamus, POMC mRNA transcripts seem to be identical to pituitary except for longer poly(A) tails (Jeannotte et al., 1987). In testis, POMC-derived transcripts are about 400 bases shorter than those in the pituitary (Chen et al., 1984; Lacaze-Masmonteil et al., 1987). This truncated POMC mRNA transcript contains no exon 1 or exon 2 sequences, and is transcribed from the transcription initiation site near the 5' end of exon 3. Since the peptide translated from this form of POMC mRNA lacks a signal peptide, it can not be secreted (Clark et al., 1990). Therefore, its role in peripheral tissues is unresolved.

POMC is a 241-amino-acid precursor polypeptide, which is cleaved in a tissue-specific fashion by prohormone convertases to yield a variety of bio-active peptides, including α-melanocortin stimulating hormone (α-MSH), β-endorphin, β-lipotropin (β-LPH) and adrenocorticotropin (ACTH). There are eight potential cleavage sites within the POMC precursor and different tissues contain specific convertases to produce a variety of biologically-active peptides. In the anterior pituitary, ACTH and

β-lipotropin are the major cleavage products. In the intermediate lobe, POMC can be cleaved into the following peptides: corticotrophin-like intermediate peptide (CLIP), γ-lipotropin (γ-LPH), β-endorphin, α-MSH and γ-melanophore stimulating hormone (γ-MSH). POMC-derived peptides play diverse roles in pathophysiology, including obesity, depression, skin pigmentation, adrenal development, and regulation of the HPA axis. In other tissues, including the hypothalamus, placenta and epithelium, all eight potential cleavage sites may be used to produce peptides responsible for energy homeostasis, pain, perception, melanocyte stimulation and immune responses.
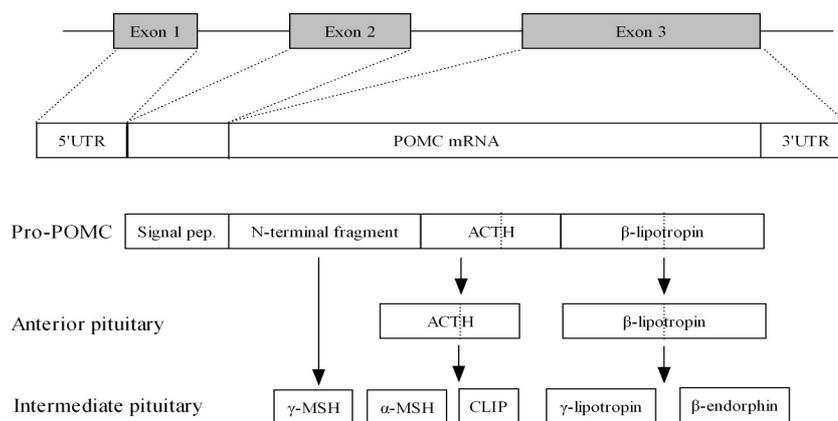
Figure 4. Mouse *Pomc* gene, mRNA, pro-hormone and peptides.The pro-opiomelanocortin (*Pomc*) gene encodes a cDNA comprising 1007 nucleotides spanning 3 exons and 2 untranslated introns. The Pro-POMC is a 241-amino-acid precursor polypeptide, which is cleaved in a tissue-specific fashion by prohormone convertases to yield a variety of bio-active peptides. In the corticotrope cells of the anterior pituitary, adrenocorticotropic hormone (ACTH) and β-lipotropin (β-LPH) are products under the control of corticotropin releasing hormone (CRH). In the intermediate lobe of the pituitary, alpha-melanocyte stimulating hormone (α-MSH), corticotropin-like intermediate lobe peptide (CLIP), γ-lipotropin and β-endorphin are products generated under the control of dopamine. α- and γ-MSH are collectively referred to as melanotropin or intermedin.

Anterior pituitary POMC synthesis and ACTH secretion are regulated by CRH released from neurohemal axon terminals in the median eminence of the hypothalamus. AVP, produced in parvocellular neurons of the hypothalamic paraventricular nucleus (PVN), acts synergistically with CRH to activate POMC transcription in the pituitary. CRH binds with high affinity to CRH-type 1 receptors (Vita et al., 1993; Timpl et al., 1998), thus stimulating cAMP production by adenylate cyclase (Giguere et al., 1982; Aguilera et al., 1983; Litvin et al., 1984; Grammatopoulos and Chrousos, 2002) and leading subsequently to activation of protein kinase A (PKA) (Reisine et al., 1985; Kovalovsky et al., 2002). This is followed by an influx of extracellular calcium through L-type voltage-dependent calcium channels (Kuryshev et al., 1996). As a consequence, calcium calmodulin

kinase II (CaMKII) becomes activated (Kovalovsky et al., 2002). These signaling events ultimately converge on POMC transcription and ACTH secretion (von Dreden et al., 1988; Kovalovsky et al., 2002).

1.4.2 Experience-dependent *POMC* methylation

To date, the methylation status of *POMC* has been studied exclusively in human tissues. The human POMC gene contains two CpG islands (Gardiner-Garden and Frommer, 1994). The intronic POMC promoter is located in the downstream CpG island and is barely expressed in most tissues. The upstream CpG island shows high tissue-specificity. Over-secretion of ACTH from non-pituitary tissues, resulting in severe Cushing's disease, is thought to be due to activation of a (normally) tissue-specific POMC promoter in ectopic tissues (Ye et al., 2005). The promoter contains a CpG island. The same study confirmed the causal relationship between DNA methylation and POMC gene expression. In ACTH-secreting tumors and POMC-expressing DMS-79 cell lines, POMC is unmethylated at the pituitary-specific promoter region. In contrast, in non-ACTH-secretion tumors, this region is heavily methylated (Newell-Price et al., 2001). In addition, POMC is heavily methylated at the same region in a number of normal ACTH-non-expressing tissues including: pancreas, spleen, lung, testes and peripheral blood leukocytes (Newell-Price et al., 2001). In thymic carcinoid patients, hypomethylation in the 5' promoter region of the POMC gene is negatively correlated with over-expression of the POMC mRNA transcript (Ye et al., 2005).

POMC DNA methylation can be altered by environmental conditions. For example, in a neonatal model of obesity, bisulfite sequencing of DNA isolated from the hypothalamus revealed hypermethylation of CpG dinucleotides within two Sp-1-related binding sequences in the POMC promoter. These two sites are essential for the mediation of leptin and insulin effects on POMC expression. Accordingly, gain of methylation within Sp1-related binding sites correlated with less activation of POMC expression by leptin or insulin signaling (Plagemann et al., 2009).

INTRODUCTION

1.5   Goals of the thesis

In both human and rodents, extensive research has shown that early-life experience has a profound impact on adult physiology and behaviour. Different environmental experiences in early life might contribute to the vulnerability for depression and anxiety later in life. However, the detailed mechanisms mediating these effects remain elusive. Using maternal separation as a paradigm of early life stress, the present work aimed to:

- Examine neuroendocrine profiles in animals that had experienced stress (maternal separation) during the first 10 days of life

- Analyze changes in *Pomc* methylation and gene expression

- Investigate age-associated changes of the expression of *Pomc* mRNA in pituitaries from animals subjected to early life stress

- Examine whether the effects of maternal separation are expressed differently in the two sexes

- Identify the molecular mechanisms underlying the long-term effects of maternal separation on altered *Pomc* expression

2 Materials and methods

2.1 Materials

2.1.1 Chemicals

Consumable	*Supplier*	*Consumable*	*Supplier*
1kb DNA ladder	Fermentas	**3mm filter paper**	Wattman
Agar	Gibco	**Agarose (low-melting point)**	Gibco
Agarose (universal)	Peqlab	**Ampicillin**	Roth
Antibiotic/antimycotic	Gibco	**Boric acid**	Biomol
Bradford assay	Biorad	**Bromophenol blue**	Biorad
Bovine serum albumin (BSA)	Sigma	**Chloroform**	Roth
Chloroform (RNase free)	Merck	**Coomassie blue**	Biorad
Developing emulsion (slides)	Kodak	**Developing solution (film)**	Kodak
Developing solution (slides)	Kodak	**DMSO**	Sigma
dNTPs (set of 4)	Fermentas	**DTT**	Sigma
Dulbecco's minimum essential medium (DMEM)	Gibco	**EDTA**	Sigma
Ethanol	Merck	**Ethidiumbromide**	Biomol
Ficoll 400	Sigma	**Fixing solution (films)**	Kodak
Fixing solution (slides)	Kodak	**bovine serum**	Gibco
Formaldehyde	Merck	**Formamide**	Sigma
L-Glutathione reduced	Sigma	**Glutathionine Sepharose**	Amersham
Glycerine	Sigma	**Glycerol**	Biomol
Glycogen	Fermentas	**Guanidine thiocyanate**	Merck
IPTG	Fermentas	**Isoamylalkohol**	Merck
β-mercaptoethanol	Merck	**Methanol**	Merck
Oligonucleotides	MWG /Sigma	**Optimem medium**	Gibco
Paraformaldehyde	Sigma	**Phosphate buffered saline (PBS)**	Gibco
Phenol	Appligene	**Ponceau**	Sigma
2-propanol	Merck	**2-propanol (RNase free)**	Merck

Protein marker	Fermentas	**Poly(d(I-C))**	Roche
Potassium chloride	Sigma	**SDS**	Biomol
Siliconising fluid	Merck	**Sodium acetate**	Merck
TEMED	Sigma	**Tris**	Riedel-de Haen
Triton X-100	Roth	**Trypsin**	Gibco
Tryptone	Roth	**X-Gal**	Sigma
Yeast extract	Gibco	**Zeocin**	Invitrogen
γ32P-ATP	Amersham	**^{32}P-dCTP**	Perkin Elmer

2.1.2 Restriction endonucleases

Enzyme	*Supplier*	*Enzyme*	*Supplier*
BamHI	Fermentas	**BglII**	Fermentas
EcoRI	Fermentas	**EcoRV**	Fermentas
HindIII	Fermentas	**NcoI**	Fermentas
PstI	Fermentas	**SacI**	Fermentas
SmaI	Fermentas	**XbaI**	Fermentas
XhoI	Fermentas		

2.1.3 Modifying enzymes

Enzyme	*Supplier*	*Enzyme*	*Supplier*
SssI CpG methylase	NEB	**T4-DNA-Ligase**	Fermentas
T4 DNA polymerase	Fermentas	**CIAP**	Fermentas
DNA pol. I, Klenow fragment	NEB	**DNA polymerase (*Taq.*)**	Fermentas
DNA polymerase (Pfu)	Fermentas	**DNaseI**	Fermentas
Proteinase K	Boehringer Mannheim	**Proteinase K (RNase free)**	Sigma
RNase	Sigma	**RNase inhibitor**	Fermentas

2.1.4 Antibodies

2.1.4.1 Primary antibodies against mouse

Antibody	Epitope	Host	Supplier
Anti-flag	M2 (monoclonal)	Mouse	Sigma
Anti-acetyl-histone H3	ARTKQTATK*APRKQLC K* is acetylated	Rabbit	Millipore
Anti-H3K9me2	R^{me2}KSTG	Rabbit	Millipore
Anti-total MeCP2	C-PRPNREEPVDSRTP	Rabbit	Upstate
Anti-total MeCP2	NH2-CSMPRPNREEPVDSRTPV-C	Rabbit	Home-made
Anti-pS421 MeCP2	C-MPRGG ^{p}SLES	Rabbit	Gifted by Greenberg's lab (Zhou et.al., 2006)
Anti-pS438 MeCP2	NH2-CMPRGGP^{p}SLES-C	Rabbit	Home-made
Anti-pS80 MeCP2	Not available	Rabbit	Gifted by Jifan Tao's lab (Tao et.al., 2009)
Anti-pS97 MeCP2	EASA^{p}SPKQR	Rabbit	Home-made
Anti-POMC	Amino acids 6-266 of Human POMC	Mouse	DAKO
Anti-total CaMKII	Amino-terminus of human CaMKII	Rabbit	Cell Signaling
Anti-phospho (Thr286)-CaMKII	Synthetic phosphopeptide flanking Thr286 of human CaMKII	Rabbit	Cell Signaling
Anti-RNA Pol II CTD	RNA Pol II CTD repeat YSPT^{p}SPS	Rabbit	Home-made
Anti-HDAC1	EEKPEAKGVKEEVKLA	Rabbit	Abcam
Anti-HDAC2	C-SGEKTDTKGTKSEQLSNP	Rabbit	Abcam
Anti-HDAC4	Not available	Rabbit	Abcam
Anti-DNMT1	EKDDREDKENAFKR	Mouse	Acris
Anti-DNMT3a	Bacteria expressed HIS-tag DNMT3a	Mouse	Acris
Anti-DNMT3b	Bacteria expressed HIS-tag DNMT3b	Mouse	Acris

2.1.4.2 Secondary antibodies

Antibody	Epitope	Host	Supplier
Anti-rabbit (594)	rabbit IgG	Goat	Perbio
Anti-mouse (488)	mouse IgG	Goat	Santa Cruz
Anti- rabbit (HRP)	rabbit IgG	Goat	Sigma

2.1.5 Vectors

Vector	Supplier
pCpGL-Basic	Gifted by Michael Rehli (Klug and Rehli, 2006)
pCpGL-Pomc	Own construct
pCpGL-Pomc-ΔCpG6-8	Own construct
pCpGL-Pomc-ΔDis-prom	Own construct
pRK7-Flag	Gifted by Anke Hoffmann (Hoffmann and Spengler, 2008)
pRK7-Flag-MeCP2	Own construct
pRK7-Flag-MeCP2-ΔC	Own construct
pRK7-Flag-S438A MeCP2	Own construct
pRK7-Flag-S97A MeCP2	Own construct
pGEM-T	Promega
His-tag MeCP2 1-250	Gifted by Adrian Bird (Kriaucionis and Bird, 2004)
CaMKII 1-280	Gifted by Anthony R Means (Planas-Silva and Means, 1992)
CaMKII T286D	Gifted by Gina Turrigiano (Pratt et al., 2003)
CaMKII	Gifted by Anthony R Means (Planas-Silva and Means, 1992)
MBD1	Own construct
MBD2	Gifted by Samson T. Jacob (Majumder et al., 2006)
MBD3	Gifted by Samson T. Jacob (Majumder et al., 2006)
GST-MeCP2	Own construct

2.1.6 Plastics

Consumable	Supplier	Consumable	Supplier	Consumable	Supplier
Filtertips	Sarstedt	PCR plates/caps	**ABgene**	Cell culture plates	Greiner
Pipette tips	Sarstedt	Scalpels	**Merck**	Micro test plates	Greiner
Cuvette 1mm	Biorad	X-ray cassette	**Kodak**		

2.1.7 Molecular biology kits

Consumable	Supplier	Consumable	Supplier
NucleoSpin PCR purification Kit	Macherey-Nagel	**96-PCR purification plate**	Macherey-Nagel
Protease inhibitor cocktail	Sigma	**Phosphatase inhibitor cocktail 1+2**	Sigma
Magna ChIP G kit	Millipore	**Montage SEQ96 sequencing reaction cleanup kit**	Millipore
BigDyeTerminator v3.1 Cycle sequencing kit	ABI	**NucleoSpin plasmid quickprep**	Macherey Nagel
RNeasy	Qiagen	**Lipofectamine reagent**	Invitrogen
Superscript II RT Kit	Invitrogen	**Picogreen DNA quantification reagent**	Molecular probes
Bio-spin 6 columns	Biorad	**LightCycler FastStart DNA master SYBR Green I**	Roche
TRIzol® **Reagent**	Invitrogen	**pGEM-T vector system**	Promega

2.1.8 Cell lines

Name	Derived tissue	Morphology	Supplier	Reference
AtT-20/D16v-F2	Mouse pituitary epithelial-like tumor cell line	epithelial	ATCC	(Buonassisi et al., 1962)
LLC-PK1	porcine kidney	epithelial	ATCC	(Perantoni and Berman, 1979)
Neuro2a	Murine neuroblastoma	Neuronal	ATCC	(Olmsted et al., 1970)
AtT20 (v1bR)	Mouse pituitary epithelial-like	epithelia	Gifted by Dr.	(Serradeil-Le Gal et al., 2007)

	tumor cell line		Eric Clauser INSERM U970	

2.1.9 Bacterial strains

DH5α from Invitrogen

PIR1 from Invitrogen

2.1.10 Primer sequences

2.1.10.1 Primers for RT-PCR

Oligo name	Sequence	Region	Product size (bp)
POMC	F, 5'-GAA GAT GCC GAG ATT CTG CT-3' R, 5'-TTT CAG TCA GGG GCT GTT C-3'	Exon2/3	221
HPRT1	F, 5'-ACC TCT CGA AGT GTT GGA TAC AGG-3' R, 5'-CTT GCG CTC ATC TTA GGC TTT G-3'	Exon7/9	168
GAPDH	F, 5'-CCA TCA CCA TCT TCC AGG AGC GAG-3' R, 5'-GAT GGC ATG GAC TGT GGT CAT GAG-3'	Exon3/4 +5	326
MeCP2	F, 5'-ACA GCG GCG CTC CAT TAT C-3' R, 5'-CCC AGTTAC CGT GAA GTC AAA A-3'	Exon3/4	237
DNMT1	F, 5'-GGA AGG CTA CCT GGC TAA AGT CAA G-3' R, 5'-ACT GAA AGG GTG TCA CTG TCC GAC-3'	Exon2/3	216
Oligo-dT	5'-TTT TTT TTT TTT TTT TTT TT-3'		

2.1.10.2 Primers for bisulfite sequencing

Primer pair	Sequence	Region	Product size (bp)
Prom-core	F, 5'-GTT TTT TAG GTA GAT GTG TTT TG-3' R, 5'-CTA CTC TTA ACC TCT TTT CTC TTC-3'	Core promoter	203

Prom-distal	5'-TTT TTT TAT TAT TGG GGA AAT TT-3'	Distal	290
	5'-CAA AAC ACA TCT ACC TAA AAA A-3	promoter	
5'-UTR	5'-TTT TTA TTT AGA TTA TTT TGT TAG TTT AGT-3'	5' UTR	283
	5'-TAA TAT CTT ATA AAA CCA AAA TCT CAA TTC-3		
Exon3	5'-TTA TTA GGT TTG GAG TAG GTT TTG G-3'	Coding	204
	5'-ACA CCC TCA CTA ACC CTT CTT ATA-3'	region	

2.1.10.3   Oligonucleotides for EMSA

Oligo name	*sequence*	
EMSA 1	For	5'-GTGGGAAATCTGCGACATAACAAATCC-3'
wild type	Rev	3'-CCTTTAGACGCTGTATTGTTTAGGGTG-5'
EMSA1	For	5'-GTGGGACACCTGCGACACACCAGACCC-3'
AT all Mut	Rev	3'-CCTGTGGACGCTGTGTGGTCTGGGGTG-5'
EMSA1	For	5'-GTGGGAAATCTGCGACACACCAGACCC-3'
AT2+3 Mut	Rev	3'-CCTTTAGACGCTGTGTGGTCTGGGGTG-5'
EMSA1	For	5'-GTGGGAAATCTGCGACATAACAGACCC-3'
AT3 Mut	Rev	3'-CCTTTAGACGCTGTATTGTCTGGGGTG-5'
EMSA2	For	5'-GTGGACGCACATAGGTAATTCCACTCCGATCT-3'
wild type	Rev	3'-CTGCGTGTATCCATTAAGGTGAGGCTAGAGTG-5'
EMSA2	For	5'-GTGGACGCACATAGGTAATTCCACTCTGATCT-3'
CpG8 Mut	Rev	3'-CTGCGTGTATCCATTAAGGTGAGACTAGAGTG-5'
EMSA2	For	5'-GTGGAAGCACATAGGTAATTCCACTCTGATCT-3'
CpG all Mut	Rev	3'-CTTCGTGTATCCATTAAGGTGAGACTAGAGTG-5'
EMSA2	For	5'-GTGGACGCACATAGGTCAGTCCACTCCGATCT-3'
AT Mut	Rev	3'-CTGCGTGTATCCTGTCTGGTGAGGCTAGAGTG-5'
Negtive control	For	5'-GTGGCCTCCGCGCTTTCCAGGCAGATGTGCC -3'
	Rev	3'-CGGAGGCGCGAAAGGTCCGTCTACACGGGTG-5'
Positive	For	5'-GTGATATGGTTTCAGAATAAGCGCTCTAAGTTTAAGAAATT-3'
control	Rev	3'-TATACCAAAGTCTTATTCGCGAGATTCAAATTCTTTAAGTG -5'

2.1.10.4   Primers for ChIP assay

Oligo name	Sequence
POMC-prom-F	5'-AAT CTG CGA CAT AAC AAA TCC CC-3'
POMC-prom-R	5'-AGA ACT GGA CAG AGG CTT AGC GT-3'
POMC-exon3-F	5'-GCT CTT CAA GAA CGC CAT C -3'
POMC-exon3-R	5'-TGA AGA TCA GAG CCG ACT GT -3'
POMC-CpGL-F	5′-GAG CAA ACA GCA GAT TAA AAG GAA T -3′
POMC-CpGL-R	5′-GAT CGG AGT GGA ATT ACC TAT GTG-3′

2.1.10.5   Primers for vector construction and sequencing

Oligo name	Sequence
POMC-pro-Luc-forward	5'-GGA TCC TGA GAT TTT GGT TTC ACA AGA TAT-3'
POMC-pro-Luc-reverse	5'-AAG CTT GTG GCC TCT CTT AGT CAC TGC T-3'
MeCP2 mut S438A-F	5'-CCC GAG GAG GCC GAC TGG AAA GCG ATG GC-3'
MeCP2 mut S438A-R	5'-GCC ATC GCT TTC CAG TCG GCC TCC TCG GG-3'
MeCP2 S97A Seq-F	5'-GAA GCC TCG GCT CGA CCC AAA CAG CGG-3'
MeCP2 S97A Seq-R	5'-CCG CTG TTT GGG TCG AGC CGA GGC TTC-3'
MeCP2-seq-1604-R	5'-ATC CAC AGG CTC CTC TCT GTT-3'
MeCP2-seq-1612-F	5'-AAA GGT GGG AGA CAC CTC CT-3'
MeCP2 mut S97A-F	5'-GAA GCC TCG GCT CGA CCC AAA CAG CGG-3'
MeCP2 mut S97A-R	5'-CCG CTG TTT GGG TCG AGC CGA GGC TTC-3'
T7	5'-TAA TAC GAC TCA CTA TAG GG-3'
Sp6	5'-CAT TTA GGT GAC ACT ATA G-3'

2.2 Methods

2.2.1 Animals and maternal separation

2.2.1.1 Animals

Pregnant C57BL/6N mice were obtained from Charles River Laboratory (Charles River, Sulzfeld, Germany), upon arrival they were housed under standard conditions at the animal facility of Max-Planck Institute of Psychiatry [temperature controlled (21°C) environment and 12h light:12h dark cycle (lights on at 06:00)]. Both male and female pups were used in this experiment. All procedures were approved by the Regierung von Oberbayern and were accordance with European Union Directive 86/609/EEC.

2.2.1.2 Separation paradigm

Maternal separation was used as early life stress (ELS) paradigm. Before pups were born, all dams were randomly assigned to one of the groups: control group (Ctrl) and early life stress group (ELS). For all groups, the day of birth was considered as postnatal day (PND) 0. For the ELS group, the pups were removed from their dam daily for 3 hours for 10 consecutive days from PND1-10. The pups were placed in a clean cage with a heat pad (~32°C) to maintain body temperature. During this period, there is no physical contact between the pups and their dam. After 3 hours separation, the pups were placed back in the home cage with their mother. For the control group, litters remained undisturbed with their mother throughout the whole experiment. In both groups, pups remained with their mother until PND21, and then they were housed in sex-matched group with 3−5 mice per cage.

2.2.1.3 Neuroendocrine measurements

For measurements of corticosterone and ACTH in plasma, commercial radioimmunoassay (RIA) kits (DRG diagnostics, Marburg) were used according to the manufacture's protocol.

2.2.2 DNA analysis

2.2.2.1   DNA extraction

Mouse pituitary DNA was purified by phenol-chloroform extraction. 500 μl lysis buffer (1% SDS, 5 mM EDTA, 100 mM NaCl, 0.5 mg/ml freshly prepared proteinase K (Roche #3115879) and 10 mM Tris-HCl, pH8.0) was added to a 1.5 ml reaction tube containing pituitary tissue, then the solution was incubated overnight at 56 °C. On the following day, the clear lysate was cooled down on ice for 30 minutes and 200 μl of salt solution (4.21 M NaCl, 0.63 M KCl, 10 mM Tris-HCl (pH 8.0)) was added. The tube was incubated on ice for 1 hour and centrifuged for 10 minutes at maximum speed (14,000 *g*) in a cooled microfuge. The supernatant was transferred to a fresh tube and 1 volume of cold Phenol /Chloroform was added. The tube was vortexed for 1 minute and centrifuged for 2–3 minutes at maximum speed at 4 °C. The upper aqueous phase was transferred carefully without touching the inter-phase to a fresh tube, 2–2.5 volume of pure ethanol and 1 μl glycogen (10 mg/ml) was added, then DNA was precipitated overnight at -20 °C. After centrifugation 15 minutes at maximum speed in a precooled centrifuge, the pellet was washed with 70% ethanol. The pellet was air dried for 5 minutes at 60 °C. 25-50 μl of TE (10mM Tris-Cl, pH 7.5, 1mM EDTA) buffer or distilled water was added to each sample. PicoGreen reagent (Molecular Probes) was used to quantify DNA concentration.

2.2.2.2   PCR reaction

Standard PCR was performed in a Biometra T-Gradient thermocycler (Biometra, Germany) with Fermentas Taq polymerase.

If not indicated otherwise, the following PCR conditions were used:

Step	Temperature	Time	Cycles	PCR mix
Initial denaturation	95 °C	5 mins	1	2 μl template
Denaturation	95 °C	1 min		2.5 μl 10×reaction buffer
Annealing	56 °C	1 min	35	1.5 μl dNTPs (10 mM each)
Elongation	72 °C	1 min		1.5 μl forward primer (10 pmol/μl)

Final elongation	72 °C	10 mins	1	1.5 µl reverse primer (10 pmol/µl)
				3 µl MgCl$_2$ (25 mM)
Storage	10 °C	pause		1U Taq polymerase
				add water to 25 µl

Table 1. Standard PCR temperature profile and PCR mix.

2.2.2.3   Agarose gel electrophoresis

Agarose gel electrophoresis was used to analyse the quality of DNA and to separate fragments by size. Depending on the size of the DNA molecules, agarose solutions ranged from 0.8 to 2% (w/v) in 1 x TBE buffer (90 mM Tris, 90 mM Boric acid, 2 mM EDTA). Ethidium bromide was added to a final concentration of 0.25 µg/µl. The samples to be analyzed were mixed with 1x loading dye (6x loading dye: 40% v/v sucrose, 0.25% xylene cyanol, and 0.25% bromophenol blue). The voltage applied depended on desired separation, gel strength and chamber sizes. In general, the voltage applied was between 4–5 V/cm. As size standard, a 1kb DNA ladder (Fermentas) was used. The DNA or RNA was visualized on a UV transilluminator.

2.2.2.4   Recovery of DNA from agarose gels

The desired DNA band was cut out from an 0.8% low melting point agarose gel on a UV transilluminator and transferred into a 1.5 ml tube. The Macherey-Nagel PCR purification kit was used to recover the DNA fragment from the gel. 100 µl of NT buffer was added to the tube and incubated at 65 °C on a thermomixer (Eppendorf, Germany) with gentle shaking until gel melting. The mixture was transferred to a PCR purification column and processed according to manufacturer's instructions. .

2.2.2.5   Bisulfite sequencing

Genomic DNA (200 ng) isolated from mouse pituitary was digested overnight with EcoRI, sodium bisulfite converted (Qiagen EpiTect Bisulfite kit) and aliquots used for PCR reactions. Products were cloned into the pGEM-T vector (Promega), and recombinant clones were picked to perform colony PCR. Products were checked for correct insert size by gel electrophoresis. After purification of PCR products

(NucleoFast PCR Cleanup Plate, Macherey-Nagel, Germany), BigDye sequencing reactions were performed. For each amplicon, at least 24 independent recombinant clones were analyzed on an ABI Prism 3700 capillary sequencer.
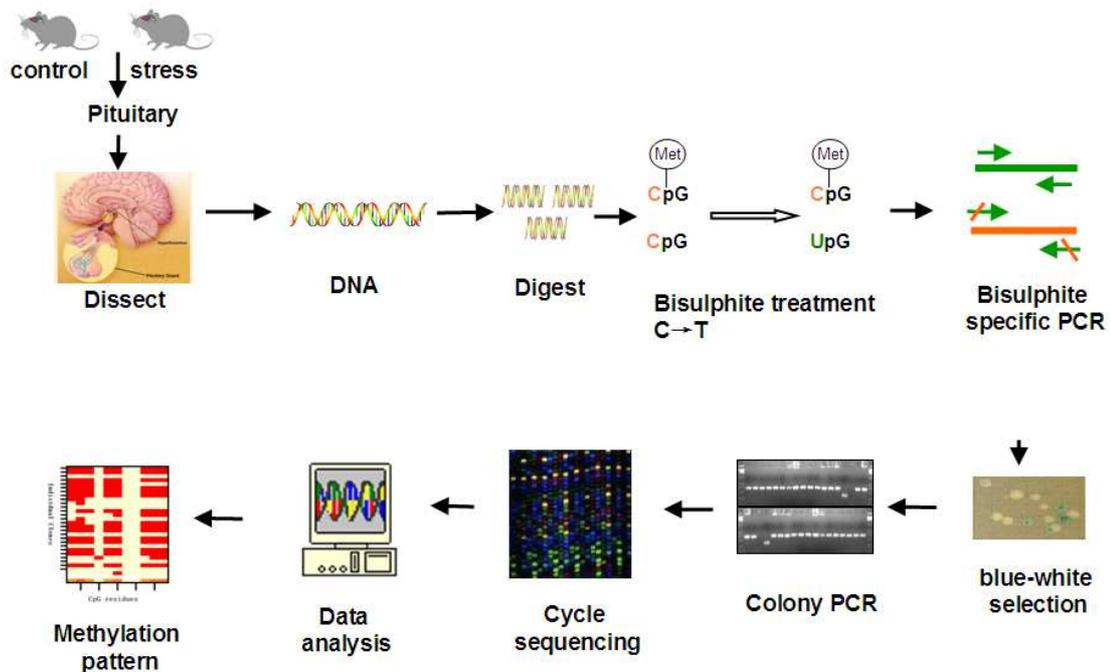
Figure 5. Bisulfite sequencing flowchart. Genomic DNA from mouse pituitary was overnight restriction enzyme digested and then bisulfite converted. Treatment of DNA with bisulfite converts cytosine (C) residues to uracil (U), but leaves 5-methylcytosine residues unaffected. In the following PCR reaction, the uracil will appear as a thymidine (T). PCR products were then subcloned into pGEM-T vector. Recombinant clones, identified by color selection, were picked as template in the colony PCR. For each amplicon, at least 24 independent recombinants were analyzed on an ABI 3730 capillary sequencer. Sequencing files were assembled by the computer program--Bioedit and methylation patterns of each animal were deduced.

2.2.2.6   Chromatin immunoprecipitation (ChIP)

Chromatin immunoprecipitation experiments were performed with AtT20 cells and mouse pituitaries to investigate the binding of MeCP2 at the *Pomc* promoter. For *in vivo* ChIP, frozen pituitary tissue was first chopped up using scissors and then washed with 1 ml 1×PBS containing protease inhibitor (1:100 dilution, Sigma). AtT20 cells or pituitary tissues were incubated for 10 minutes at 37 °C in the presence of 1% formaldehyde. Formaldehyde treatment was quenched by addition of glycine to a final

concentration of 125 mM. The chromatin immunoprecipitation protocol was based on the Upstate Biotechnology ChIP Kit (Magna ChIP G, Millipore) protocol with the following modifications: samples were sonicated for 12 cycles of: [30 seconds "ON" / 30 seconds "OFF"] with the Bioruptor TM from Diagenode (cat # UCB-200) in a wet ice bath. After sonication, 5 μl of the sheared material was loaded on a 1% agarose gel to check fragment sizes. The DNA smear on the gel should range between 200 bp and 1000 bp. DNA concentrations of the chromatin samples were determined with a *SmartSpec Plus* spectrophotometer (Bio-Rad). The sonicated samples were either subjected to immunoprecipitation or stored at -20 °C until further use. Chromatin samples 5 OD were then subjected to immunoprecipitation using antibodies specific to the MeCP2 C-terminus or phospho-RNA pol II according to the Upstate ChIP kit protocol. To reduce unspecific binding in the immunoprecipitation, antibodies were pre-incubated with chromatin DNA on a rotating platform in the cold room overnight, and the Dynabeads Protein G (Invitrogen) were added on the following day and incubated for an additional 1 hour in the cold room with rotation. After reverse crosslinking, protein digestion, and DNA purification, immunoprecipitates were dissolved in 50 μl TE buffer and subjected to standard or real-time PCR.

2.2.2.7 Sequential ChIP

For sequential ChIP assays, the initial ChIP was performed with the indicated antibodies, chromatin was eluted with 50 μl dithiothreitol (DTT) (10 mM), and a second ChIP was then carried out. Amplified products were quantified by real-time PCR. The relative binding of the immunoprecipitated proteins at the *Pomc* locus was calculated from real-time PCR data.

2.2.3 RNA analysis

2.2.3.1 RNA isolation

Total RNAs from pituitary tissues or cell lines were isolated using the TRIzol reagent (Invitrogen). All plastic and glassware used was rinsed with water containing 0.05% diethypyrocarbonate (DEPC) and autoclaved before use to inactivate RNAses. All experiments were performed on ice. Pituitary tissues or cell lines were homogenized

in 1 ml of TRIzol reagent. The homogenized samples were incubated for 5 minutes at room temperature to permit complete disruption of nucleoprotein complexes. 0.2 ml of chloroform was added to the sample per 1 ml TRIzol reagent. Tubes were shaken vigorously by vortexing for 15 seconds and incubated at room temperature for 2–3 minutes. Then all the samples were subjected to centrifugation at no more than $12,000 \times g$ for 15 minutes at 4 °C. RNA stays exclusively in the aqueous phase. The aqueous phase was transferred to a fresh tube, and 0.5 ml of isopropyl alcohol (2-propanol) was added per 1 ml of TRIzol reagent. Samples were incubated at room temperature for 10 minutes and centrifuged at no more than $12,000 \times g$ for 10 minutes at 4 °C. The supernatant was entirely discarded. The RNA pellet was washed once with 75% ethanol, adding at least 1 ml of 75% ethanol per 1 ml of TRIzol Reagent. Then the samples were mixed by vortexing and centrifuged at no more than $7,500 \times g$ for 5 minutes at 4 °C. RNA pellets were air dried for 5–10 minutes and dissolved in 30 µl of DEPC-treated water. RNA concentrations were measured by RiboGreen.

2.2.3.2   cDNA synthesis and subsequent gene-specific PCR

Synthesis of cDNAs was carried out in 20 µl reaction volume. Total RNA (200 ng) isolated from mouse pituitary or cell lines was subjected to reverse transcription in the presence of 1 µl oligo (dT) (100 pm), 1.5 µl dNTP (10 mM each) mix and filled up with distilled water to 12 µl. Then the mixture was heated to 65 °C for 5 minutes and quick chilled on ice. The contents of the tube were collected by brief centrifugation. $5 \times$ First-Strand buffer and 0.1M DTT were added to the tube, and then the samples were incubated at 42 °C for 2 minutes. In the next step, either 1 µl (200 units) of Superscript II RT transcriptase or 1 µl water for the negative control was added to the tube and then all the samples were incubated at 42 °C for 50 minutes. Finally, the reaction was terminated by heating at 70 °C for 15 minutes. The cDNA was used as template for amplification in PCR reactions.

2.2.3.3   Quantitative PCR analysis

Pomc mRNA expression level in the pituitary was analyzed by qRT-PCR, using the LightCyclerR FastStart DNA MasterPLUS SYBR Green I reagent (Roche Diagnostics GmbH, Germany). All experiments were performed according to manufacturer's instructions. Reaction volumes were adjusted to 10 µl in each

experiment and contained 5 µl of distilled water, 0.5 µl of forward primer (10 pmol/µl), 0.5 µl of reverse primer (10 pmol/µl) and 5x PCR-Mix (prepared by adding 14 µl of reagent 1a to 1b from the Roche kit). Primers used for qRT-PCR were designed across exons to avoid genomic DNA contamination. The primers for POMC, MeCP2, DNMT1 and the housekeeping genes glyceraldehyde-3-phosphate dehydrogenase (GAPDH) and hypoxanthine guanine phosphoribosyl transferase 1 (HPRT1) were listed in the previous parts. Experiments were performed in triplicates on the LightcyclerR 2.0 instrument (Roche Diagnostics GmbH) under the following PCR conditions: initial denaturation: 40 cycles of denaturation, annealing, and elongation (see Table 2 reaction conditions in the LightCyclerR for POMC, MeCP2 and the housekeeping genes GAPDH and HPRT1 for reaction conditions). Fluorescence was assessed each cycle after the elongation phase. At the end of each run, a melting curve (50−95°C with 0.1 °C/sec) was generated to asses linearity of the amplification process. Crossing points (Cp) were calculated with the LightCyclerRSoftware 4.0 (Roche Diagnostics GmbH, Germany) using the absolute quantification fit-points method. Threshold and noise band were set in all compared runs to the same level. Relative gene expression was determined by the $2^{-\Delta CT}$ method (Livak and Schmittgen, 2001) using the real PCR efficiency calculated from an external standard curve. Cp was normalized to the housekeeping genes GAPDH and HPRT, respectively, and values calculated relative to the expression mean of each group.

genes	Preincubation	Denaturation	Annealing	Elongation
Pomc	95 °C/10 min	95 °C/10 sec	56° C/5 sec	72 °C/8 sec
Mecp2	95 °C/10 min	95 °C/10 sec	56° C/5 sec	72 °C/10 sec
Dnmt1	95 °C/10 min	95 °C/10 sec	61°C/5 sec	72 °C/10 sec
Gapdh	95°C/10 min	95 °C/10 sec	65 °C/5 sec	72 °C/13 sec
Hprt1	95 °C/10 min	95°C/10 sec	57 °C/5 sec	72° C/8 sec

Table 2. Amplification conditions of qRT-PCR

2.2.4 Plasmids

2.2.4.1 Standard and parental plasmids

pCpGL-Basic vector (graciously gifted by Michael Rehli, University Hospital Regensburg, Germany) was created by replacement of the enhancer/promoter region (PstI/NheI fragment) of the CpG-free plasmid pCpG-mcs (Invivogen, San Diego, CA) to a short CpG-free linker (5'-CTG CAG GAC TAG TGG ATC CAG ATC TTA AGC TTA GTC CAT GGA CAA TTG CTA GC-3') containing several restriction sites. A CpG-free luciferase coding region was released from pMOD-LucShS (Invivogen) by digestion with MfeI (blunted using Klenow polymerase) and NcoI, and subcloned into NheI (blunted) and NcoI digested, linker ligated CpG-free backbone. The CpG-free luciferase vector containing R6K origin of replication was maintained in E.coli PIR1 cells (Invitrogen, Karlsruhe, Germany). This bacterial strain was grown in low salt LB medium (Tryptone, 10 g/l; yeast extract, 5 g/l; NaCl, 5 g/l and pH 7.0 adjusted by NaOH) supplied with 25 µg/ml of Zeocine (Invitrogen) as antibiotics.

pRK7-FLAG vector was created by cloning the oligonucleotides encoding the FLAG-epitope into the HindIII and BamHI digested pRK7 vector. These oligonucleotides encode for the short hydrophilic 8 amino acid (aa) peptide Asp-Tyr-Lys-Asp-Asp-Asp-Asp-Lys. This epitope is likely to be located on the surface of a fusion protein due to its hydrophilic nature and, therefore, accessible to antibodies. The small size limits interference with the fusion protein's function and transportation.

2.2.4.2 Reporter constructs

pCpGL-Pomc luciferase vector contains the promoter region of the mouse *Pomc* gene. A fragment spanning 550 bp of the mouse *Pomc* gene was amplified from genomic DNA isolated from the mouse corticotrope cell line AtT20 by PCR. The primers used for this PCR reaction contained a BamHI site in the forward primer and a HindIII site in the reverse primer. The PCR product was first cloned into pGEM-T (Promega) vector and verified by sequencing. The *Pomc* promoter fragment was then released from the pGEM-Pomc vector by BamHI and HindIII double digestion and purified on an agarose gel. CpGL-basic vector which contained a CpG free backbone was also

double digested with BamHI and HindIII and dephosphorylated by adding 1U of calf intestinal alkaline phosphatase (CIAP) to avoid recircularization of the cloning vector. After gel purification of the backbone vector, the *Pomc* promoter fragment was ligated into the BamHI/HindIII site of pCpGL-Basic vector.

pCpGL-Pomc-ΔCpG6-8 containing a deletion of CpG residues 6–8 was generated by insertion of a BglII/HindIII fragment of previously described pCpGL-Pomc into the BglII/HindIII site of the pCpGL-basic vector. pCpGL-Pomc-ΔDis-prom vector containing only the proximal *Pomc* promoter was obtained by cloning a PstI/HindIII fragment of previously described pCpGL-Pomc into the PstI/HindIII site of the pCpGL-basic vector.

2.2.4.3 Expression vectors

The MeCP2 expression vectors (graciously gifted by Adrian Bird, University of Edinburgh, UK) consist of the mouse MeCP2_alpha variant in pRL-SV40 (Promega) and of a cDNA for the first 205 amino acids of human MeCP2 with a C-terminal His-tag in the pet30b vector (Novagen), respectively. N-terminal Flag-tagged forms of different MeCP2 constructs were obtained by PCR-cloning of wild type (F; aag gga tcc gcc gcc gct gcc gcc acc gc, R; tct gat atc ctc agc taa ctc tct cgg tc) or of a form deleted of the 45 C-terminal amino acids of MeCP2 (F; aag gga tcc gcc gcc gct gcc gcc acc gc, R; tct gat atc ctc agc taa ctc tct cgg tc) into the BamHI and EcoRI sites of pRK7-Flag (Hoffmann et al., 2006). The MeCP2 riboprobe (nt 612–1,604; Acc. No. NM_010788) contains the conserved sequence within exons 3 and 4 of the mouse *Mecp2* gene. A corresponding PCR-product (F; aaa ggt ggg aga cac ctc ct, R; tcc aca ggc tcc tct ctg tt) was cloned in the pGEM-T vector (Promega) and antisense riboprobes were generated as previously described (Dragich et al., 2007). Expression vectors for MBD2 and MBD3 (graciously gifted by Samson T. Jacob, Ohio State University, US) contain the mouse MBD2 or MBD3 cDNAs in the pcDNA3.1 vector (Invitrogen) (Ghoshal et al., 2004). The MBD1 expression vector contains the full length cDNA for mouse MBD1 (Acc. No. NM_013594; F; tac ctc tag aat ggc tga gga ctg gct gga ctg, R; ttt cta gaa aca att tgc aaa gaa ttt tca gg) inserted in the pRK7 expression vector. CaMKII expression vectors contained either full-length CaMKII (1-317) or CaMKII (1-290), which is constitutive active due to the absence of the calmodulin-binding domain (graciously gifted by Anthony R Means Dept. of

Pharmacology and Cancer Biology, Duke University Medical Center, P. O. Box 3813 Durham, NC). The constitutive active CaMKII (T286D) contains a replacement of Thr 286, which locates in the autoinhibitory domain by Asp (graciously gifted by Gina Turrigiano, Department of Biology, Volen National Center for Complex Systems, Brandeis University, Waltham, MA 02454, USA).

2.2.4.4   Recombinant protein construct

The plasmid GST-MeCP2 (pGex2tk-MeCP2) was used to produce recombinant MeCP2 protein for EMSA experiment. For prokaryotic expression, the MeCP2-alpha cDNA was PCR amplified (F; aag gga tcc gta gct ggg atg tta gg, R; tct gat atc ctc agt ggt gga gga gga g) and inserted into the BamHI and SmaI sites of pGex2tk (Pharmacia). All constructs used in this study were entirely sequence verified.

2.2.4.5   Site-directed mutagenesis

In order to test the specificity of phospho-MeCP2 antibodies, the phospho residue Ser 97 and Ser438 were replaced in MeCP2 by alanine using site-directed mutagenesis. Site-directed mutagesis was performed using a two step PCR method. The pRK-Flag-MeCP2 vector was used as the parental vector. The oligonucleotides for this mutagenesis are listed below:

S97A Sense: 5'-GAA GCC TCG GCT CGA CCC AAA CAG CGG-3'

S97A Antisense: 5'-CCG CTG TTT GGG TCG AGC CGA GGC TTC-3

S438A Sense: 5'-CCC GAG GAG GCC GAC TGG AAA GCG ATG GC-3'

S438A Antisense: 5'-GCC ATC GCT TTC CAG TCG GCC TCC TCG GG-3'

Briefly, the first PCR contained 50 ng vector DNA, 125 ng of oligonuleotide (sense or antisense), 1 µl of dNTP (10mM), 10x Pfu reaction buffer, 1 µl Turbo Pfu polymerase (Fermentas) and filled up to 50 µl with distilled water. After initial denaturation for 3 minutes at 95 °C, 10 amplification cycles (95 °C, 30 sec; 60 °C , 60 sec; 68 °C, 10 mins) were carried out.

In the second PCR reaction, 25 µl of sense and 25 µl of antisense PCR product were taken from the first PCR. Following addition of 0.5 µl of Pfu polymerase, PCR

reactions were performed as below. After the first initial denaturation of 3 minutes at 95 °C, 20 amplification cycles (95 °C, 30 sec; 56 °C, 60 sec; 68 °C, 10 mins) were performed. 2 µl of PCR product were taken to check amplification progress by gel electrophoresis. Then PCR products were purified by spin column (Macherey-Nagel). 50 µl of water was added to elute the PCR product. In order to remove the parental vector, DpnI digestion was performed which contained 45 µl of eluate, 5 µl of 10x buffer and 1 µl of DpnI (10U/µl). After incubating the sample at 37 °C for 90 minutes, the sample was heat inactivated at 65 °C for 10 minutes, then purified by phenol/chloroform and ethanol precipitation. Finally, DNA was resuspended in 10 µl of water. 2 µl of vector DNA was transformed in electrical competent bacteria. Sequencing was carried out to verify the mutation.

2.2.4.6   *In vitro* methylation

The CpG methyltransferase, M.SssI (New England Biolabs), can methylate all cytosine residues (C^5) within the double-stranded dinucleotide recognition sequence 5'...CG...3'. The protocol was as follows: in the first step, 32 mM SAM stock was freshly diluted to 1600 µM. Then reaction was set up in a volume of 20 µl by adding the following reagents: 11 µl of nuclease free water, 2 µl of 10×NEBuffer, 2 µl of diluted SAM from previous step, 4 µg of plasmid DNA and 1 µl of SssI methylase (4 U/µl). The reaction was incubated at 37 °C for 1 hour. Then the reaction was stopped by heating at 65 °C for 20 minutes. After phenol/chloroform purification and ethanol precipitation, the vector was ready to use.

2.2.4.7   Site-directed DNA methylation

Site-directed DNA methylation was performed to methylate specific CpG dinucleotides (CpG 6−8) in a *Pomc* promoter vector (CpGL-Pomc). 5 µg of CpGL-Pomc vector was double digested with BglII and HindIII whereby only CpG 6−8 remained in the backbone vector. To prevent recircularization of the cloning vector, Calf Intestinal Alkaline Phosphatase (CIAP), which removes 5´ phosphates from the vector DNA, was added to the digestion system. The vector DNA was first purified on a PCR cleanup column; then *in vitro* methylation was carried out as mentioned above. In the control, all steps remained the same with one exception: in the *in vitro* methylation step, 1 µl of water was added instead of 1U of Methylase SssI. In

parallel, 5 µg POMC PCR products were also double digested with BglII and HindIII. After PCR product purification, the PCR product was ligated to the backbone vector which contained methylated CpG 6−8. After overnight ligation, the product was subjected to phenol/chloroform purification and ethanol precipitation. To verify the methylation status of the plasmid vector, bisulfite sequencing was performed. The final patch DNA methylation product was enough for 3 transfections (3 wells) in a 12-well plate.

2.2.4.8   Plasmid preparations

I) Small-scale preparations

In order to screen positive recombinants, plasmid DNA was extracted from *E.coli*. Colonies were picked from an agar plate and incubated in 1.5 ml growth medium supplemented with appropriate antibiotics (Zeocin, 25 µg/ml; Ampicilin 100-200 µg/ml). The cultures were incubated 6−8 hours or overnight at 37 °C in a shaker (rotation 200 rpm). 1.5 ml of each overnight culture was transferred in a 1.5 ml reaction tube and centrifuged (10 min, 9000 *g*, RT) to pellet the bacteria. The cell pellet was resuspended in 200 µl TEG (25 mM Tris pH 8.0, 10 mM EDTA, 100 µg/ml RNase A, and 1% glucose) on a shaking platform or vortexer, lysed by adding 200 µl alkaline SDS (200 mM NaOH, 1% (w/v) SDS) and mixed by inverting the tube for 6−8 times. After incubation at RT for 5 minutes, 200 µl of 3M KAc was added. The tube was inverted again for 6−8 times and then kept on ice for 10 minutes before centrifugation (10 min, 13,000*g*, RT). The plasmid DNA in the supernatant was transferred into a new 1.5 ml tube and 500 µl of isopropanol was added. The tube was incubated on ice for 30 minutes and then centrifuged (20 min, 13,000 *g*, 4 °C) to pellet the plasmid DNA. The pellet was washed with 70% ethanol and centrifuged (5 min, 13,000 *g*, 4 °C). The supernatant was carefully aspirated; the pellet was air-dried and redissolved in 25 µl TE (10 mM Tris, 1 mM EDTA). The plasmid DNA can be used immediately or stored in a -20 °C freezer.

II) Large-scale preparations

To obtain 100 µg of plasmid DNA or more, maxiprep was performed. A single clone was picked from the agar plate, then incubated overnight at 37 °C with vigorous shaking in 2 ml of SOB (tryptone 20 µg/ml, yeast extract 5 µg/ml, NaCl 10 mM, KCl

2.5 mM) medium with appropriate antibiotics. On the next day, 2 ml of the overnight culture was added to a 500 ml flask containing 40 ml of TB_A (tryptone, 12 μg/ml; yeast extract, 24 μg/ml; glycerol, 0.4%) and 10 ml of TB_B (KH_2PO_4, 0.17 M; K_2HPO_4, 0.72 M) with appropriate antibiotics. The culture was incubated overnight at 37 °C with shaking (200 rpm). The plasmids were purified using a Macherey-Nagel plasmid maxiprep kit.

2.2.5 Cell culture and transfection experiments

2.2.5.1   Cell cultures

LLC-PK1 cells are an epithelial cell line (ATCC No. CL-101) originally derived from porcine (pig) kidneys. The cells show a fibroblastic-like morphology and were grown in Dulbecco's Modified Eagle Medium (DMEM) supplemented with 10% fetal calf serum (FCS). In this study, LLC-PK1 cells were used for transfection of pRK-MeCP2 vectors by electroporation to validate MeCP2 antibodies.

AtT-20/D16v-F2 (mouse pituitary epithelial-like tumor cell line) cells (ATCC No. CRL-1795) are corticotrope and are derived from a neuroendocrine tumor, which endogenously expresses two distinct somatostatin receptor subtypes (SRIF). They are used in transfection studies to investigate endocrine and exocrine secretory pathways, in particular ACTH (adrenocorticotropic hormone) and beta-endorphin. The F2 subclone of AtT-20 (see ATCC CCK-89) was developed by B. Gumbiner. This clone had been used successfully by Moore et al. (Moore et al., 1983a, b) for several DNA mediated transfection studies relating to endocrine and exocrine secretory pathways. In this study, AtT20 cells were used for the investigation of *Pomc* gene activation by various treatments and stimuli. AtT20 cells were grown in DMEM supplemented with 10% FCS.

Neuro2A is a mouse neuroblastoma cell line (ATCC No. CCL-131) established by R.J. Klebe and F.H. Ruddle in 1969 (Klebe, 1969) from a spontaneous tumor of an albino mouse strain and are neuronal in morphology. In this study, we extracted DNA from Neuro2A cells and performed bisulfite sequencing to check *Pomc* DNA methylation status. Neuro2A cells were grown in DMEM supplemented with 10% FCS.

AtT-20 (V1bR) cells are corticotrope cells with the mouse vasopressin V1b receptor stably expressed. These cells were kindly gift from Dr. Eric Clauser (INSERM U970, Paris, France). They were used in transfection studies to investigate *Pomc* luciferase activity after AVP treatment as well as in ICC experiments to examine MeCP2 phosphorylation after AVP treatment. AtT20 (V1bR) cells were grown in 50% MF12/50% DMEM Glutamax supplemented with 10% FCS, 10% Nu serum (BD biosciences), geneticin (0.5 mg/ml) and 1% Penicillin/streptomycin (Biochrom) as antibiotic.

2.2.5.2   Primary pituitary cell culture

For mouse primary pituitary cell culture, tissues were removed from adult male mice (~6 weeks old) and stored in HD-buffer (Hepes 25 mM, NaCl 137 mM, KCl 5 mM, Na_2HPO_4 0.7 mM, glucose 10 mM, Partricin (A2812, Biochrom) 25 mg/l, and Penicillin/Streptomycin (A2213, Biochrom) 105 units/l). After washing several times with HD-buffer, pituitaries were chopped up into small pieces by scissors. The HD-buffer was removed, then 5 ml of collagenase (Worthington Biochem) solution was added to the cells to dissociate the extracelluar matrix. After incubation of the cells in a 37 °C incubator about 2 hours, 35 ml of cell culture medium (50 ml FCS (Gibco), 5 ml glutamine (Biochrom), 5 ml Pen/Strep (Biochrom), 5 ml Partricin (Biochrom), MEM-vitamins (Biochrom), 2.5 mg insulin (Sigma), 2.5 mg transferrin (Sigma), 30 pm T3 (Sigma), 10 µg sodium selenite (Sigma) in 500 ml DMEM medium (Gibco)) was added to stop the reaction. Living cells were counted by acridine orange/ethidium bromide staining and pituitary cells were seeded into 12-well culture plates at a concentration of 100.000 cells/ml. Two days later, growth medium was replaced with fresh culture medium and cells treated either with KCl (55 mM) or AVP (100 nM). The calmodulin kinase II inhibitor (1 µM, EMD Chemicals, Gibbstown, USA) or the AVP V1b receptor antagonist--SSR149415 (1 µM, Axon1114, Axon medchem) were added to the medium 30 minutes before stimulation.

2.2.5.3   Transfection

LLC-PK1 cells were seeded one day before electroporation. They were harvested by trypsinisation and resuspended in 1x Electroporation buffer (1x EP buffer) (50 mM K_2HPO_4, 20 mM CH_3KO_2, 20 mM KOH) to adjust to a concentration of 2 x 10^7

cells/ml. 1 x 10^6 cells in 50 µl of this was added to a 100 µl mixture containing 200 ng of pRK-MeCP2 vector, 2 µg CaMKII vector, 4 µl MgSO$_4$, 20 µl 5 x EP buffer, 2 µg PAM carrier DNA, and water. This was incubated at room temperature for 10 minutes, placed in a cuvette and then electroporated using a BTX 600 electroporator (290 V, 500 µF, 360 Ω). After pulse delivery, the cells were immediately transferred to 6-well culture dishes containing 2 ml of DMEM+10% FCS and incubated overnight at 37 °C with 5% CO$_2$.

AtT20 cells were transfected using lipofectamine reagent. One day before transfection, 1 x 10^5 AtT20 cells were seeded in 1 ml DMEM+10% FCS onto 12-well tissue culture dishes and grown until 50–80% confluence. The medium was removed prior to transfection and the cells were rinsed with 200 µl of Opti-MEM without FCS. For each well, 6 µl of lipofectamine reagent was mixed with 2 µg of pCpGL-Pomc-luciferase vector and 0.5 µg pRK7-β-gal which was mixed in 100 µl of Opti-MEM medium without serum. The plasmid Opti-MEM mixture was added to Lipofectamine Opti-MEM mixture dropwise, then the mixtures was incubated for 45 minutes at room temperature to allow complexes to form. These complexes were added to the rinsed cells and incubated for 6 hours. After this 400 µl of DMEM+20%FCS was added, and cells incubated overnight at 37 °C. 24 hours after transfection, luciferase activity was measured.

2.2.5.4   Luciferase assays

To measure promoter activity, cells were washed twice with PBS and then thoroughly lysed in 100 µl lysis buffer (75 mM Tris-HCl, 10 mM MgCl2, 1% Triton X-100, 2 mM ATP, 1 mM DTT). 80 µl of aliquots were measured in a LKB luminometer for 20 seconds. As an internal control of transfection efficiency, the luciferase readings were nomalized on β-galactosidase activity from a cotransfected expression vector (pRK7-β-gal) (Hoffmann et al., 2003). The β-gal activity in the extracts was measured as described previously (Spengler et al., 1993).

2.2.6 Protein preparations

2.2.6.1   Recombinant proteins

Recombinant GST-MeCP2 fusion proteins were used for EMSA experiment. Following transformation of pGEX-2TK-MeCP2 into DH5α bacteria, single colonies were grown at 37 °C in 50 ml 2YT (0.16% tryptone, 0.1% yeast extract, 0.1% NaCl) overnight, to which a futher 450ml 2YT was added and grown for 3 hours until an OD 600 of 0.5−1.0 was reached. After that, they were incubated at a final concentration of 1 mM IPTG for another 2 hours at 30 °C. The GST-MeCP2 protein was purified using glutathione-sepharose beads (Hoffmann et al., 2003). Eluted GST-MeCP2 was shown to be of at least 95% purity as judged by Coomasie blue staining. The concentration of GST-MeCP2 was determined using Bradford assays and aliquots were stored at -80 °C until usage.

2.2.6.2   Protein concentration and purity

Bradford assays were applied to determine the concentration of all proteins used in this study. The assay is based on the observation that the absorbance maximum for an acidic solution of Coomasie Brilliant Blue G-250 shifts from 465 nm to 595 nm when binding of the dye to proteins occurs. Both hydrophobic and ionic interactions stabilize the anionic form of the dye, causing a visible colour change. The concentrated assay buffer was first diluted 1:5 and standards were prepared containing a range of 20 to 200 μg protein (BSA). The samples were diluted (3 μl in 200 μl water) to an estimated concentration of 20 to 200 μg/ml. 800 μl Bradford reagent was added to each sample and protein standards, and the absorbance was measured at 590 nm. Protein concentrations of samples were deduced from the standard curve. Coomassie blue staining was then further used to assess the purity and integrity of recombinant protein preparations. Protein samples were loaded onto an SDS-PAGE gel with a size marker and fractionated at 150 V. The gel was then soaked in 0.2% Coomassie blue for 1 h and destained in 40% methanol, 50% acetic acid solution over night. The gel was then blotted on to paper and dried. All proteins used in the study were of at least 95% purity.

2.2.6.3   Electrophoretic mobility shift assay (EMSA)

EMSA was used to determine the affinity of a protein for a particular DNA sequence. In these EMSA experiments, recombinant GST-MeCP2 protein was incubated with 20,000 cpm of double-stranded end labelled oligonucleotides. Sense and antisense

oligonucleotides contained the CpG dinucleotide neighboured by an AT rich sequence and an overhanging GTG for end labelling. The oligonucleotides used for EMSA experiment are listed in Figure 6. In order to show the importance of the methylated CpG dinucleotide and the adjacent AT rich sequence to MeCP2 binding, a series of mutated oligonuleotides were designed. They either contained a mutated CpG dinucleotide to abolish DNA methylation or carried mutation(s) in the AT rich region. An oligonucleotide encoding a previously reported MeCP2 binding site was used as positive control. This binding site was identified previously as high affinity MeCP2 binding site (Klose et al., 2005).
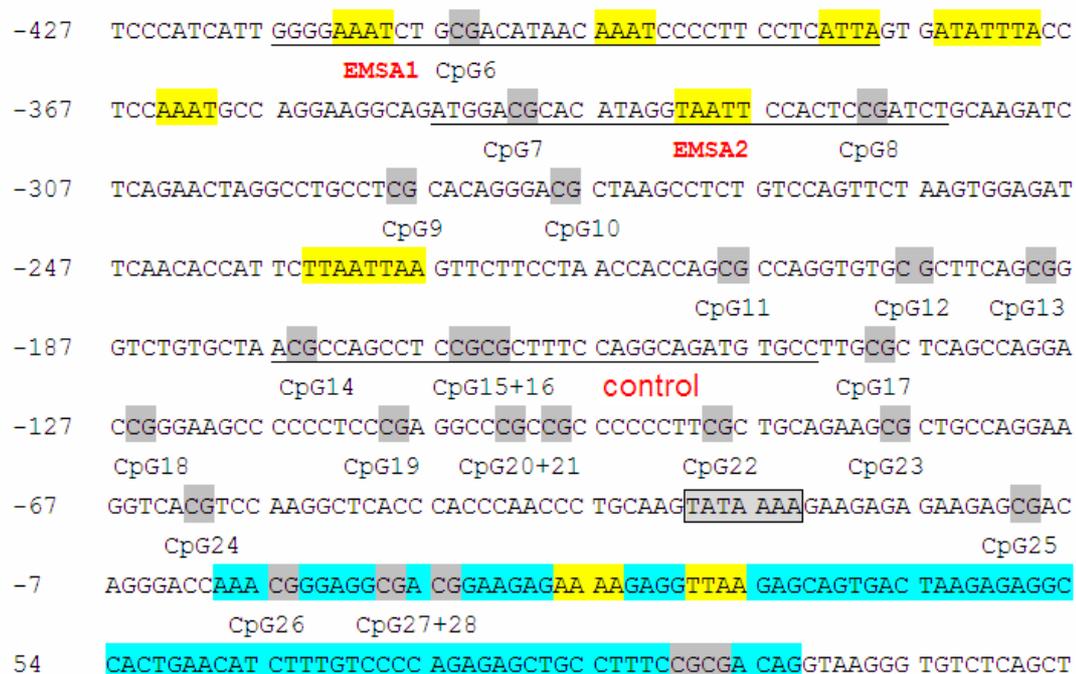
Figure 6. Oligonucleotides derived from the *Pomc* promoter region used in the EMSA experiments. CpG dinucleotides are shadowed in gray and AT runs in yellow. The location and sequence of the oligonucleotides used for the EMSA experiments are underlined. The sequence marked in cyan indicates *Pomc* exon1.

In the EMSA experiment, oligonucleotides were annealed in a reaction volume of 40 µl containing 1 µg/µl of each of the sense and antisense oligonucleotides and 4 µl of annealing buffer (1.5 M NaCl, 100 mM Tris-HCl pH 7.9). The oligonucleotides were heated at 85 °C for 10 minutes to ensure DNA double-strand separation, and then slowly cooled down to room temperature by switching off the heat-block to allow for efficient annealing of the sense to the antisense strands. The double-strand oligonucleotides were *in vitro* methylated (see *in vitro* methylation) by CpG methyltransferase (M.SssI, NEB). Unmethylated and methylated oligonucleotides

were diluted to 50 ng/ml and used in parallel in the labelling reaction. For the labelling reaction, the mastermix was prepared as follow: 1.5 μl of oligo mix (50 ng/μl), 2.0 μl of 10×Klenow buffer, 3.0 μl ^{32}P-dCTP, 4.0 μl of dATG, 1 μl of Klenow enzyme and water to 20 μl. This mastermix was incubated at room temperature for 45 minutes and 4 μl of dCTP (5 mM) was added. The mixture was incubated again for 5 minutes at room temperature and the oligonucleotides were purified by biospin column. 1 μl of the mixture was taken for counting. The labelled oligonucleotides were dissolved to 20.000 cpm/μl by distilled water. A working stock of 20.000 cpm/μl labelled oligonucleotide was used for all EMSA experiments. The binding reaction was then performed using 5 μg of GST-MeCP2 protein in a volume of 20 μl reaction buffer (10 mM Tris-HCl pH 8, 3 mM MgCl$_2$, 66 mM KCl, 100 μg/ml BSA, 12% glycerol, 1 μg/μl of dI/dC, 1 mM DTT). This was incubated on ice for 5 minutes and then 20,000 cpm of labelled oligonucleotide was added and the whole reaction was incubated for a further 25 minutes at room temperature. 3 μl of 6×DNA loading dye was added and the samples were loaded on a 5% polyacrylamide gel (non denaturating). The gel, which was pre-run for 30 minutes (4°C; 150V; 0.5x TBE) was run with the samples at 100V for around 1 hour at 4°C. Hereafter, the gel was dried and subjected to autoradiography overnight.

2.2.6.4   Western blots

Transfected or non-transfected AtT20 and LLC-PK1 cells were used for western blots. Cells were seeded in 10 cm or 6-well plates 24 hours before harvesting. The cells were first washed twice with cold 1−5 ml 1x PBS. Then cells were scrapped in 0.2 to 0.5 ml TE buffer with protease inhibitor cocktail (1/100) and phosphatase inhibitor cocktail (1/100). The cells were disrupted by ultrasonification for 3 minutes (30-second interval) in an ice bath. An aliquot of 3 μl was kept at this step for measuring protein concentration by Bradford. The remaining cell lysates were added 4x Laemmli buffer (200 mM Tris-HCl pH 6.8, 8% SDS, 40% glycerol, 0.4% Bromophenol blue, 0.1% β-mercaptoethanol) according to the volume. The cells were heated to 95 °C in a heatblock for 5 minutes to denature proteins. All the samples were kept in the -20 °C freezer ready to use. An 8% SDS-PAGE gel was prepared. 50 μg of whole cell extract (WCE) was loaded to each well. The SDS-PAGE gel was run at 120 V in the cold room with a water flow for cooling. When the 35 kD pre-stained

maker reached the bottom of the gel, the proteins were transferred to a nitrocellulose membrane in a transfer chamber at 50 V for 2 hours in the cold room. The membrane was briefly stained with Ponceau red to check if the proteins had transferred from the gel to the membrane. Unspecific binding of the antibodies to the membrane was blocked by placing the membrane in blocking buffer (10 mM Tris, 0.5 M NaCl, 0.1% Tween, 5% BSA, pH 7.6) which was incubated on a shaker at room temperature for 1 hour. The blocking solution was poured off and the membranes incubated with the primary antibody in a shaker over night at 4 °C. Membranes were then washed 5 minutes three times with TBST (0.1 % Tween-20) to remove unbound antibody and then incubated for 1 hour at RT with the second conjugated antibody. The membranes were washed as before. A 1:1 mixture of the chemiluminescent reagent was prepared and added to the membrane for 2 minutes. Then the membrane was dried slightly and wrapped in saran wrap. The first film was exposed for 30 second to check signal appearance and then exposure time was adjusted to the strength of the signals.

2.2.6.5   Protein de-phosphorylation

De-phosphorylation was performed to demonstrate the specificity of the phospho-438 MeCP2 antibody. For an antibody that only binds its phospho-site when the protein is denatured, treating the membrane with phosphatase post-transfer is preferable to treat the non-denatured lysate. After SDS-PAGE gel electrophoresis, the proteins were transferred to a nitrocellulose membrane which had been blocked by pretreatment with 5% BSA in TBS with 0.1% Triton X-100 for one hour at room temperature. The membrane was cut to obtain a slot containing at least one sample duplicated in the other piece. The two pieces of membrane were placed in separate containers with 3−5 ml CIP buffer inside. The CIP enzyme was added to the container with the piece to be de-phosphorylated. After incubation at 37°C for one hour, the samples were subjected to the standard western blot procedure.

2.2.6.6   Immunohistochemistry

Pituitary slides, primary pituitary or AtT20 cells were fixed with 4% paraformaldehyde in phosphate-buffered saline (PBS) for 5 minutes. Coverslips were washed with PBS for 5 minutes, and then blocked for 2 hours with blocking solution (50 mg/ml BSA, 50 mg/ml goat serum, 0.5% Triton X-100, 50 mM Tris-HCl, 50 mM

NaCl and pH7.4). Coverslips were incubated with the following primary antibodies diluted in blocking solution overnight in a humidifying chamber at 4°C: total MeCP2 (1:400); pS438-MeCP2 (1:400), CaMKII (1:500), pCaMKII (1:500) and ACTH (1:400). Coverslips were washed three times with PBS for 10 minutes. Secondary antibodies were diluted in blocking solution, and incubations were performed at room temperature for 2 hours. Coverslips were washed with PBS three times for 10 minutes then DAPI was added at 1:6000 in PBS for 5 minutes. After washing with PBS three times for 10 minutes, the coverslips were mounted.

2.2.7 Statistical analysis and computer software

CpG island analyses was performed using the online program CpG Plot (http://www.ebi.ac.uk/Tools/emboss/cpgplot/) and EMBOSS (Rice et al., 2000). The heatmap was generated using the online free software Heatmap Builder. Primers were designed according to the general guidelines by the software Oligo 6. For pituitary corticotrope cell counting, the total cell number was counted automatically by the software of Cell C; and the corticotrope cell number was counted manually using the software Image J. Graphs were drawn by the software Sigma Plot and Microsoft Excel. All statistical analyses were performed by Microsoft Excel. All figures were designed through CoralDraw software version 10 (Corel Corporation, Ottawa).

3 Results

3.1 Biometric data

3.1.1 Experimental design

We carried out maternal separation (MS) to model early life stress. This maternal separation model is based on the fact that in the wild field, the dam will leave the nest ranging from 15 minutes to 3 hours for foraging. The higher rank of the mother, the less time she will spend. During her absence, it is very stressful for the litters. It is also suggested that the first 10 days of life is a critical time window for mouse development. This traumatic event early in life can lead to severe consequences at later stage when they reach adulthood.
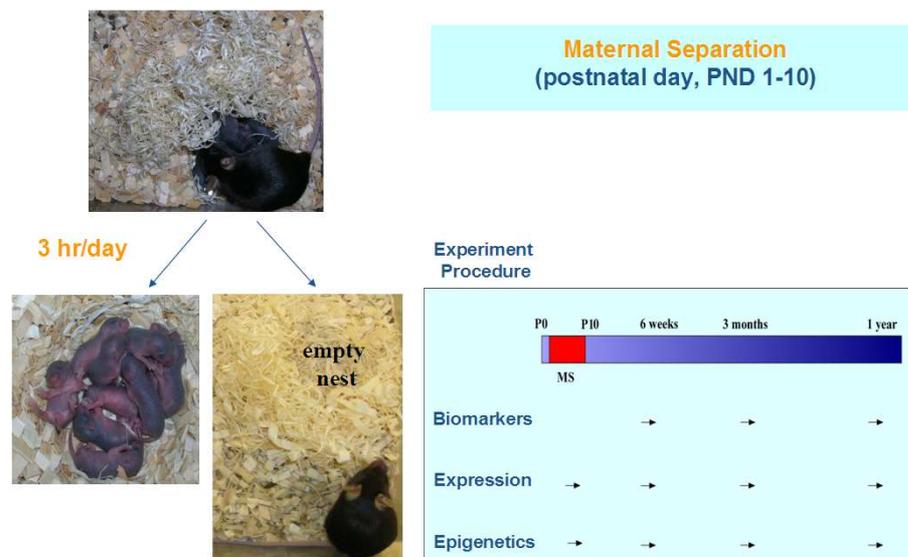
Figure 7. Maternal separation model and experimental design.

The procedure of maternal separation is as following: the new born mice were separated 3 hours daily from their mother from postnatal day 1 to day 10. After P10, all the mice lived with their mother. In this experiment, 4 time-points were investigated: P10, 6 weeks, 3 months and 1 year. Both male and female mice were used for biometric, neuroendocrine, gene expression and DNA methylation analysis. Male mice were used for the behavioral tests and the investigation of molecular mechanisms.

3.1.2 Behavioral analysis of adult offspring

To assess long-term alterations in behavior due to early life stress exposure, we performed a series of behavioral tests. Only male mice were used in the experiments, and these data had been published previously (Murgatroyd et al., 2009). In summary, early life stress (ELS) produced long-lasting behavioral changes for the following criteria. First, adult ELS mice (6-week-old) showed memory deficits in an inhibitory avoidance task. Second, ELS mice had increased immobility in the force swim test. In contrast, anxiety-like behavior was unaffected by early life stress in the elevated plus-maze, novelty-induced hypophagia and light-dark avoidance test.

3.1.3 Biometric data

3.1.3.1   Body weight

There were no significant body weight differences ($p > 0.05$, t-test) between ELS and control mice through all timepoints (6 weeks, 3 months and 1 year) in both sexes (Figure 8). These data supported the idea that ELS is a psychological stressor rather than a physical intervention such as sickness or famine.
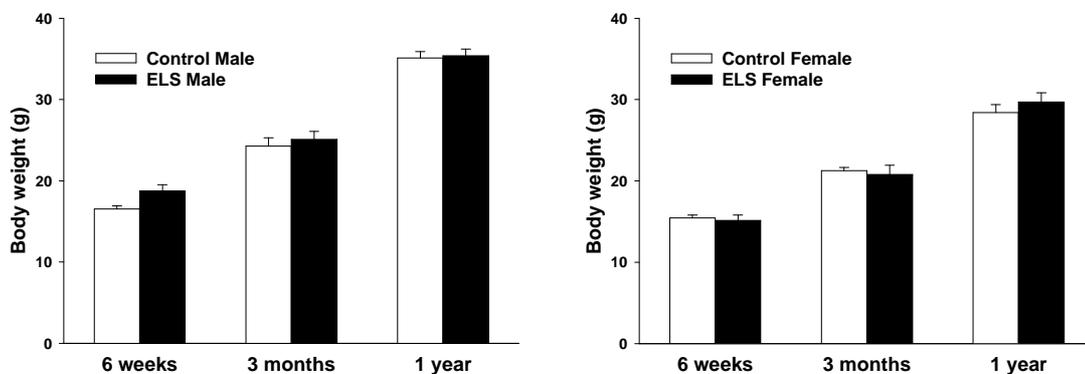
Figure 8. Mouse body weight after early life stress. There is no difference in body weight between control and early life stress (ELS) mice at all ages in both sxes. Data are mean ± S.E.M (n=8−10/group).

3.1.3.2   Thymus weight

Thymus glands of control and ELS mice were dissected and weighed at each timepoint. The relative weight (mg/100g BW) of the thymus in ELS mice was significantly lower ($p < 0.05$, t-test) than controls (Figure 9), which is in according

with the fact that ELS mice had higher levels of corticosterone (Figure 11) in the plasma.
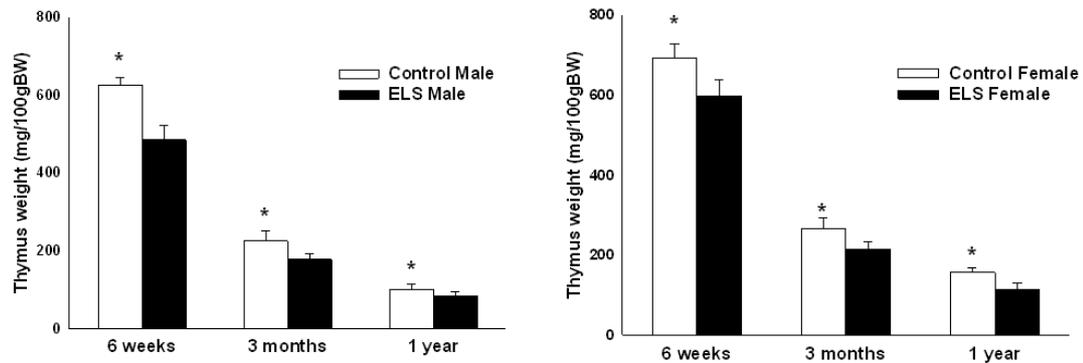
Figure 9. Reduced thymus weight after early life stress. As compared with controls, early life stress mice showed involution of thymus weight at all ages in both genders, indicative of higher levels of corticosterone (Cort) in the blood. Data are mean ± S.E.M (n=8-10/group). *p<0.05 (t-test).

3.1.3.3   Adrenal weight

Adrenal glands from male and female mice were also dissected and weighed. The relative weight of adrenal gland (mg/100g BW) was significantly higher in the ELS group than the controls (p < 0.05, t-test) in both genders (Figure 10). Furthermore, adrenals weighed significantly less in males than females irrespective of rearing condition. Previous study demonstrated that adrenal gland growth and function is under the control of pituitary derived ACTH. The hypertrophy of the adrenals in the ELS group predicted a hyper-secretion of ACTH compared with control mice.
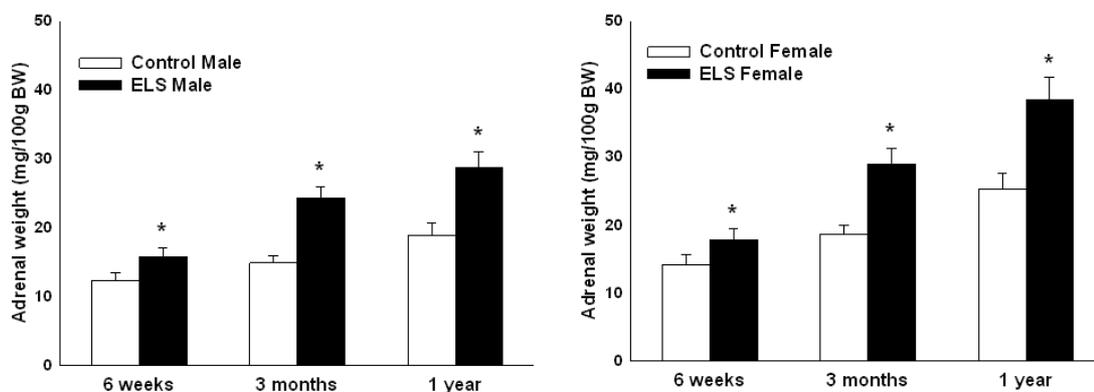
Figure 10. Increased adrenal weight after early life stress. As compared with controls, early life stress mice showed larger adrenals at all ages in both genders, predicting higher level of adrenalcorticoal (ACTH) in the blood. Data are mean ± S.E.M (n=8−10/group). *p < 0.05 (t-test).

3.1.4 Plasma corticosterone (Cort) levels

Basal evening and morning plasma corticosterone levels were measured. In both conditions, plasma corticosterone concentrations were higher in ELS mice compared with controls in both genders. Female animals had a higher overall concentration of corticosterone than males (Figure 11).
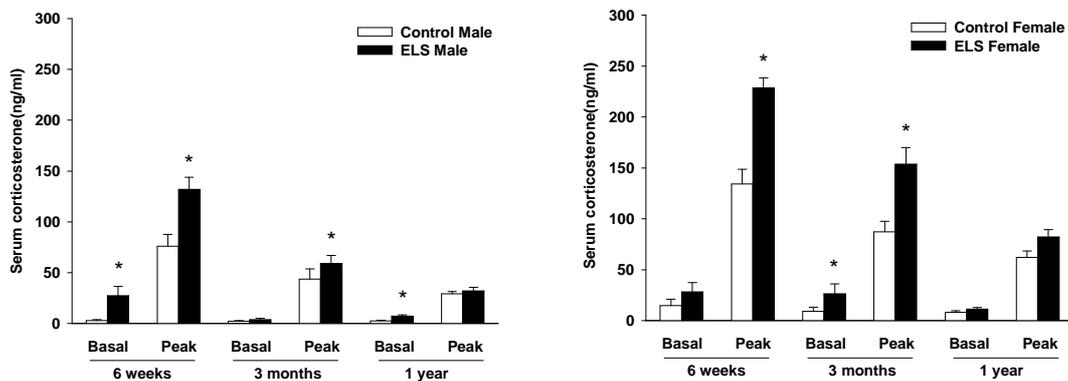
Figure 11. Increased serum levels of corticosterone (Cort) after early life stress. ELS mice at 6 week, 3 month and 1 year time points presented with increased serum corticosterone levels under peak and basal conditions. Data are mean ± S.E.M (n=8−10/group). *p < 0.05 (t-test).

3.1.5 *Pomc* mRNA expression

Basal Pomc mRNA expression in mouse pituitary was measured by quantitive real time PCR (q-PCR). As shown in Figure 12, ELS mice produced a significant increase of *Pomc* mRNA level in the pituitary compared with controls from 10 days old mice up to 1 year. To facilitate comparation of relative mRNA level between different timepoints and between genders, cDNA from mouse pituitary AtT20 cells was used as the general standard throughout the experiments. As shown in Figure 12, basal Pomc mRNA expression slightly increased with age irrespective of gender. Furthermore, when compared the *Pomc* mRNA levels between genders, baseline Pomc mRNA expression in females was significantly higher than in males.
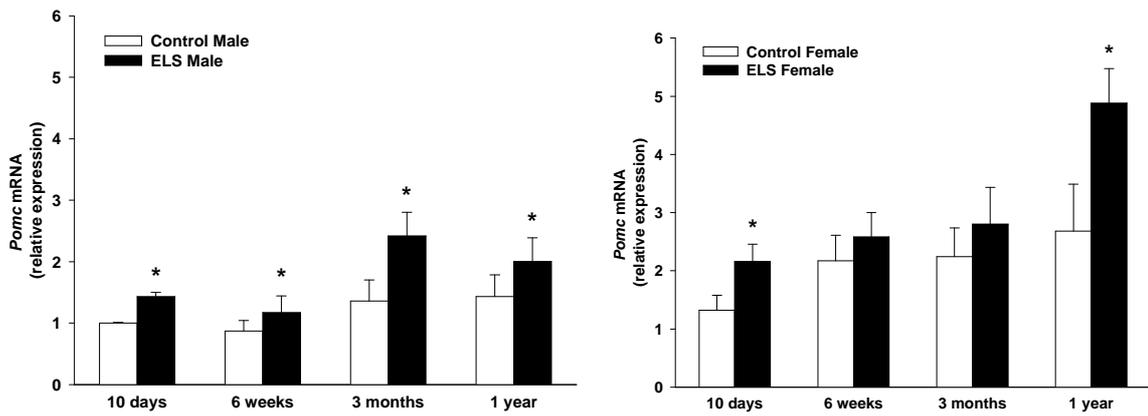
Figure 12. *Pomc* mRNA level after early life stress. Pomc mRNA was significantly higher in the pituitaries of ELS mice at all time points both in male (left) and female (right) animals as determined by qPCR analysis. Data are mean ± S.E.M (n = 8−10/group). *p < 0.05 (t-test).

Pomc mRNA is expressed both in the anterior lobe and intermediate lobe of the pituitary, but processed differently by cell type specific enzyme usage. To address the question whether *Pomc* mRNA expression could be altered due to early life stress exposure in the intermediate lobe, we dissected the intermediate lobe (6-week-old) from the anterior pituitary and tested the *Pomc* mRNA levels from anterior lobe and intermediate lobe separately by real-time PCR. The results showed that early life stress resulted in upregulation of *Pomc* mRNA in the anterior pituitary. On the contrary, early life stress did not influence *Pomc* mRNA in the intermediate lobe (Figure 13).
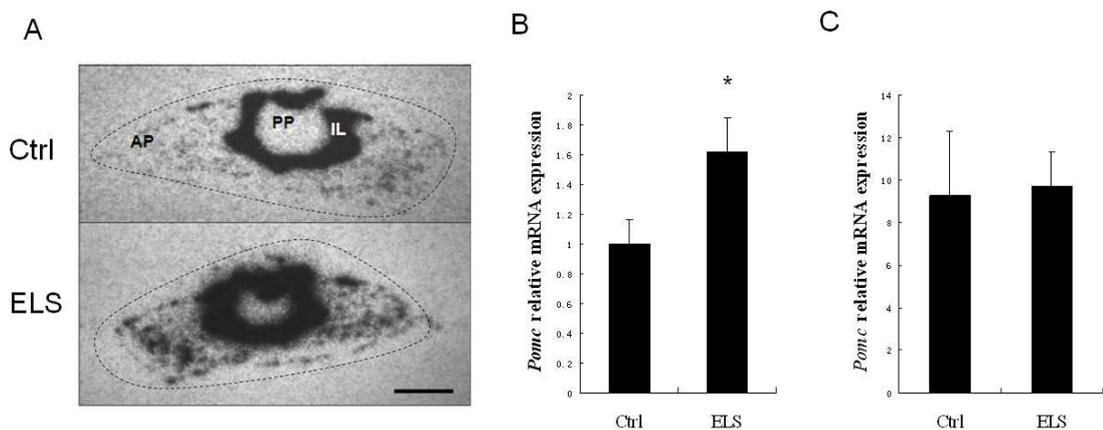
Figure 13. Early life stress produced increased level of *Pomc* mRNA in the anterior pituitary. (A) Representative bright-field autoradiographs of pituitary sections (6-week-old males) hybridized with a ^{35}S-labeled oligonucleotide probe complementary to *Pomc* mRNA from a Ctrl (upper) or ELS (lower) mouse. AP, anterior pituitary; IL, intermediate lobe; PP, posterior pituitary. Scale bar, 500 µm. In situ hybridization showed that *Pomc* expression is much higher in ELS mice. (B) *Pomc* mRNA expression was significantly higher in ELS than controls in the mouse anterior pituitary (6-week-old males). (C) ELS did not influence *Pomc* mRNA expression in the intermediate pituitary. Data are mean ± S.E.M (n = 8−10/group). *p < 0.05 (t-test).

3.1.6 Serum ACTH level and AVP-CRH challenge test

ACTH, which is cleavaged enzymatically from POMC in the antior pituitary, was also measured in the blood of 6-week-old mice. Consistent with the *Pomc* expression patterns in the pituitary, blood ACTH levels were also higher in ELS mice than controls in both genders. Early life stress also increased sensitivity of the pituitary-adrenal axis to the hypothalamic secretagogues CRH and AVP in both genders. When the mice were treated with AVP and CRH peptides, the early life stress (ELS) group mice displayed much higher responsiveness compared with control mice (Figure 14).
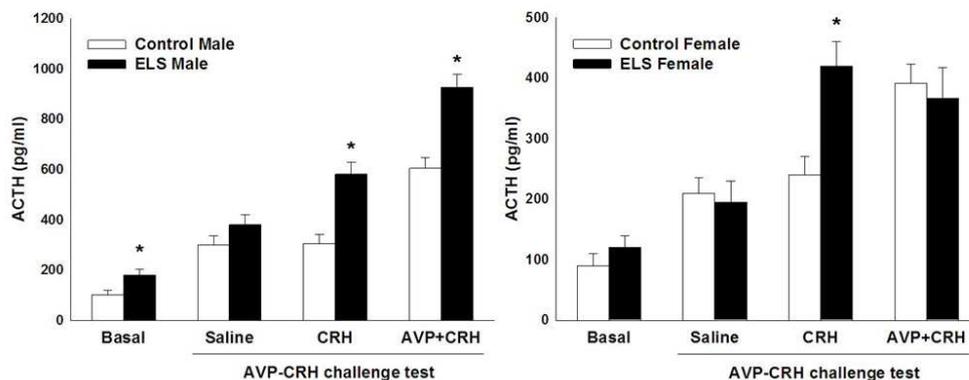
Figure 14. Early life stress increased sensitivity of the pituitary-adrenal axis to CRH and AVP in both genders. Under basal conditions, blood ACTH levels were higher in ELS mice (6-week-old) in both genders. ELS mice displayed much higher responsiveness compared with control mice after AVP and CRH application. Data are mean ± S.E.M (n = 8−10/group). $^{*}p < 0.05$ (t-test).

3.2 *Pomc* DNA methylation status

3.2.1 DNA methylation at the *Pomc* gene locus in naïve mice

Here, we used the in-bred mouse strain C57BL/6N. All mice were housed under the same condition. The only difference between control mice and ELS mice came from the maternal separation procedure. External stimulations can change the phenotypes later in life; we hypothesized that epigenetic processes could be responsible for this fact. DNA methylation is a stable epigenetic mark at CpG dinucleotides, which often couples to lasting changes in gene transcription. Methylation of cytosine residues

within CpG dinucleotides can result in gene silencing; such CpGs are conspicuously under-represented in mammalian genomes and typically cluster with GC-rich regions called CpG islands (CGI). In the case of *Pomc* gene, computational analysis (CpGPlot, EMBOSS) and previous literature (Gardiner-Garden and Frommer, 1994) revealed 2 CpG islands within mouse *Pomc* gene locus: CpG island 1 (CGI 1) which surrounds the *Pomc* transcription start site and CpG island 2 (CGI 2) which lies approximately 5 kb downstream, encompassing the third exon of *Pomc* gene.
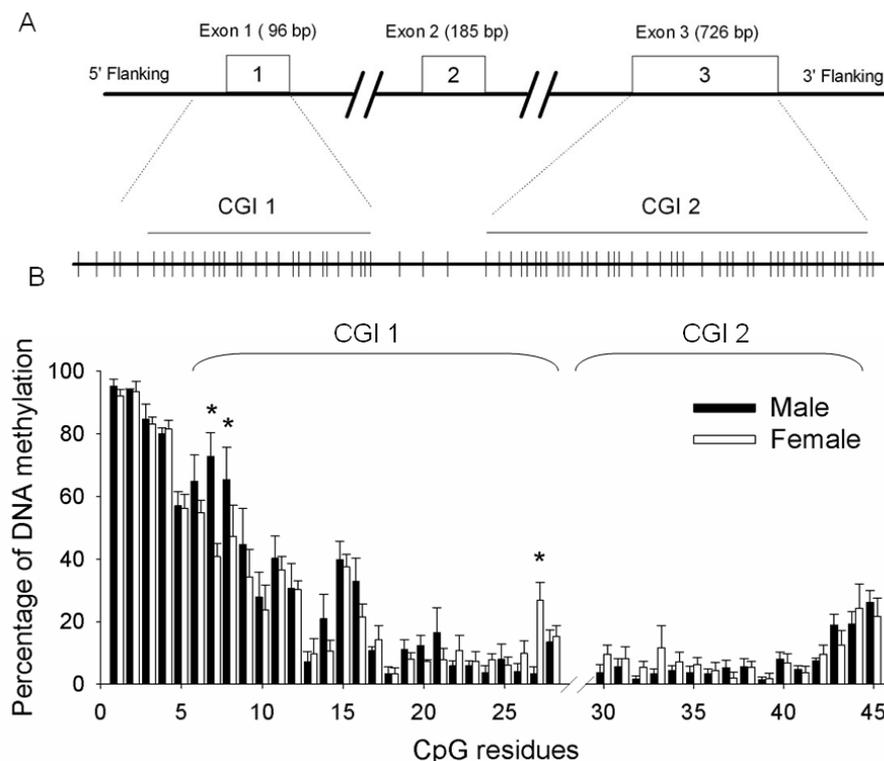
Figure 15. DNA methylation status at the *Pomc* gene locus. (A). Schematic diagram of the mouse *Pomc* gene. Exons are indicated by open (numbered) boxes and CGIs by numbered bars, and the distribution of CpG residues are listed according to their position. (B). Sequence analysis of bisulfite-converted DNA isolated from the pituitaries of naive C57/BL6 mice (3-month-old) showed sparse methylation in the core promoter (CGI 1) and the coding region (CGI2). In contrast, high levels of CpG methylation were found at the far distal promoter region of the *Pomc* gene. Comparing the DNA methylation level between male and female revealed that males show higher level of DNA methylation than females. Data are mean ± S.E.M (n=8-10/group). *p < 0.05 (t-test).

To investigate the DNA methylation status at the *Pomc* gene locus, sodium bisulfite conversion was performed with genomic DNA isolated from pituitaries. Four pairs of primers were designed to cover the entire CGI 1 and part of CGI 2 (Figure 15). Sodium bisulfite treatment of DNA samples converts non-methylated cytosines (C) to uracils (U), which are then replaced by thymidine (T) in the subsequent PCR

reactions. Methylated cytosines (mC) are unaffected by sodium bisulfite reaction and the differences in methylation status are thus apparent and easily detected on sequence reads.

The pituitary was dissected away from the brain, and genomic DNA was isolated and treated with sodium bisulfite. Sequence analysis of bisulfite-converted DNA isolated from the pituitaries of naive C57BL/6N mice (3 months old) showed sparse methylation in the core promoter CGI 1 and the coding region CGI 2. In contrast, we found high levels of CpG methylation clustered at the far distal promoter region of *Pomc* encompassing CpG1 to CpG16 (Figure 15); this region has been shown in the previous literature to play a critical role in *Pomc* gene regulation. When DNA methylation was compared between genders, male mice showed higher levels of DNA methylation than females at the *Pomc* distal promoter region (Figure 15 and Figure 16).

3.2.2 Early life stress dependent DNA methylation

As shown in the previous chapter (Figure 12), ELS induced higher levels of *Pomc* mRNA in the pituitary; therefore we wondered whether DNA methylation might play a role in regulating *Pomc* gene expression during early life adverse events. Bisufite sequencing was performed between ELS and control mice aged 10 days, 6 weeks, 3 months and 1 year in both genders. The results showed that no differential DNA methylation was observed at all time points either in the coding region, which is confined as CGI 2 (CpG 30-45), or in the core promoter region (CpG 17-28) as well as in the 5' UTR (CpG 1-5). By contrast, ELS induced hypomethylation at the *Pomc* distal promoter region ranging from CpG 6 to CpG 16. To facilitate the comparison of DNA methylation through age and between genders, heatmaps were deduced to illustrate the DNA methylation status. DNA methylation levels were transformed into graded-color, ranging from 0% of methylation (yellow) to 100% of methylation (red). In these heatmaps, the x-axis represents a single CpG residue from CpG 6 to CpG 16 at the *Pomc* distal promoter region, and every single row stands for a single mouse subjected to bisulfite mapping.

The heatmap showed that early life stress produced a significant decline of DNA methylation through the *Pomc* distal promoter in ELS mice aged 10 days, 6-week, 3 months, and 1 year in both genders. Importantly, this region has been shown to be a

critical area both for pituitary specific *Pomc* gene expression and *Pomc* activation from upstream secretagogues, such as CRH and AVP. Overall, these findings revealed that ELS triggered a heterogeneous response in CpG hypomethylation and indicated a functional role for the detected changes.

In addition, examination of the methylation status of all CpGs found within the *Pomc* promoter of naïve mice revealed a general decline in methylation in 1-year aged mice compared with 6-week aged animals, with 30% of all CpG residues showing a significant decline (Figure 16B). Correspondingly, increased levels of *Pomc* mRNA expression was observed in 1 year old naïve mice compared with 6 weeks animals (Figure 12), indicating that age-associated DNA hypomethylation might contribute to the elevated *Pomc* mRNA expression. However, in contrast to males, females did not show any age-associated drift in DNA methylation (Figure 16D).
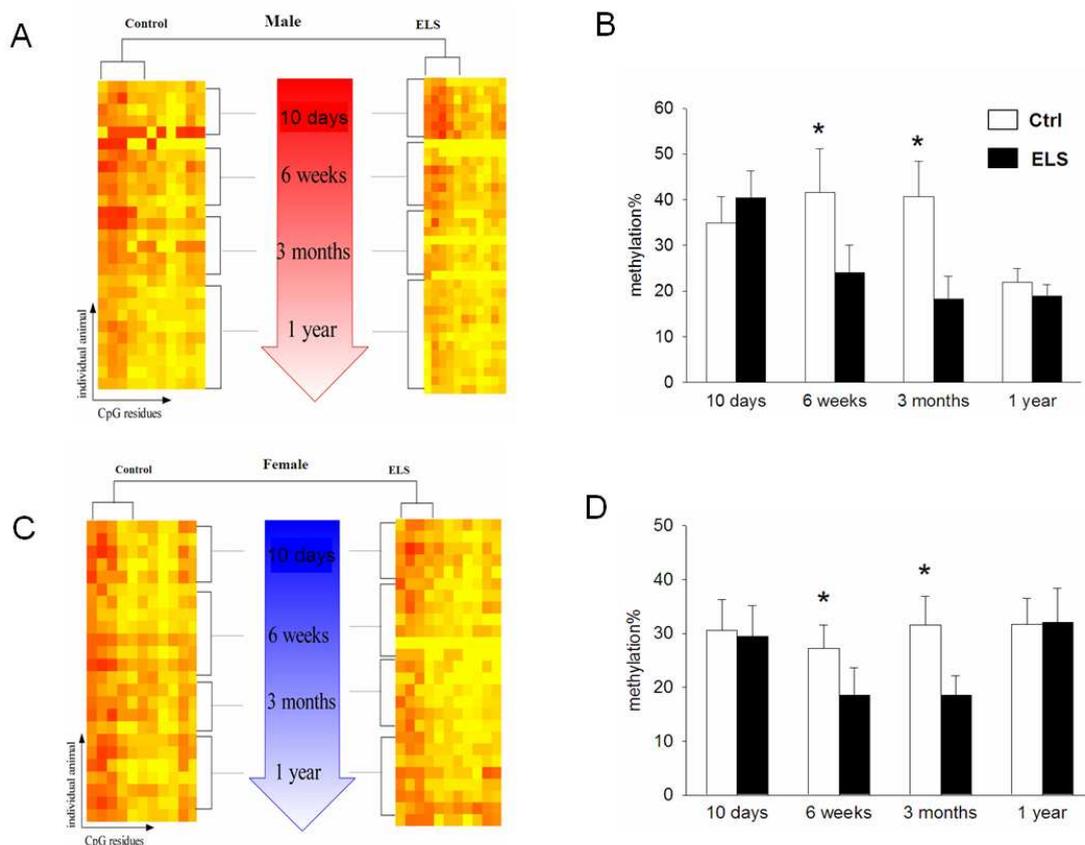
Figure 16. Early life stress induced hypomethylation at the *Pomc* distal promoter region. (A and C). Comparison of the DNA methylation status from ELS and control mice aged 10 days, 6 weeks, 3 months and 1 year, the results showed hypomethylation of multiple CpG residues throughout the far distal promoter region in ELS mice both in males (A) and females (C). (B). Analysis of overall methylation of the distal promoter revealed age-related substantial reductions in methylation. (D) Overall DNA methylation of female control mice did not show any age-associated drift. *p < 0.05 (t-test)

3.2.3 *Pomc* DNA methylation in different tissues

The DNA methylation status at the *Pomc* distal promoter ranging from CpG 6 to CpG 16 from different tissues was studied by bisulfite mapping. As shown in Figure 17, the *Pomc* gene showed a tissue-specific DNA methylation pattern. In normal non-expressing tissues, such as adrenal, kidney, spleen, thymus, hippocampus and the non-expressing cell line Neuro2A (data not shown), the *Pomc* distal promoter was hyper-methylated. In contrast, *Pomc* gene had relatively less methylation in the pituitary. Furthermore, in the corticotrope cell line AtT20 in which *Pomc* was highly expressed, the promoter region was free of DNA methylation.
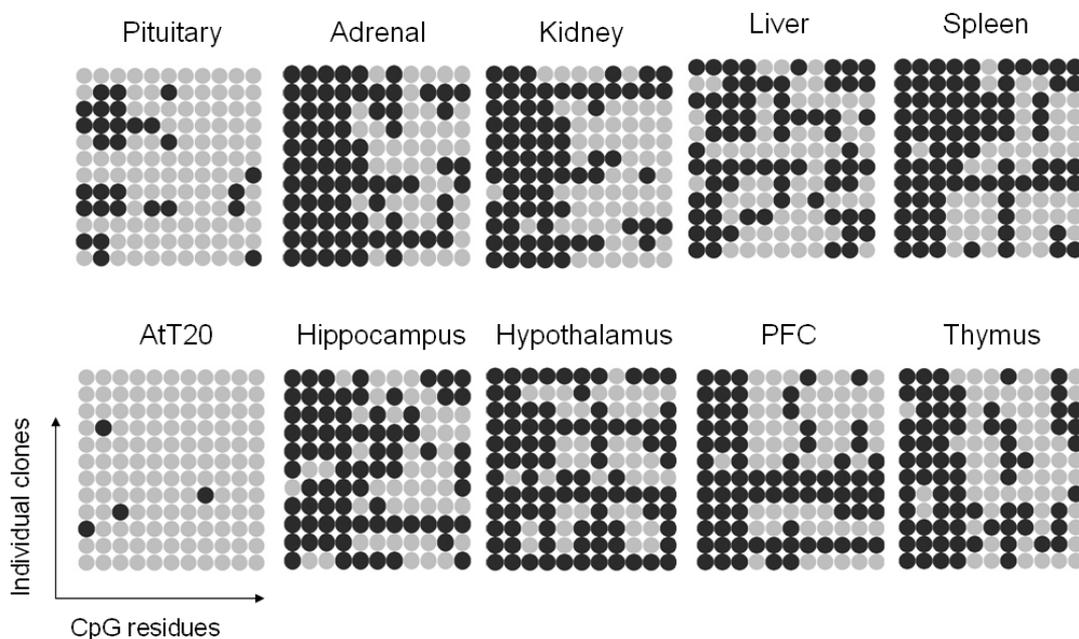
Figure 17. *Pomc* DNA methylation status in different tissues. Bisulfite sequencing analysis using DNA from different mouse tissues (6-week-old) including pituitary, hypothalamus, hippocampus, prefrontal cortex (PFC), adrenal gland, kidney, liver, spleen and thymus revealed a tissue-specific DNA methylation pattern. In normal *Pomc* non-expressing tissues such as kidney, thymus and adrenal, *Pomc* was hyermethylated at the distal promoter, especially at the region ranging from CpG6 to CpG8.

3.2.4 DNA methylation of *Pomc* pseudogene

In the early stage of our research, we found that the DNA methylation pattern in exon 3 (CGI 2) always displayed an all-or-nothing pattern. In short, if one CpG residue was unmethylated in the clone, all the CpGs were totally free of methylation. In contrast however, if one CpG residue was methylated, all the CpGs in the clone were fully

methylated. Careful sequence analysis detected however slight difference in DNA sequence between the two classes of clones. A sequence blast was performed, and we found that the fully methylated sequence belonged to the *Pomc* pseudogene (also known as *Pomc*2 or *Pomc*-ps1) which locates to chromosome 19 in the mouse genome. Sequence alignment between *Pomc* and its pseudogene was performed and the results showed that this non-transcribed *Pomc* pseudogene was a homology of *Pomc* exon 3 with an identity of 90% (data not shown).

3.3 DNA methylation controls *Pomc* gene expression

Given the role of DNA methylation in controlling gene expression, we next examined whether methylation alone is sufficient to repress *Pomc* gene activity. Bisulfite sequencing results showed differential DNA methylation pattern between ELS and controls at the *Pomc* distal promoter, especially in the region ranging from CpG 6 to CpG 8. *Pomc* reporter constructs with methylated or unmethylated CpGs were transfected into the AtT20 mouse pituitary cell line. In this experiment, selectively methylated CpG 6-8 induced a 43% reduction of *Pomc* promoter activity, while deletion of this region diminished reporter activity by 68% (Figure 18B). These results demonstrated the functional importance of this region for regulation of *Pomc* gene expression. We also examined *Pomc* reporter activity after *in vitro* methylation of the entire promoter, including the core promoter and the distal promoter. Such methylation completely abolished luciferase activity. Taken together, these findings suggested that DNA methylation at CpG 6-8 is critical for controlling *Pomc* gene expression. Bisulfite sequencing proved the success of site-directed DNA methylation (Figure 18C).
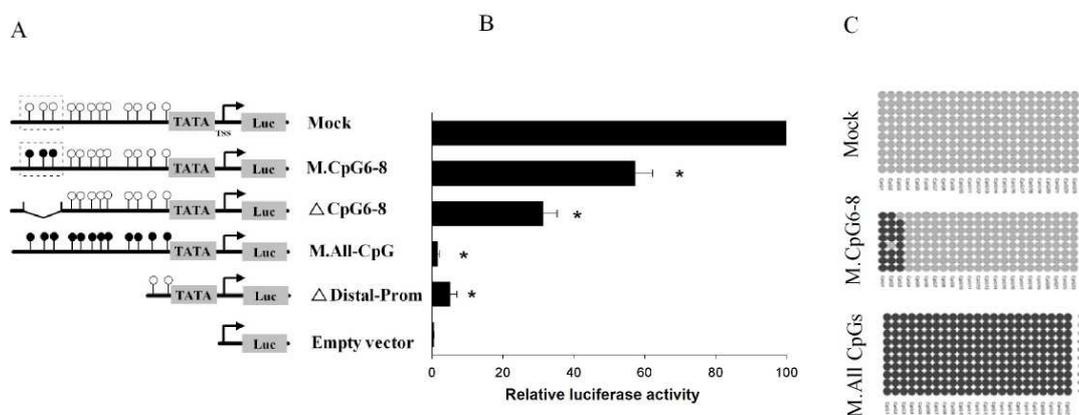
Figure 18. DNA methylation controls *Pomc* gene expression. (A) Schematic representation of *Pomc* luciferase constructs. The parental *Pomc*-Luc construct (mock) contains the entire mouse *Pomc* promoter. M.CpG6-8 indicates that only CpG 6-8 were *in vitro* methylated by site-directed DNA methylation using a CpG-free vector. ΔCpG 6-8 is devoid of CpG 6 to 8. M.All-CpG indicates that all the CpGs in the *Pomc* promoter were completely methylated by CpG methylase SssI. ΔDistal-Prom lacks the entire distal promoter. (B) Entire vector or site-specific promoter (CpG 6-8) methylation reduced reporter activity by 99% and 40%, respectively. Deletion of either CpGs 6-8 or the entire distal promoter reduced reporter activity by 68% and 90%, respectively, in AtT20 cells. (C) Bisulfite sequencing confirmed the success of site-directed DNA methylation. Data are mean ± SD, three independent experiments were performed. *p < 0.05 (t-test).

Hypothalamic derived peptides corticotrophin-releasing-hormone (CRH) and arginine vasopressin (AVP) stimulate transcription of *Pomc* and secretion of ACTH *in vivo* and in ACTH producing pituitary tumor AtT20 cells. Previous studies showed the importance of the distal promoter for the regulation of *Pomc* activity after CRH and AVP stimulation. In our study, we questioned whether DNA methylation in the *Pomc* distal promoter could affect AVP and CRH-dependent stimulation of *Pomc* expression. From the literature (Ventura et al., 1999) and our RT-PCR experiment, we know that AVP v1b receptor expression is barely detectable in normal AtT20 cells. To overcome this problem, a new AtT20 cell line with v1b receptor stably expressed was used. In this cell line, the mouse AVP v1b receptor gene was intergrated into the mouse genome resulting in stable expression of the mouse v1b receptor. Methylated and unmethylated *Pomc* reporter were transfected into AtT20 cells (AVP v1bR), 24 hours after transfection, the cells were treated with the peptides AVP (10^{-7} M), CRH (10^{-8} M) or both. After 2 hours of treatment, luciferase activity was measured. According to the results in Figure 19, if the reporter is unmethylated, the *Pomc* promoter activity was increased by 38%, 22% and 67% respectively upon CRH, AVP or CRH+AVP treatment in the cultured cells compared with the non-treated control. However, if the *Pomc* reporter was methylated at CpG 6-8, CRH treatment alone failed to activate *Pomc* expression. On the contrary, AVP treatment alone can still increase the *Pomc* mRNA expression by 22% when compared with the non-treated control. A synergic effect of *Pomc* promoter activation (31% increases) was also observed when the methylated reporter was treated with both AVP and CRH. Taken together, DNA methylation plays a critical role in the regulation of *Pomc* gene expression both under basal condition and activated conditions.
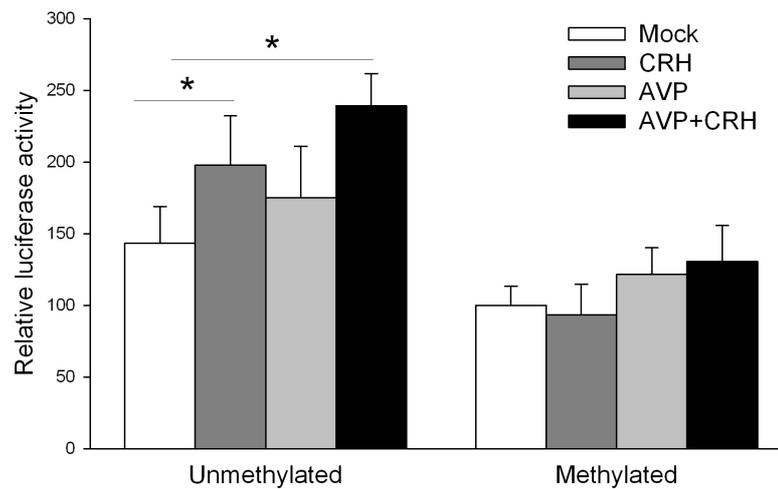
Figure 19. DNA methylation at CpGs 6-8 strongly blocked *Pomc* activation stimulated by CRH, but not by AVP. AVP (10^{-7} M) and CRH (10^{-8} M) activated *Pomc* promoter activity when the *Pomc* reporter was free of DNA methylation. If the *Pomc* reported was site-directed methylated at CpG 6-8, CRH treatment alone failed to stimulate *Pomc* mRNA expression. In contrast, AVP or AVP+CRH treatment increased *Pomc* luciferase activity compared with non-treated control. Values represent mean ± S.D. Three independent experiments were performed. The asterisks indicate significant difference. (*, $P<0.05$)

3.4 MeCP2 binds to the *Pomc* promoter and represses gene activity

3.4.1 MeCP2 represses *Pomc* gene expression

In our previous results (Figure 18), we proved that DNA methylation could repress *Pomc* gene expression. The next question was, by which mechanism does DNA methylation repress *Pomc* gene expression? It is generally accepted that DNA methylation at CpG dinucleotides (^{m}CG) is interpreted by a family of methyl CpG-binding domain (MBD) proteins. These epigenetic readers (except MBD4) can serve as an epigenetic platform. Histone deacetylases (HDACs) and DNA methyltransferases (DNMTs) can be recruited to confer transcriptional repression and gene silencing. After cotransfecting a series of MBD family proteins with the methylated reporter plasmid into AtT20 cells, we found that MBD1, MBD2 and MBD3 have moderate effects on DNA methylation-directed *Pomc* repression. In

contrast, we found that the founding member of MBD family protein, MeCP2, significantly suppressed *Pomc* gene activity (Figure 20A).
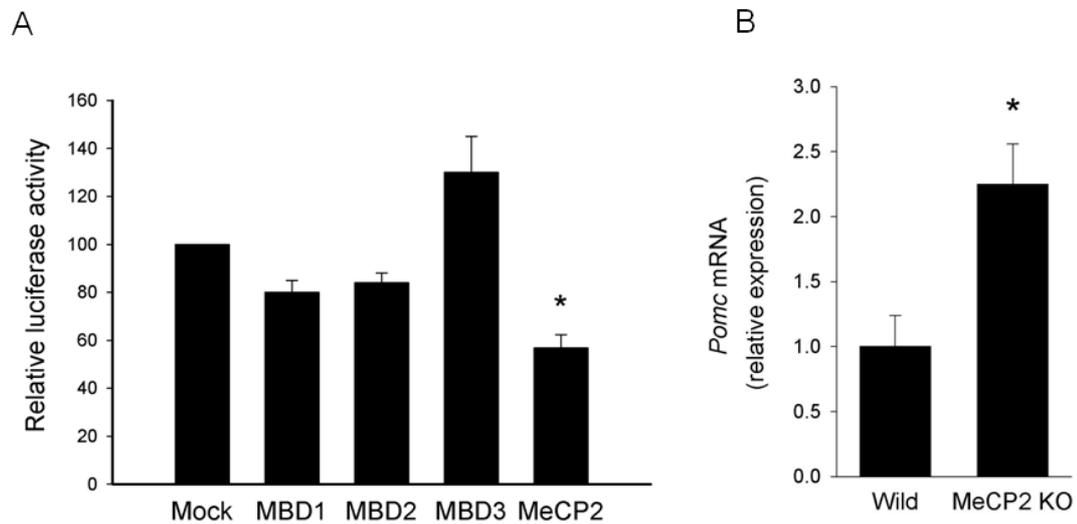
Figure 20. MeCP2 strongly represses *Pomc* gene expression *in vitro* and *in vivo*. (A) After cotransfecting a series of MBD proteins with methylated reporter plasmid into AtT20 cells, we found that MeCP2 significantly suppressed *Pomc* gene activity, while MBD1, MBD2 and MBD3 had moderate effect. (B) *Pomc* mRNA level between wild type and MeCP2 KO was tested by qRT-PCR. The results showed a two-fold increase of *Pomc* mRNA levels in MeCP2 KO mouse pituitary compared with controls.

Since these experiments were done under over-expression, we were interested to know whether MeCP2 is expressed in pituitary cells. RT-PCR, western blot and immunohistochemistry results revealed the presence of MeCP2 in pituitary cells (Figure 21A). To examine the repressive role of MeCP2 *in vivo*, pituitaries from MeCP2 knockout mice were subjected to gene expression analysis. The results confirmed the repressor role of MeCP2 for *Pomc* expression as evidenced by over 2-fold increased mRNA levels compared with wild type mice (Figure 20B).
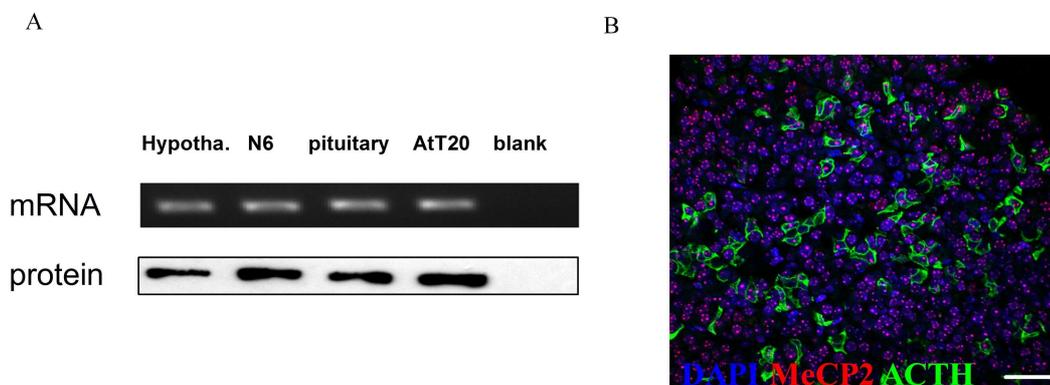
Figure 21. MeCP2 is expressed in pituitary cells. (A) RT-PCR and western blot results showed that MeCP2 is expressed in mouse pituitary and the pituitary cell line-AtT20 both at the mRNA

and protein levels. Mouse hypothalamic tissue and the hypothalamic cell line N6 were used as positive controls. (B) MeCP2 is strongly expressed in the cell nuclei of the mouse pituitary and colocalizes with ACTH-positive cells. Scale bar, 50 μm.

To further investigate the distribution of MeCP2 in the mouse pituitary, immunohistochemistry experiments were performed using antibodies against total MeCP2 (red) and ACTH (green) in naïve mouse pituitary slides. The results in Figure 21B showed that MeCP2 is ubiquitously expressed in the cell nuclei of the mouse pituitary and colocalized with ACTH positive cells.

3.4.2 MeCP2 binds to the *Pomc* promoter *in vitro*

To investigate whether MeCP2 can be directly bound to the *Pomc* promoter, electrophoretic mobility shift assay (EMSA) experiments were performed using recombinant GST-MeCP2 protein. According to previous reports, MeCP2 DNA binding depends on two criteria: firstly, MeCP2 preferentially binds to methyl-CpG sites and secondly, binding is increased in case A/T bases ([A/T$\geq$4]) are present adjacent to methyl-CpG. The sequence [A/T$\geq$4] was found previously to be essential for high-affinity binding at selected sites and at known MeCP2 target regions such as in the *Bdnf* and *Dlx6* genes. Based on these MeCP2 binding criteria, *Pomc* DNA sequences of far upstream 5' UTR, promoter (CGI 1) and exon3 (CGI 2) were analyzed. The results revealed that only the DNA sequence in the distal promoter fulfilled the two criteria for MeCP2 binding. The far upstream promoter failed the test because of the very low density of CpG sites in that region. In contrast, exon3 behaved differently. Although there were plenty of CpG sites (CGI 2), A/T ([A/T$\geq$4]) runs were rarely found adjacent to methyl-CpG. Three pairs of oligonucleotides were designed for the EMSA experiments. Oligonucleotide EMSA1 was located in the distal promoter which contained CpG 6 together with 3 A/T runs adjacent to CpG 6. EMSA2 was located next to EMSA1 which covered CpG 7 and CpG 8. As a negative control, we also designed a pair of oligonucleotides named control (Ctrl) in the promoter spanning CpG 14-16, but in this sequence there were no A/T ([A/T$\geq$4]) runs adjacent to CpG dinucleotides (Figure 22A).
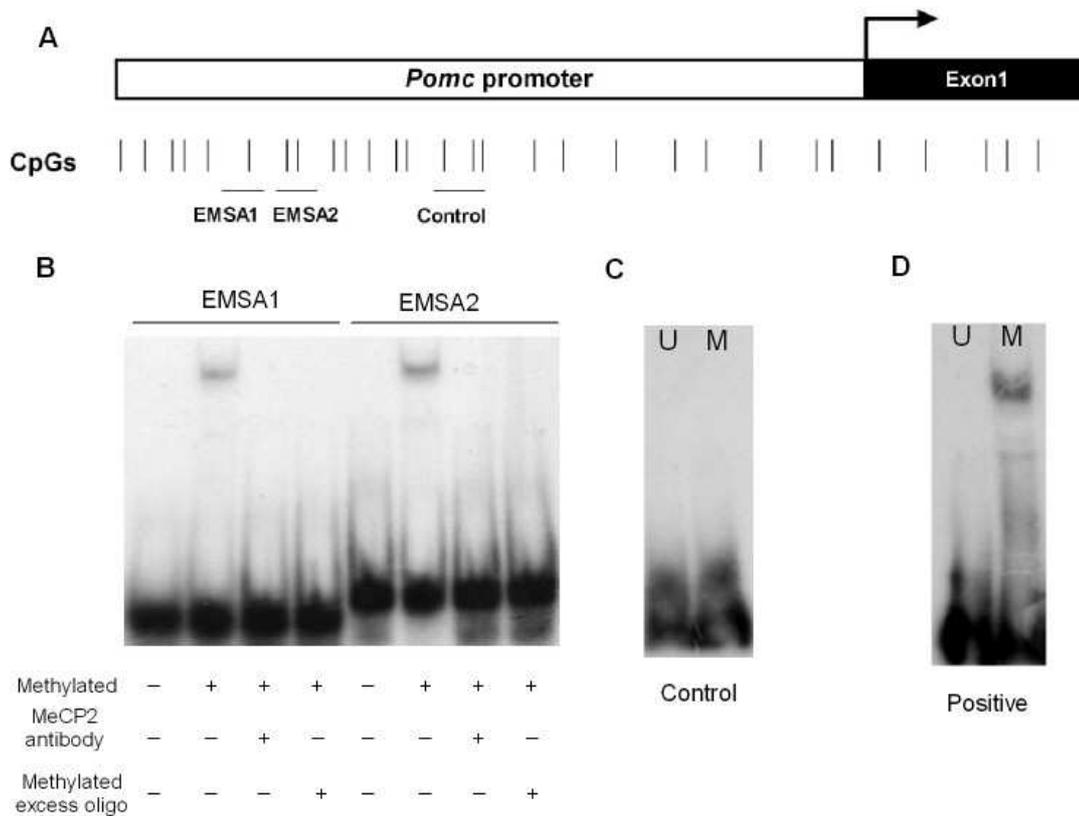
Figure 22. MeCP2 is bound to the *Pomc* promoter *in vitro*. (A) Schematic diagram of the *Pomc* promoter. The distribution of CpG residues is indicated according to their position by vertical bars. The positions of the respective oligonucleotides used for EMSA experiments are shown. (B) EMSA experiments showed that MeCP2 recognized specifically methylated CpG oligonucleotides. MeCP2 was bound strongly to methylated, but not to unmethylated EMSA1 and EMSA2 oligonucleotides as well as the positive control. Self-competition experiments and pre-incubation with the MeCP2 antibody proved the specificity of MeCP2 binding to the methylated EMSA1 and EMSA 2. (C) MeCP2 showed no binding in the middle of the *Pomc* promoter (Control) irrespective of its methylation status. (D) The positive control shows that MeCP2 preferentially binds to methylated oligonucleotides. Representative autoradiograms (n = 3 independent experiments each) are shown.

Sense and antisense oligonucleotides were first slowly annealed to form a double strand and then *in vitro* methylated. Both methylated and unmethylated oligonucleotides were subjected to an end-labeling step with ^{35}S. End-labeled oligonucleotides together with GST-MeCP2 protein were loaded on the PAGE gel and were fractionated.

The results of the EMSA experiments in Figure 23B agree with previous evidence for high affinity MeCP2 binding, to methylated CpGs adjacent to A/T sites. MeCP2 specifically bound to the region spanning CpG 6 to CpG 8 (EMSA1 and EMSA2), with an affinity (K_D =6.48 nM and 5.86 nM respectively), which is comparable to the positive control (Figure 22D). In contrast the control

oligonucleotide in the middle of the *Pomc* promoter showed no binding at all irrespective of the methylation status (Figure 22C). The specificity of the protein/DNA complex was further confirmed by a super shift assay, in which the protein/DNA complex disappeared during the gel electrophoresis upon addition of MeCP2 antibody. Self-competition tests were also performed using an excess (1:10, 1:100, 1:1000) of unlabelled methylated or unmethylated oligonucleotides. The results showed that DNA binding was gradually reduced with increased amount of methylated oligonuceotide, while the unmethylated oligonucleotide had much less effect.

To further decipher the importance of methyl-CpG and the adjacent A/T sites for MeCP2 binding, a series of mutations were generated. The set of mutations tested is shown in the left part of Figure 23, with the parent oligonucleotide sequence depicted above. In the case of EMSA1 (CpG 6), A/T runs were essential for MeCP2 binding. For example, if AT3 was mutated alone, the binding was reduced by 75%, and if AT2 and AT3 were mutated together, only 14% binding remained compared with the wild type. Furthermore, if AT runs were completely mutated; the MeCP2 binding was almost abolished (Figure 23A). In the case of EMSA2, it might have a different binding mechanism compared with EMSA1 because there were two CpG sites (CpG 7 and CpG 8) and only one A/T run in the oligonucleotide. As shown in Figure 23B, mutations occurring in one of the CpGs impaired protein/DNA complex formation, while mutations in both CpG 7 and CpG 8 completely destroyed the protein/DNA complex. The AT run was also a key element for MeCP2 binding in EMSA2. As shown in Figure 23B, the DNA/protein complex was strongly impaired after mutation of A/T sites adjacent to CpG dinucleotides.

In summary, *in vitro* binding experiments showed that MeCP2 was efficiently bound to sequences present at the *Pomc* distal promoter region spanning CpG 6 to CpG 8, while MeCP2 showed less binding to other parts, such as the proximal promoter (CpG 14-16). Mutational studies revealed that both the methylated CpG(s) and the AT runs were essential for high affinity MeCP2 binding.
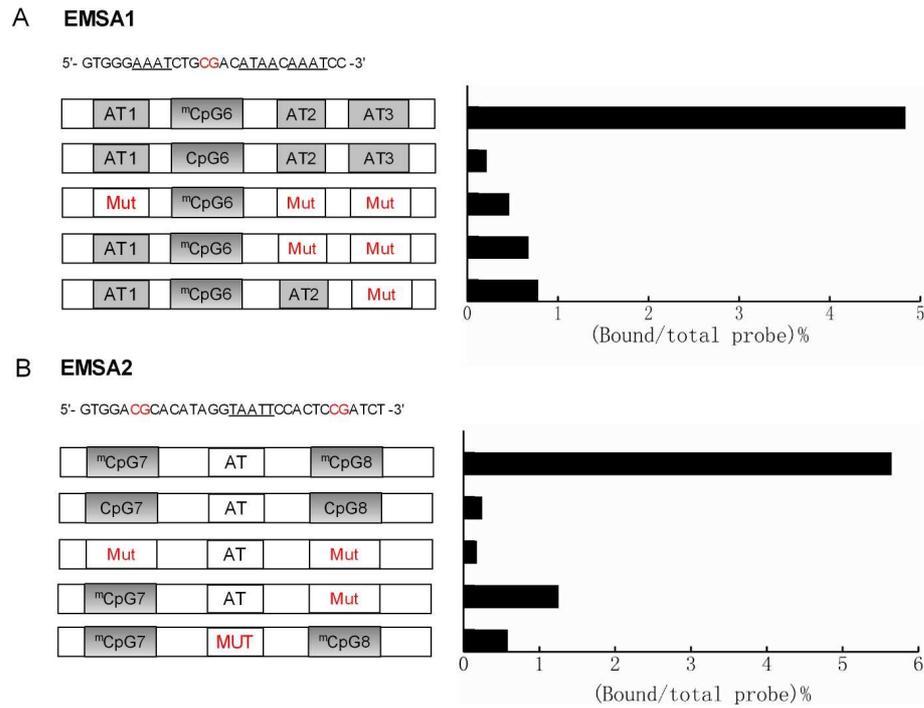
Figure 23. Methylated CpGs and AT runs were essential for MeCP2 binding to *Pomc* promoter derived oligonucleotides. (A) Binding specificity of MeCP2 for EMSA1 was investigated by base substitutions of AT clusters adjacent to the methylated CpG. The sequence of the parent oligonucleotides is listed above the scheme. The results indicated a strong decline of MeCP2 binding resulting from the absence of AT sequences adjacent to methylated CpG 6. (B) Binding specificity of MeCP2 for EMSA2 was investigated by mutagenesis of either CpG(s) or AT cluster adjacent to methylated CpG residues. The results indicated a strong decline of MeCP2 binding for mutated CpG sites or mutated AT sequences flanking methylated CpGs.

3.4.3 MeCP2 represses *Pomc* gene expression *in vivo*

Chromatin immunoprecipitation (ChIP) is a technique to investigate the binding of a particular protein of interest to chromatinized DNA. In our experiment, we sought to confirm the repressive function of MeCP2 at the *Pomc* locus *in vivo*. A sequential-ChIP experiment from mouse pituitary was performed to prove this hypothesis. The first (primary) round of the ChIP was carried out with antibodies against acetylated histone H3 (H3Ac), a mark of transcriptional active chromatin, or dimethylhistone H3 Lys-9 (H3K9me2), a mark of transcriptional repressive chromatin. The anti-C-terminal MeCP2 antibody was used for the second (secondary) round of ChIP, which we performed on half of the product of the primary ChIP; the remaining product from the first ChIP was saved for analysis of the primary ChIP. DNA recovered from both ChIP steps was analyzed by real-time PCR for the presence of the *Pomc* promoter. By

doing so, we were able to simultaneously evaluate the activity of *Pomc* as well as MeCP2 occupancy at the *Pomc* promoter. Two pairs of primers were designed for this ChIP experiment. The first primer pair was located in the *Pomc* distal promoter region spanning CpG 6 and CpG 10 and producing a 154 bp PCR amplicon. As a control, the second primer pair was designed in the coding region (exon3) which lies 6 kb downstream (Figure 24A).
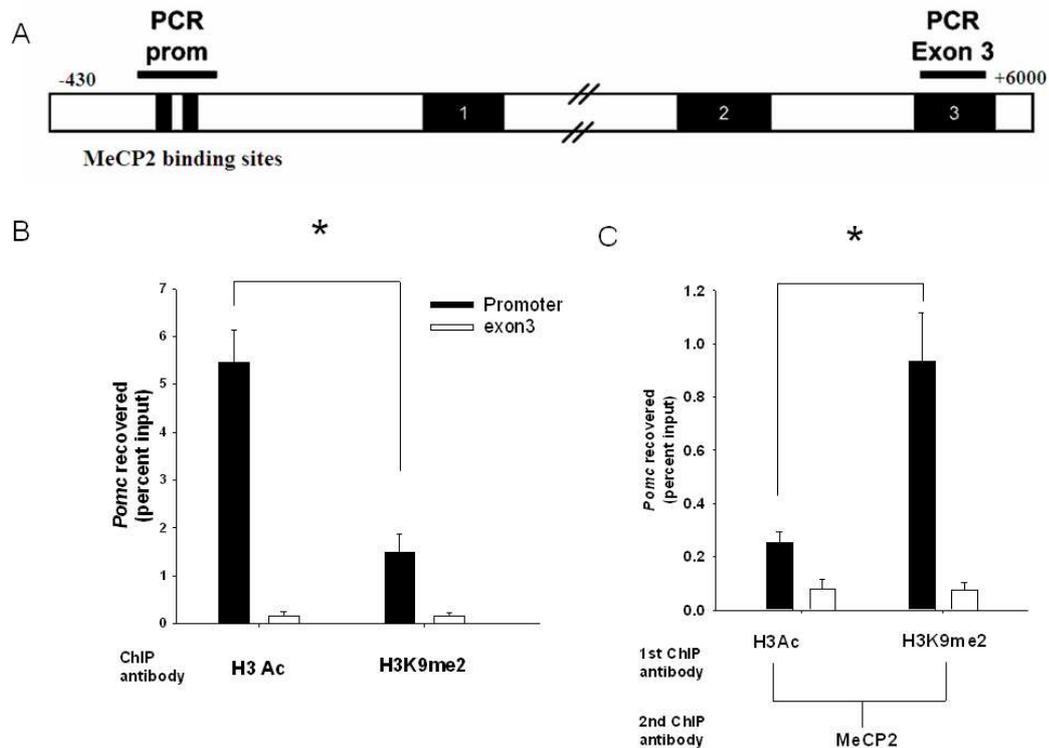
Figure 24. MeCP2 is bound to the repressed state of the *Pomc* promoter *in vivo* Seq-ChIP was performed on pituitary chromatin isolated from naïve mice. (A) Schematic representation of the mouse *Pomc* gene indicating the position of PCR-amplified regions in the ChIP experiment. (B) More *Pomc* DNA was recovered when the primary ChIP was conducted with anti-acetyl histone H3 (H3Ac) than with anti-dimethyl-histone H3 Lys9 (H3K9me2). (C) Secondary ChIP with anti-C-terminal MeCP2 on the samples recovered from B indicated that MeCP2 preferentially associates with dimethyl-histone H3 Lys-9 at the *Pomc* promoter. Values represent mean ± SD. Three independent experiments were performed. The asterisks are used to indicate significant difference (*, $P < 0.05$).

When we performed the primary ChIP, we recovered more *Pomc* DNA with anti-acetyl histone H3 than with anti-dimethyl histone H3 Lys-9 (Figure 24B). However, when we performed the second round ChIP with anti-MeCP2, we recovered significantly more *Pomc* from chromatin that had been initially immunoprecipitated with anti-dimethyl-histone H3 Lys-9 than from chromatin that had been initially

immunoprecipitated with anti-acetyl histone H3 (Figure 24C). In summary, the results from Seq-ChIP indicated that MeCP2 is preferentially associated with the transcriptionally inactive, dimethyl-histone H3 Lys-9 marked *Pomc* promoter in mice pituitaries.

3.4.4 MeCP2 recruits repressor complexes to the *Pomc* promoter

MeCP2 suppresses gene transcription by recruiting corepressors, such as HDACs and DNMTs, to its target DNA binding sites. To determine which corepressors coexist within the same protein complex resident at the promoter region of *Pomc*, sequential ChIP assays were performed. In this sequential ChIP assay, an initial ChIP was performed with an antibody that recognizes MeCP2. The precipitated chromatin-DNA complex was washed and eluted, and a second immunoprecipitation (IP) was performed with MeCP2, Hdac1, Hdac2, Hdac4, Dnmt1, Dnmt3a, Dnmt3b or control istope IgG antibodies. When the first ChIP was performed with anti-MeCP2, the second ChIP showed the presence of Hdac2, Dnmt1, and to a lesser extent Hdac1, in the MeCP2-DNA complex (Figure 25). In contrast, the *Pomc* promoter was not enriched for Hdac4, Dnmt3a and Dnmt3b binding. The specificity of these results was supported by performing the sequential ChIP experiment in the reverse order (data not shown).

ChIP was first performed with antibodies against either MeCP2, corepressors (HDACs and DNMTs) or control rabbit IgG on chromatin derived from naïve mouse pituitaries. Immunocomplexes were dissociated from the beads and 50% of the first immunoprecipitation (IP) were reverse cross-linked and subjected to PCR analysis. The remaining eluate of the first IP reaction was subject to a second round of ChIP with an antibody against MeCP2 or control rabbit IgG. PCR analysis was performed on the eluates both from the first ChIP and second ChIP. The results revealed that Hdac1, Hdac2 and Dnmt1 exist in *Pomc* distal promoter region in the first ChIP. The co-occupancy of Hdac1 with MeCP2, Hdac2 with MeCP2 and Dnmt1 with MeCP2 was proved by the second ChIP with MeCP2.
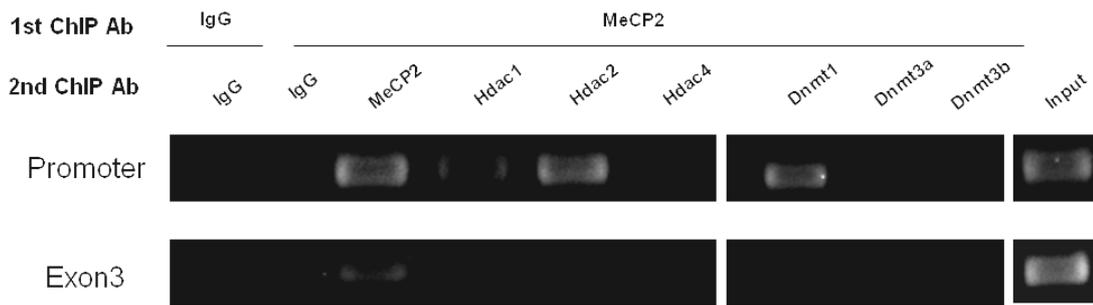
Figure 25. MeCP2 is associated with repressor complexes (HDACs and DNMTs) at the *Pomc* promoter region. Sequential ChIP assays were performed after an initial immunoprecipitation (IP) with anti-MeCP2. After a second IP with anti-Hdac1, anti-Hdac2, or anti-Dnmt1, DNA from the distal promoter, but not from the coding region (exon3) could be amplified. No DNA was recovered following immunoprecipitation by Hdac4, Dnmt3a, Dnmt3b or isotype IgG antibodies.

3.5 Phosphorylation of MeCP2 in pituitary cells

3.5.1 Depolarization dependent MeCP2 phosphorylation in pituitary cells

Protein phosphorylation is an important posttranslational modification that can modulate the function of a protein by adding a phosphate group to serine, tyrosine, or threonine residues. Previous results showed that phosphorylation of MeCP2 at serine 421 in cultured rat neurons can precede the release of MeCP2 from the *Bdnf* promoter resulting in an increase in BDNF expression (Zhou et al., 2006; Tao et al., 2009). We wondered whether such phosphorylation of MeCP2 is also present in pituitary cells. To address this question, immunocytofluorescence (ICC) experiments were performed using an antibody against total MeCP2, which recognizes MeCP2 irrespective of its phosphorylation status and an antibody against pS438 of MeCP2 (which is homologous to S421 MeCP2 in rat) in pituitary primary cells. Double staining experiments using antibodies against MeCP2 and ACTH, the later is a marker for pituitary corticotrope cells, revealed the ubiquitous expression pattern of MeCP2 in pituitary cells with higher expression levels in corticotropes (Figure 21 and 26A). Moreover, MeCP2 was phosphorylated at serine 438 in cultured mouse primary pituitary cells upon membrane depolarization by 55 mM KCl. Under basal conditions, the pS438 MeCP2 signal was barely detectable. In contrast, when primary cells were subjected to membrane depolarization using elevated levels of extracelluar potassium

to activate L-type voltage-sensitive calcium channels (L-VSCCs), MeCP2 S438 phosphorylation could be readily detected in cultured mouse pituitary cells (Figure 26B).
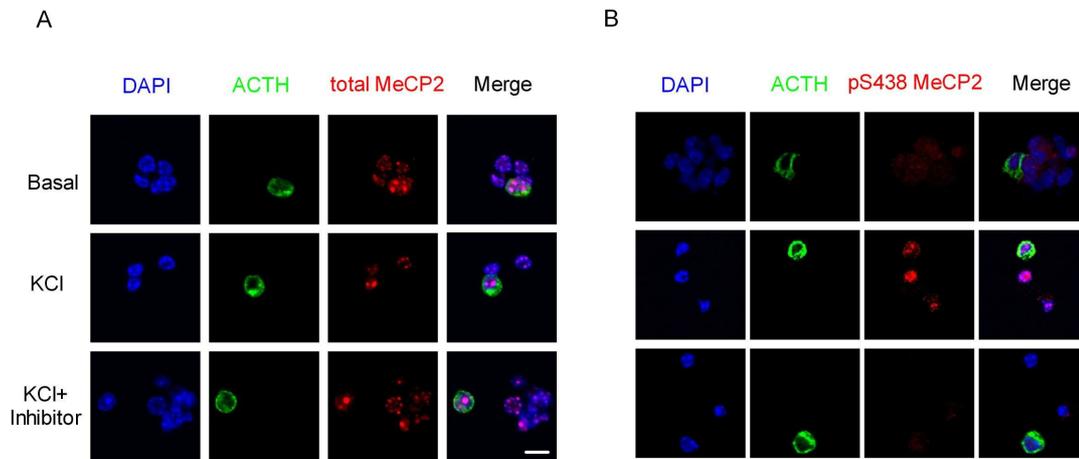
Figure 26. MeCP2 is phosphorylated at serine 438 in pituitary primary cells upon membrane depolarization. (A) Total MeCP2 (red) showed similar levels of immunoreactivity under different conditions. MeCP2 colocalizes with the corticotrope cell marker ACTH (green) in primary pituitary cells. (B) MeCP2 is phosphorylated at serine 438 after KCl treatment of primary pituitary cells. Pre-treatment of the cells with a CaMKII inhibitor prevented the increase of phospho-MeCP2 after membrane depolarization by KCl treatment. Scale bar, 10 µM.

Previous research showed that cells treated with KCl undergo calcium influx resulting in activation of calmodulin-dependent Protein Kinase II (CaMKII). To address this question, pituitary primary cells were treated with 55 mM KCl for 1 hour and the activity of phospho-CaMKII, which is the activated form of CaMKII, was monitored by immunostaining. As shown in Figure 27A, the phosphorylated form of CaMKII was significantly increased after KCl treatment without influencing the total level of CaMKII (Figure 27B). Previous research revealed that MeCP2 phosphorylation was mediated by CaMKII activity, therefore we asked whether pS438 phosphorylation was affected if CaMKII activity is blocked by pharmacological treatment. The results supported the role of CaMKII in the mediation of MeCP2 phosphorylation on serine 438 as evidenced by reduced pS438 MeCP2 immunostaining when the primary cells were pre-treated with a CaMKII inhibitor before KCl stimulation.
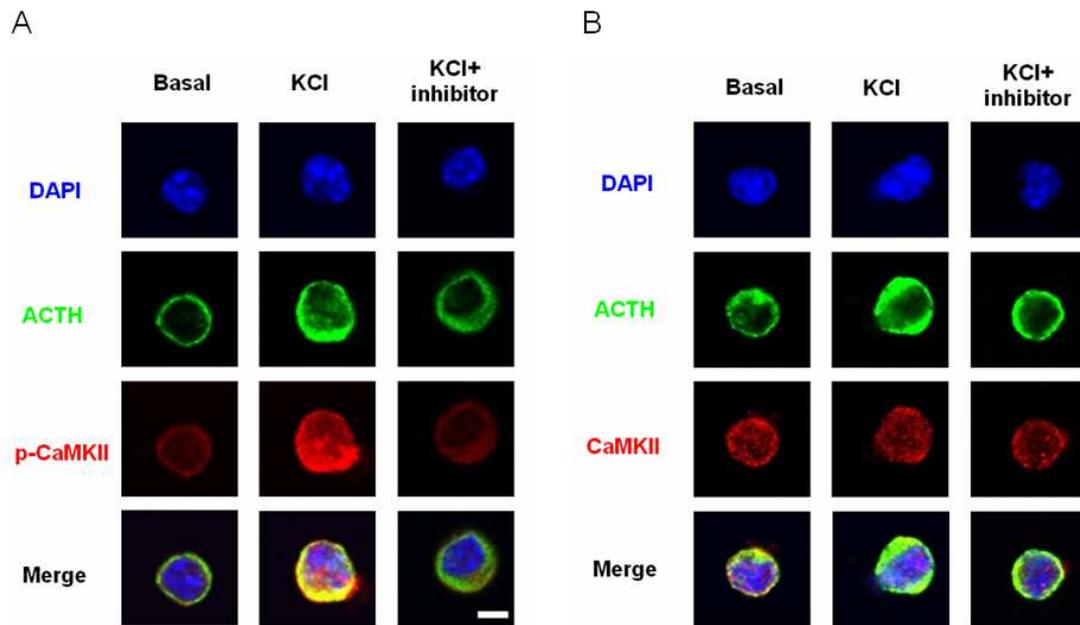
Figure 27. Phospho-CaMKII immunostaining was increased after membrane depolarization of primary pituitary cells. (A) KCl treated pituitary primary cells showed increased pCaMKII (red) and ACTH (green) staining as compared with the non-treated condition. Pre-treatment with a CaMKII inhibitor prevented the increase of phospho-CaMKII immunoreactivity after membrane depolarization by KCl treatment. (B) In contrast, total CaMKII immunoreactivity was unchanged under both conditions. Scale bar, 5μM.

Given the heterogeneous nature of pituitary primary cells, we asked whether phosphorylation of MeCP2 at serine 438 could take place in the homogeneous corticotrope cell line-AtT20.
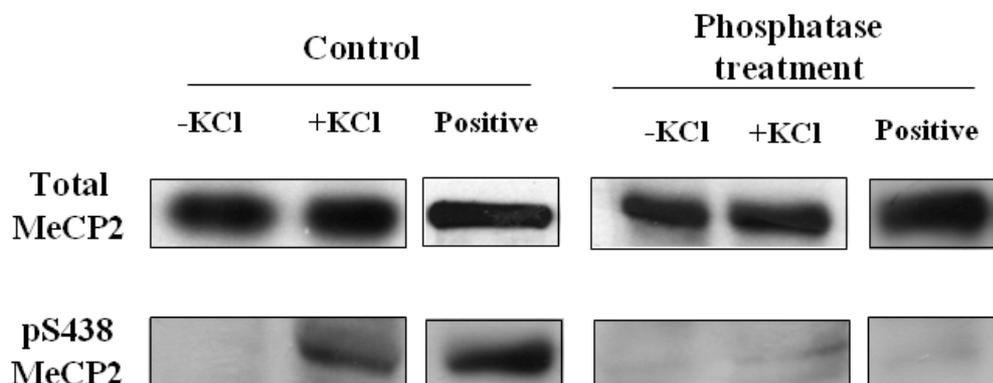
Figure 28. MeCP2 is phosphorylated at site 438 in AtT20 corticotrope cells upon membrane depolarization. Western blots of whole cell extracts from AtT20 cells demonstrated an increased level of phosphorylation of MeCP2 at serine 438 when cells were depolarized by KCl. CIP treatment proved the specificity of the pS438 MeCP2 antibody. Total MeCP2 levels remained the same for all testing conditions.

Immunoblot analysis of MeCP2-S438 phosphorylation in corticotrope AtT20 cells showed that depolarization increased levels of MeCP2-pS438 immunoreactivity when compared with controls without influencing levels of total MeCP2. To confirm

the specificity of pS438 MeCP2, calf intestinal phosphatase (CIP) treatment was carried out to dephosphorylate MeCP2 residues before primary antibody incubation. After phosphatase treatment, the pS438 MeCP2 antibody can not detect any signal any more. Total MeCP2 signal was not affected by this treatment (Figure 28).

3.5.2 Phosphorylation of MeCP2 at S438 reduces *Pomc* promoter occupancy

As already shown, MeCP2 overexpression suppresses methylated *Pomc* reporter activity; we further hypothesized that *Pomc* expression is regulated by MeCP2 phosphorylation. To address this hypothesis, CpG 6−8 methylated *Pomc* reporter plasmids were cotransfected with the expression vector MeCP2, constitutively active CaMKII, or MeCP2 together with CaMKII in AtT20 cells. MeCP2 transfection alone reduced *Pomc* reporter activity, while, CaMKII has the opposite effect. When MeCP2 was cotransfected with CaMKII, we observed complete reversal of the repression by MeCP2. To further investigate the role of phosphorylation of MeCP2 at serine 438 in regulating *Pomc* gene activity, a Flag-tagged mutant MeCP2 expression plasmid (S438A) was constructed, in which serine 438 was replaced by alanine. As a consequence, MeCP2 can not be phosphorylated at this site any more. When AtT20 cells were transfected with MeCP2 (S438A) in the absence or presence of CaMKII, the reporter activity was repressed by MeCP2 (S438A), while cotransfection of CaMKII could not reverse MeCP2-directed repression any more (Figure 29A).

Previous reports indicated that phosphorylation of MeCP2 at serine 421 (pS438 in mouse) can derepress gene activity by loss of MeCP2 binding from its target DNA sequence. To test whether MeCP2 occupancy is altered upon membrane depolarization at the *Pomc* locus, ChIP experiments were carried out using CpG 6−8 methylated reporter constructs in control or membrane-depolarized cells. The results showed a strong reduction of MeCP2 occupancy and increased *Pomc* luciferase activity following depolarization, while pretreatment with a specific CaMKII inhibitor reversed the depolarization-induced dissociation (Figure 29B).

A   B
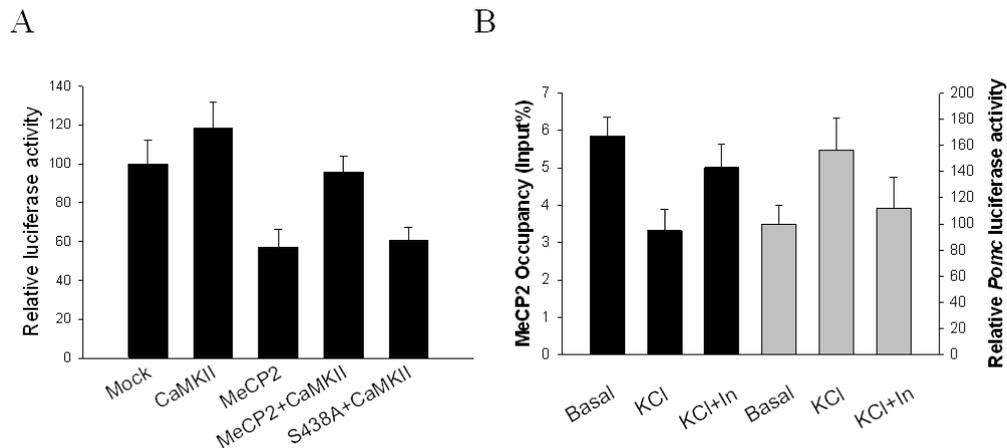
Figure 29. Phosphorylation of MeCP2 at serine 438 can rescue *Pomc* expression by promoting dissociation of MeCP2 from the *Pomc* promoter. (A) CaMKII modulates repressive actions of MeCP2 at the *Pomc* promoter. Cotransfecting a constitutively active CaMKII plasmid with a *Pomc* site-dircted methylated vector stimulated *Pomc* expression and overrided the repressive effects of further cotransfection with MeCP2. Activated CaMKII could not rescue Pomc expression when cotransfected with the mutated form MeCP2 (S438A). (B) Membrane depolarization relieved MeCP2 occupancy at the *Pomc* promoter. AtT20 cells were depolarized with 55 mM KCl (1 hour). ChIP experiments showed reduced MeCP2 occupancy at *Pomc* promoter (black bar, left), paralleled by increased *Pomc* luciferase activity of the promoter (gray bar, right). Pretreatment of AtT20 cells with a CaMKII inhibitor reversed these effects. Data are mean ± SD. Three independent experiments were performed.

3.5.3 AVP elicits MeCP2 phosphorylation in pituitary cells

Previous research showed that AVP actives *Pomc* mRNA expression through calcium pathways. We hypothesized that CaMKII activity might be altered during AVP treatment in primary pituitary cells. To address this question, pituitary primary cells were treated with AVP (10^{-7} M) for 2 hours, the activity of phospho-CaMKII was monitored by immunostaining. As shown in Figure 30A, the phosphorylated form of CaMKII was significantly increased after AVP treatment without influencing the total levels of CaMKII. As we have already shown that MeCP2 phosphorylation is mediated by CaMKII activity, we hypothesized that MeCP2 could be phosphorylated when primary pituitary cells were treated with AVP peptide. The results showed that this was indeed the case. Interestingly, most of the pS438-MeCP2 positive cells colocalized well with ACTH suggesting that MeCP2 phosphorylation at serine 438 occurred predominantly in corticotrope cells (Figure 30B). The reason for this result could be explained by the fact that the AVP v1b receptor only exists in corticotrope

cells in the pituitary. Pre-incubation with 10^{-6} M SSR149415, a specific antagonist of the v1b receptor, completely abolished AVP-induced MeCP2 phosphorylation.
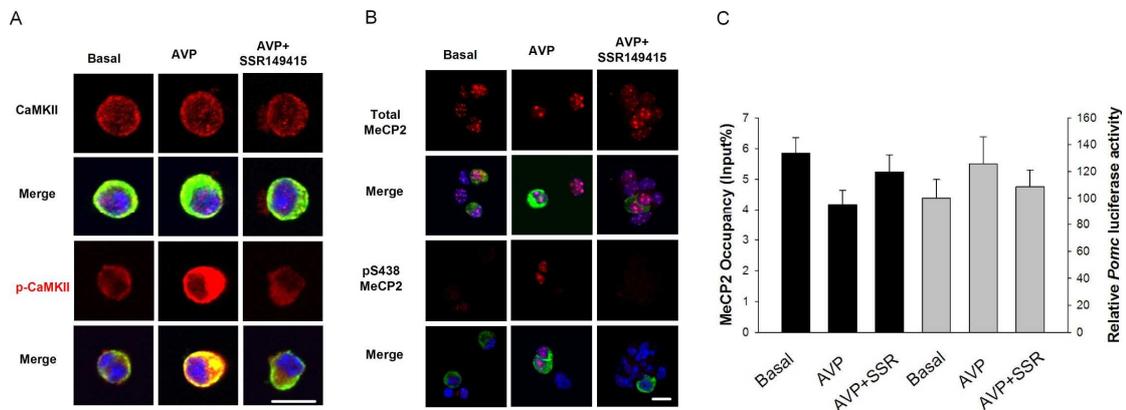
Figure 30. AVP induced MeCP2 phosphorylation and dissociation from the *Pomc* promoter region. (A) Immunostaining of total and activated p-CaMKII in primary pituitary cells. AVP treatment activated p-CaMKII without changing the level of total CaMKII. Pretreatment of the cells with the AVP v1b receptor antagonist SSR149419 completely abolished AVP induced activation of p-CaMKII. Both CaMKII and p-CaMKII (red) colocalized with the corticotrope cell marker ACTH (green). Scale bar: 10 μM. (B) AVP induced MeCP2 phosphorylation at serine 438 without altering total MeCP2 level. Scale bar: 10 μM (C) AVP treatment of AtT20 cells relieved MeCP2 occupancy at the *Pomc* promoter. AtT20 cells were treated with 100 nM AVP for 2 hours. ChIP experiments showed reduced MeCP2 occupancy at the *Pomc* promoter (black bars, left), paralleled by increased *Pomc* luciferase activity of the promoter (gray bar, right). Pretreatment of AtT20 cells with SSR149415 reversed these effects. Data are mean ± SD. Three independent experiments were performed.

Next we asked whether AVP can induce MeCP2 phosphorylation in corticotrope cells. To answer this question, homogeneous corticotrope AtT20 cells were used to monitor MeCP2 phosphorylation level using immunostaining. Previous research showed that AVP activates *Pomc* expression through binding to its specific V1b receptor at the corticotrope cell membrane, and triggers intracellular calcium influx. However, from the literature (Ventura et al., 1999) and our experiments, we know that AVP v1b receptor expression is barely detectable in normal AtT20 cells. To solve this problem, an AtT20 cell clone with v1b receptor stably expressed was used. Corticotrope AtT20 cells were treated with 10^{-7} M AVP or DMSO for 2 hours. After treatment the cells were fixed and stained with MeCP2 and ACTH. As the results show in Figure 31, pS438-MeCP2 can only be detected when AtT20 cells were treated with AVP. Pre-treatment of cells by SSR149415 half an hour before AVP treatment completely abolished AVP-induced MeCP2 phosphorylation in AtT20 cells suggesting the specificity of AVP for MeCP2 phosphorylation.
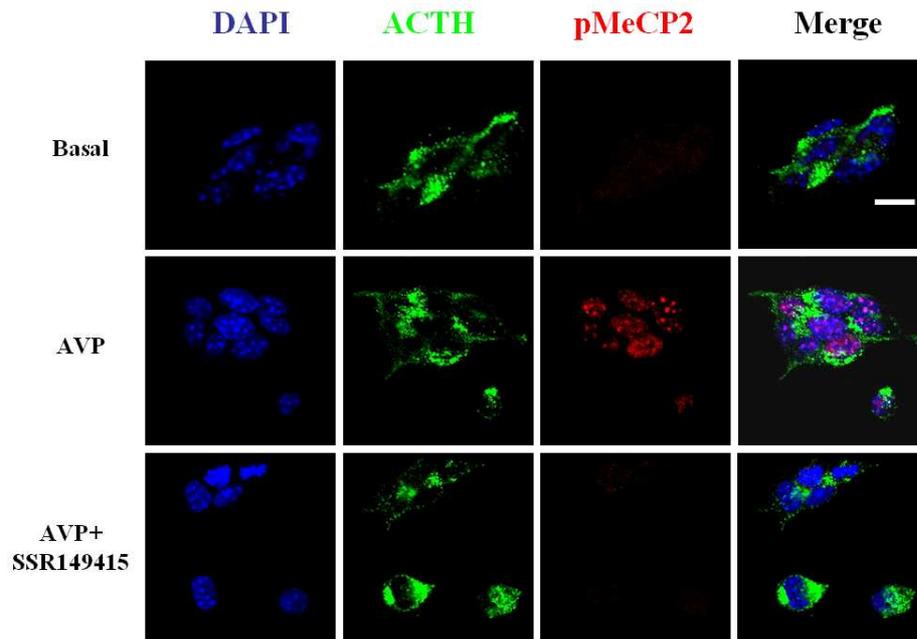
Figure 31. AVP induced MeCP2 phosphorylation in AtT20 (v1bR) cells. AVP induced MeCP2 phosphorylation at serine 438 through binding to the v1b receptor. Nuclear staining of p-MeCP2 (red) colocalized with ACTH (green). Scale bar: 10 μM

AVP-induced phosphorylation of MeCP2 at serine 438 can also reduce MeCP2 occupancy at the *Pomc* promoter as tested by ChIP experiments. CpG 6−8 methylated *Pomc* reporter was transfected into the AtT20 (v1b receptor expressed) cell line. 24 hours after transfection, the cells were treated with 10^{-7} M AVP peptide for 2 hours. Then the cells were harvested, fixed and sonicated to obtain the DNA fragments in the size ranging from 200 to 500 bp. ChIP experiments were performed using the antibody against total MeCP2, in parallel, luciferase assays were carried out to monitor *Pomc* promoter activity. To recover *Pomc* fragment only from the transfected reporter, the forward ChIP primer targeted the vector backbone, and the reverse primer was located in the *Pomc* insert. The results showed a 29% of reduction of MeCP2 occupancy and increased *Pomc* luciferase activity following AVP treatment. Pretreatment of AtT20 cells with SSR149415 completely blocked the dissociation of MeCP2 due to AVP treatment (Figure 30C).

3.5.4 Early life stress induces phosphorylation of MeCP2 in the pituitary

Previous results showed that MeCP2 is phosphorylated in pituitary cells upon membrane depolarization or AVP stimulation. We sought to know whether MeCP2

phosphorylation status is altered after early life stress in mouse pituitary sections. To address this issue, immunohistochemistry was performed on formalin fixed paraffin embedded pituitary sections obtained from ELS and control mice. The results revealed no differential regulation in total MeCP2 protein in the pituitary between ELS and control mice (data not shown).
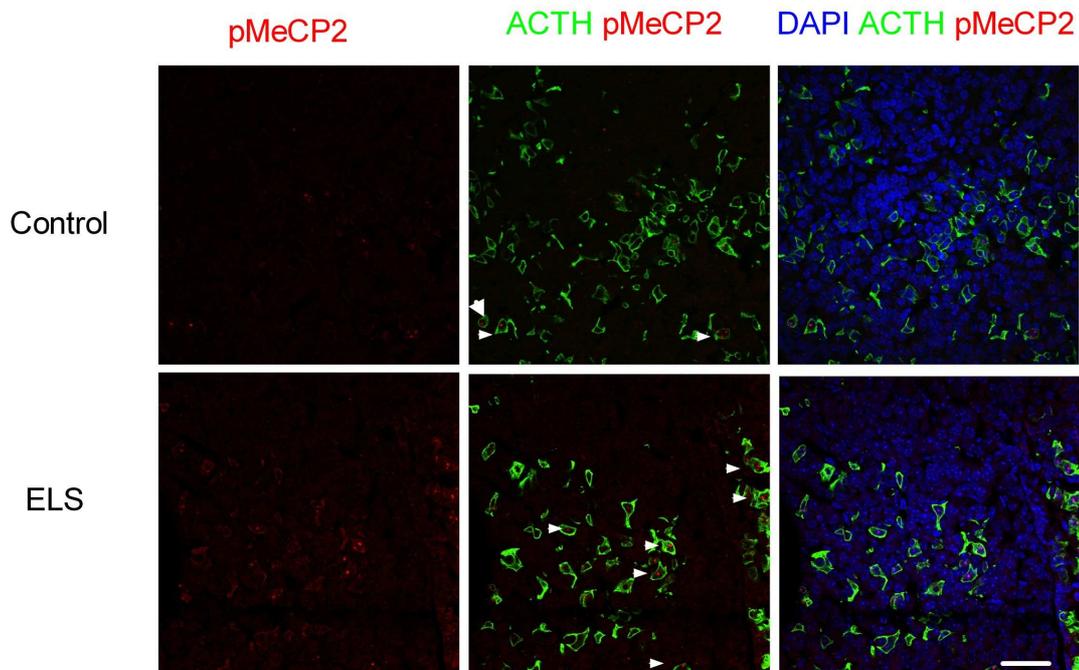
Figure 32. Early life stress induces phosphorylation of MeCP2 in mouse pituitary. ELS led to increased immunostaining of pS438-MeCP2 (red) and ACTH (green) in the anterior pituitary of 3-month-old mice. pMeCP2 is colocalized with ACTH, which is the marker for pituitary corticotrope cells. White arrow heads indicate positive pS438-MeCP2 staining. The images that are shown are representative of five mice per group. Scale bar: 50 μM

However, comparing pS438 MeCP2 immunoreactivity revealed an increased immunostaining of pS438-MeCP2 in ELS mice compared with controls. Interestingly, most pS438-MeCP2 positive cells were colocalized well with ACTH. This supports our hypothesis that the early-life stress paradigm produced increased levels of AVP from the PVN of the hypothalamus which induced a tissue-specific phosphorylation of MeCP2.

3.6 Reduced occupancy of MeCP2 after ELS

3.6.1 ELS did not affect the corticotrope cell number

Early life stress leads to higher levels of *Pomc* mRNA expression in the pituitary. ACTH, which is enzymatically cleaved from Pro-POMC in pituitary corticotrope cells, was also upregulated after early maternal separation. As we know, pituitary cells proliferate postnatally. We wondered whether early life adversity could affect the development of corticotrope cells.

	Total cells counted	ACTH positive	Ratio
PND-10 Ctrl	32288±2826	1475±172	4.56±0.15
PND-10 ELS	32203±725	1496±82	4.65±0.31
3-month Ctrl	39422±1671	1551±102	3.93±0.16
3-month ELS	39669±776	1570±28	3.95±0.14
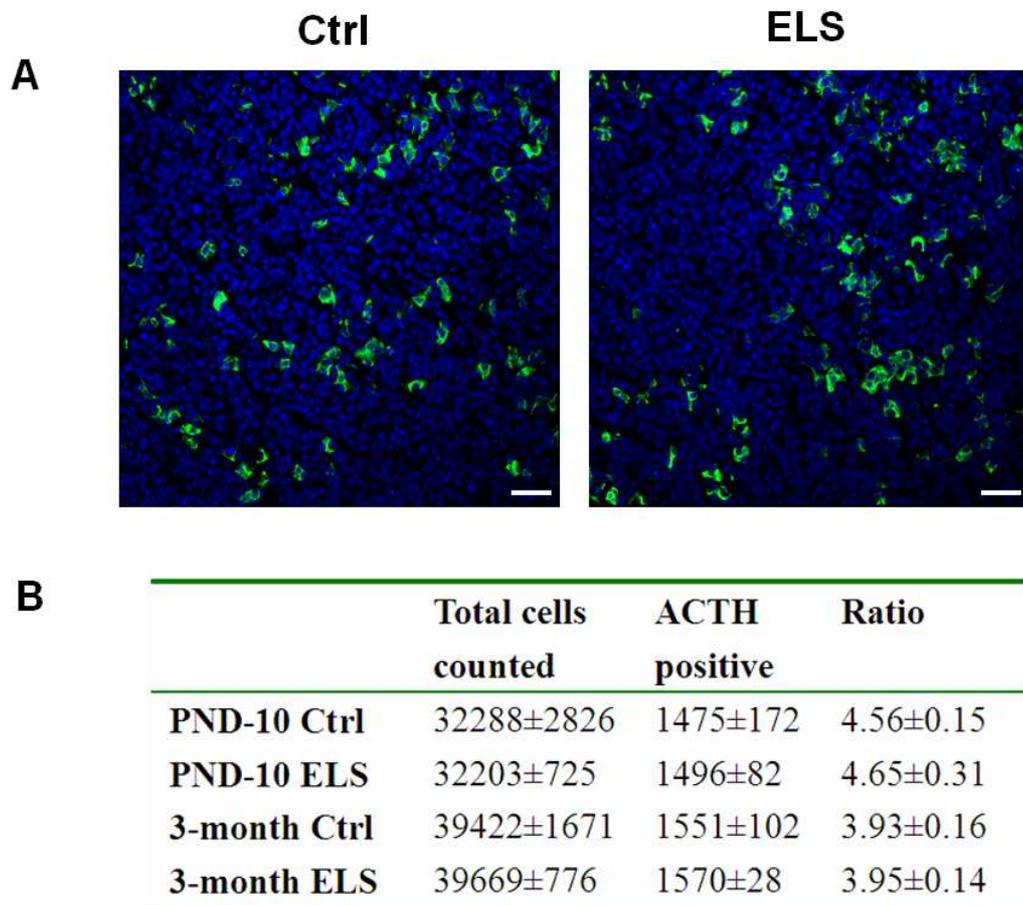
Figure 33. Corticotrope cell number is not altered during early life stress. Representative pictures of immunostaining showed no difference in corticotrope cell ratios between control (Ctrl) and early life stress (ELS) in 3-month old pituitaries. DAPI (blue) staining was used to mark the cell nuclei in all cells, while ACTH (green) positive cells indicated the corticotrope cells in the anterior pituitary. Scale bar: 50 µM. (B) The number of labeled cells with DAPI (total number) and ACTH (corticotrope cell) in 10-day old and 3-month old mice pituitaries. Pituitary slides (8 sections/animal, 5 mice per group)

To answer this question, immunohistochemistry experiments were performed using an antibody against ACTH to mark corticotrope cells in the anterior pituitary

and DAPI to stain the total cell population. The total cell number of anterior pituitary and ACTH-positive cells were counted and compared between control and ELS mice. Pituitary slides (8 sections/animal, 5 mice per group) from10-day and 3-month-old mice were used for this experiment (Figure 33). The results revealed no difference in the ratio of the corticotrope cells with 4.56 ± 0.15 in the control group and 4.65 ± 0.31 in the ELS group at PND 10 and ratios of 3.93 ± 0.16 and 3.95 ± 0.14 at 3 months of age, respectively. In summary, these immunohistochemistry results imply that ELS did not affect postnatal development of the corticotrope cell population.

3.6.2 ELS reduces MeCP2 occupancy at the *Pomc* promoter

Previous EMSA experiments indicated that MeCP2 preferentially binds to methylated DNA sites in the *Pomc* distal promoter region. Sequential ChIP experiments performed in mouse pituitary revealed that MeCP2 was associated with a transcriptional inactive state of the *Pomc* promoter. In addition, bisufite sequencing results showed that early life stress (ELS) induced hypomethylation at the *Pomc* distal promoter. Taken together, we speculated that the difference in DNA methylation would result in differential occupancy of MeCP2 at the *Pomc* promoter, which in turn will affect *Pomc* mRNA expression. To test this hypothesis, *in vivo* ChIP experiments were performed using mouse pituitaries from 6 weeks old mice. Two antibodies were used in this *in vivo* ChIP: activated RNA Pol II, which is an indicator of *Pomc* transcription and C-terminal MeCP2 (antibody against total MeCP2). Two pairs of primers were designed for this ChIP experiment. The first primer pair was located in the *Pomc* distal promoter region spanning CpG 6 and CpG 10 and producing a 154 bp PCR amplicon. As a control, the second primer pair was designed in the coding region (exon3) which lies 6 kb downstream (Figure 24A).
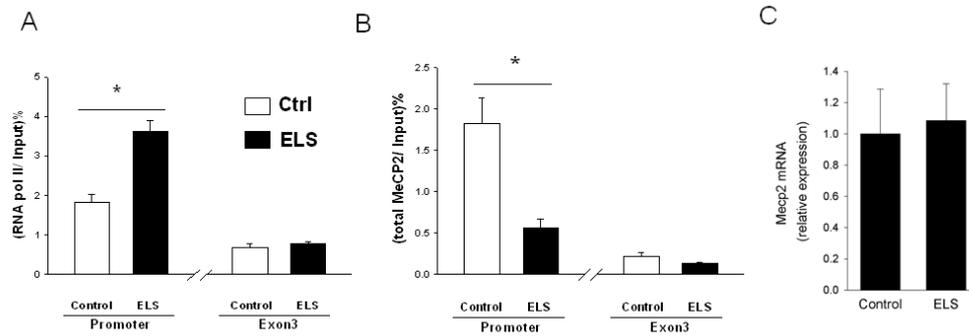
Figure 34. ELS altered MeCP2 and RNA polI II occupancy at the *Pomc* locus in 6 weeks old mice pituitaries. (A) ChIP analysis using the pituitaries of control and ELS mice revealed increased binding of RNA pol II at the *Pomc* promoter region. (B) ChIP analysis showed that ELS mice displayed decreased binding of MeCP2 at the *Pomc* promoter region. (C) Monitoring MeCP2 mRNA expression levels showed no difference between pituitaries from ELS mice and control mice in 6 weeks old mice. Values expressed as mean ± S.E.M; ChIP, n = 8 animals/group; RT-PCR, n = 6-8/group * $P < 0.05$.

In vivo ChIP analysis revealed increased activated RNA pol II occupancy at the *Pomc* promoter of ELS mice, reflecting increased *Pomc* gene transcription (Figure 34A). When we performed the ChIP experiment using anti-MeCP2 antibody, the results showed that total MeCP2 occupancy was reduced in the ELS group (Figure 34B). These results agree with the findings of less DNA methylation in the ELS group. A statistical analysis was performed and the results demonstrated a negative correlation between total MeCP2 antibody and RNA Pol II binding ($p < 0.05$, data not shown). Monitoring MeCP2 mRNA expression levels showed no differences between pituitaries from ELS mice and control mice in 6 weeks old mice (Figure 34C).

We also investigated MeCP2 occupancy status in 10 days old mouse pituitary. ELS mice also displayed reduced MeCP2 occupancy at the *Pomc* promoter region compared with control litters (Figure 35A). Although *Pomc* mRNA level was markedly increased in 10 days old mice (Figure 12, 35A), the DNA methylation level did not differ between control and ELS mice of this age. Given that 10 days old control and ELS mice have similar methylation patterns, the differences in MeCP2 occupancy indicated that ELS-induced phosphorylation of MeCP2 at serine 438 leads to relief of MeCP2 occupancy from the *Pomc* promoter. There was no difference for MeCP2 mRNA expression levels between pituitaries from ELS mice and control mice in 10 days old mice (Figure 35C).
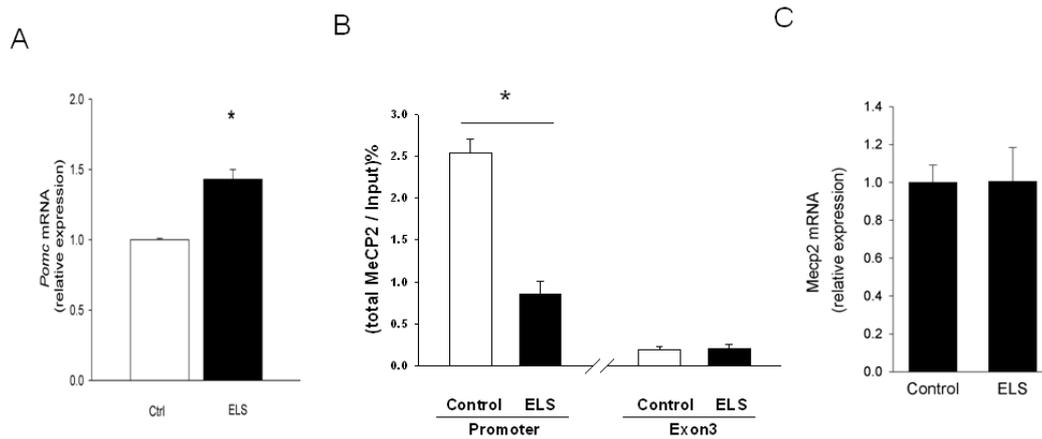
Figure 35. ELS leads to reduced occupancy of MeCP2 at the *Pomc* locus in 10 days old mice. (A) qRT-PCR analysis revealed ELS mice displayed increased level of *Pomc* mRNA expression compared with controls in 10-days old mice pituitaries. (B) ChIP analysis showed that ELS mice displayed decreased binding of MeCP2 at the *Pomc* promoter region. (C) Monitoring MeCP2 mRNA expression levels showed no difference between pituitaries from ELS mice and control mice in 10-days old mice. Values expressed as mean ± S.E.M; ChIP, n = 8 animals/group; RT-PCR, n = 6–8/group * P < 0.05.

3.6.3 Early life stress reduces recruitment of Dnmt1 occupancy to the *Pomc* promoter

Which mechanism is responsible for the loss of methylation during early life experience? As we know, the pituitary gland almost doubles in volume during the first 10 days of life and continutes to enlarge until adulthood. The mitosis of existing cells contributes to the increase in number during early postnatal development. To maintain DNA methylation pattern during cell mitosis, DNA methyltransferases are recruit. Dnmt1 is known control DNA methylation maintenance during cell division. MeCP2, which can directly bind to methylated or hemimethylated DNA sequence, can tether Dnmt1 and promote DNA methylation. Our previous experiment showed that Dnmt1 is associated with MeCP2 at the *Pomc* promoter. Early life stress leads to reduced MeCP2 occupancy at the *Pomc* promoter. We questioned whether ELS could affect Dnmt1 recruitment at the *Pomc* promoter resulting in loss of DNA methylation during pituitary cell proliferation.
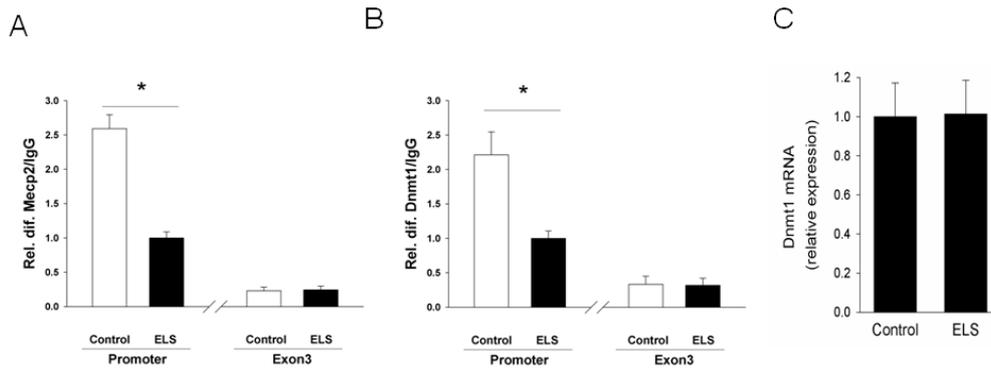
Figure 36. Sequential ChIP experiment showed that ELS reduced MeCP2 and Dnmt1 occupancy at the *Pomc* locus in 6 weeks old mice pituitaries. (A) The first ChIP using an antibody against MeCP2 revealed decreased binding of MeCP2 at the *Pomc* promoter region. (B) The second ChIP using an antibody against Dnmt1 showed that ELS mice displayed lower level binding of Dnmt1 at the *Pomc* promoter region compared with controls. (3 pituitaries were pooled, n = 8/group; * $P < 0.05$) (C) Monitoring Dnmt1 mRNA expression levels showed no difference between pituitaries from ELS and control mice in 6 weeks old animals. Values expressed as mean ± S.E.M; ChIP, three pituitaries were pooled, n = 8/group; RT-PCR, n = 8/group * $P < 0.05$.
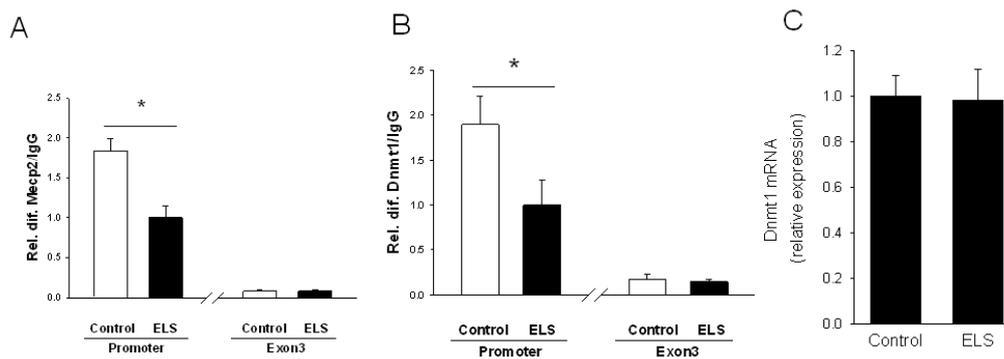
Figure 37. Sequential ChIP experiment showed that ELS reduced MeCP2 and Dnmt1 occupancy at the *Pomc* locus in 10 days old mice pituitaries. (A) The first ChIP using an antibody against MeCP2 revealed decreased binding of MeCP2 at *Pomc* promoter region. (B) The second ChIP using an antibody against Dnmt1 showed that ELS mice displayed lower level binding of Dnmt1 at *Pomc* promoter region compared with controls. (C) Monitoring Dnmt1 mRNA expression levels showed no difference between pituitaries from ELS and control mice in 10 days old animals. Values expressed as mean ± S.E.M; ChIP, five pituitaries were pooled, n = 8/group; RT-PCR, n = 8/group * $P < 0.05$.

To address this question, a sequential ChIP experiment was performed using the first antibody against MeCP2 and the second antibody against Dnmt1 for comparing ELS and control pituitaries. When we performed the ChIP experiment using anti-MeCP2 antibody, the results showed that total MeCP2 occupancy was reduced in ELS group (Figure 36A, 37A) as we showed previously by simple ChIP both in 10-day-old pituitary and in 6-week-old mice (Figure 34, 35). When we performed the second round ChIP with anti-Dnmt1, we recovered significantly more *Pomc* from chromatin

from control mice than from ELS mice both in 10-day old and 6-weeks old mice pituitaries (Figure 36B, 37B). Monitoring the mRNA expression of Dnmt1 by qRT-PCR revealed no difference in basal Dnmt1 expression levels between pituitaries from ELS and control mice both in 10-day and 6-week-old mice (Figure 36C, 37C).

3.7 Home-made MeCP2 antibody generation
3.7.1 Peptides used for MeCP2 antibody generation

The polyclonal antibody antitotal MeCP2 that recognizes MeCP2 irrespective of its phosphorylation status was generated by injecting New Zealand White rabbits with the KLH-conjugated peptide NH2-CSMPRPNREEPVDSRTPV-CONH2 corresponding to amino acids 480-496. The antiserum was purified by affinity-chromatography on a column that was coupled to MeCP2 480-496 peptide, and the affinity-purified anti-total MeCP2 antibody was eluted.

The polyclonal antibody MeCP2 pS438 that recognizes the phosphorylated serine 438 was generated by injecting New Zealand White rabbits with the KLH-conjugated peptide NH2-CMPRGGpSLES-CONH2 (phosphor-serine). The antiserum was purified by affinity chromatography on a column that was coupled to unphosphorylated MeCP2 S438 peptide. The flow-through was then passed over a second column that was conjugated to phosphorylated MeCP2 S438 peptide, and the affinity-purified anti-MeCP2 pS438 antibody was eluted.

The polyclonal antibody MeCP2 pS97 that recognizes the phosphorylated serine 97 was generated by injecting New Zealand White rabbits with the KLH-conjugated peptide NH2-EASA^{P}SPKQR (phosphor-serine). The antiserum was purified by affinity chromatography on a column that was coupled to unphosphorylated MeCP2 S97 peptide (Figure 38).

Figure 38. Protein sequence alignment of e1 forms of mouse, human and rat MeCP2. The peptides used for generation of the different MeCP2 antibodies are boxed in color. pS97 and pS438 phosphorylation sites are pointed out by arrows in the MeCP2 protein sequence.

3.7.2 MeCP2 constructs used for antibody validation

MeCP2 expression constructs were transfection into LLC-PK1 cells for testing MeCP2 antibodies. The position of the S97 and S438 phosphorylation site and the total MeCP2 site are marked in the wild type MeCP2 construct in Figure 39. Wild type, mutated or truncated versions of MeCP2 were tagged at their amino termini with the Flag-epitope. The phosphor-acceptor residue serine 97 was replaced by alanine in MeCP2 (S97A) and the phosphor-acceptor residue serine 438 was replaced by alanine as well (S438A). In the case of MeCP2ΔC, the terminal 45 amino acids containing the recognition sequence for anti-MeCP2 were deleted.

RESULTS
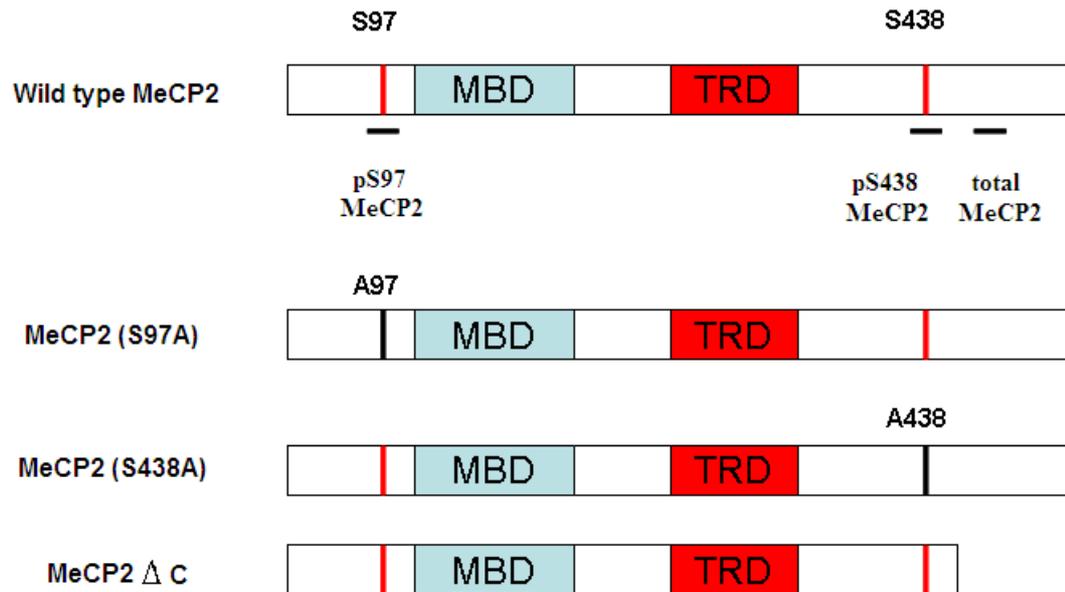
Figure 39. Schematic of MeCP2 expression constructs used for MeCP2 antibodies validation. The position of the S97 and S438 phosphorylation site and the total MeCP2 site are marked in the wild type MeCP2 construct. Wild type, mutated or truncated versions of MeCP2 were tagged at their amino termini with the Flag-epitope. The phosphor-acceptor residue serine 97 was replaced by alanine in MeCP2 (S97A) and the phosphor-acceptor residue serine 438 was replaced by alanine as well (S438A). In the case of MeCP2ΔC, the terminal 45 amino acids containing the recognition sequence for anti-MeCP2 were deleted.

3.7.3 Antibody validation by western blot

3.7.3.1 Characterization of the anti-total MeCP2 antibody

Flag-tagged MeCP2 (0.1 µg each) expression vector was transfected into LLC-PK1 cells and immuoblotted whole cell extracts (WCE) were tested with anti-MeCP2 (1:1,000), a commercial MeCP2 antibody (1:1,000, Up-MeCP2), or an anti-Flag antibody (1:1,000). No signals were detected in mock-transfected cells, MeCP2 transfected cells tested with the preimmune serum, or following pre-absorption of the MeCP2 antibodies on a GST-MeCP2 fusion protein (Figure 40).

Similar signals were detected by anti-MeCP2 antibodies in MeCP2 transfected cells. In contrast to the Flag-antibody, neither of the anti-MeCP2 antibodies detected transfected MeCP2ΔC, indicating their specificity.
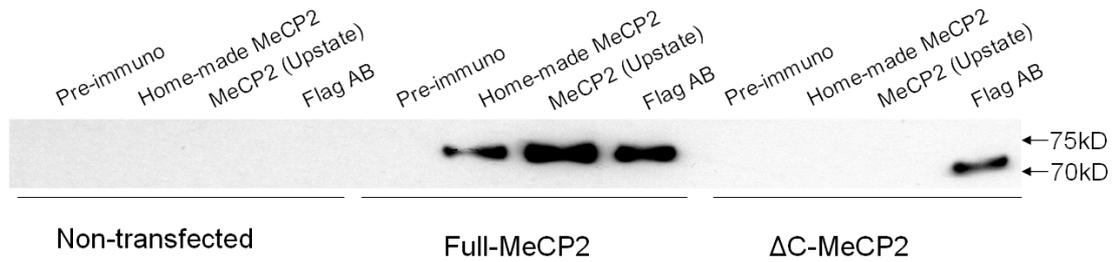
Figure 40. Characterization of the anti-total MeCP2 antibody.

3.7.3.2 Characterization of the anti-phospho MeCP2-S438 antibody

MeCP2 was cotransfected in the absence or presence of calmodulin kinase (CaMKII) or of two different forms of constitutively active calmodulin kinases [containing either a C-terminal truncation (CaMKII*) or a point mutation (T286D)]. Immunoblots were tested with either anti-MeCP2 or anti-MeCP2-pS438. Signals detected by MeCP2-pS438 were specific to the phosphorylated form of MeCP2 (Figure 41A).

In the following experiment, the specificity of MeCP2-pS438 was tested. Wild type MeCP2 and mutated MeCP2 (S438A) were separately transfected in the absence and presence of CaMKII* and immunoblots were tested with anti MeCP2-pS438 or anti-Flag antibodies, respectively. MeCP2-pS438 detected MeCP2 solely in the presence of CaMKII* and of serine 438. Retesting of the same immunoblots with the anti-Flag antibody proved that all samples contained comparable levels of MeCP2 proteins (Figure 41B).

Calf intestine phosphatase (CIP) was used to further confirm the specificity of the MeCP2-pS438 antibody. WCE from cells cotransfected with Flag-tagged MeCP2 and CaMKII* were treated with calf intestine phosphatase. Preincubation with CIP entirely abolished the detection of MeCP2 by the MeCP2-pS438 antibody. In contrast, the anti-Flag antibody detected similar levels of MeCP2 expression, irrespective of CIP pretreatment. In parallel, we also tried to dephosphorylate the protein after SDS-PAGE. After protein transfer, the blotting membrane was treated with CIP by incubation at 37 °C for 1 hour. Both methods lead to similar results (Figure 41C).
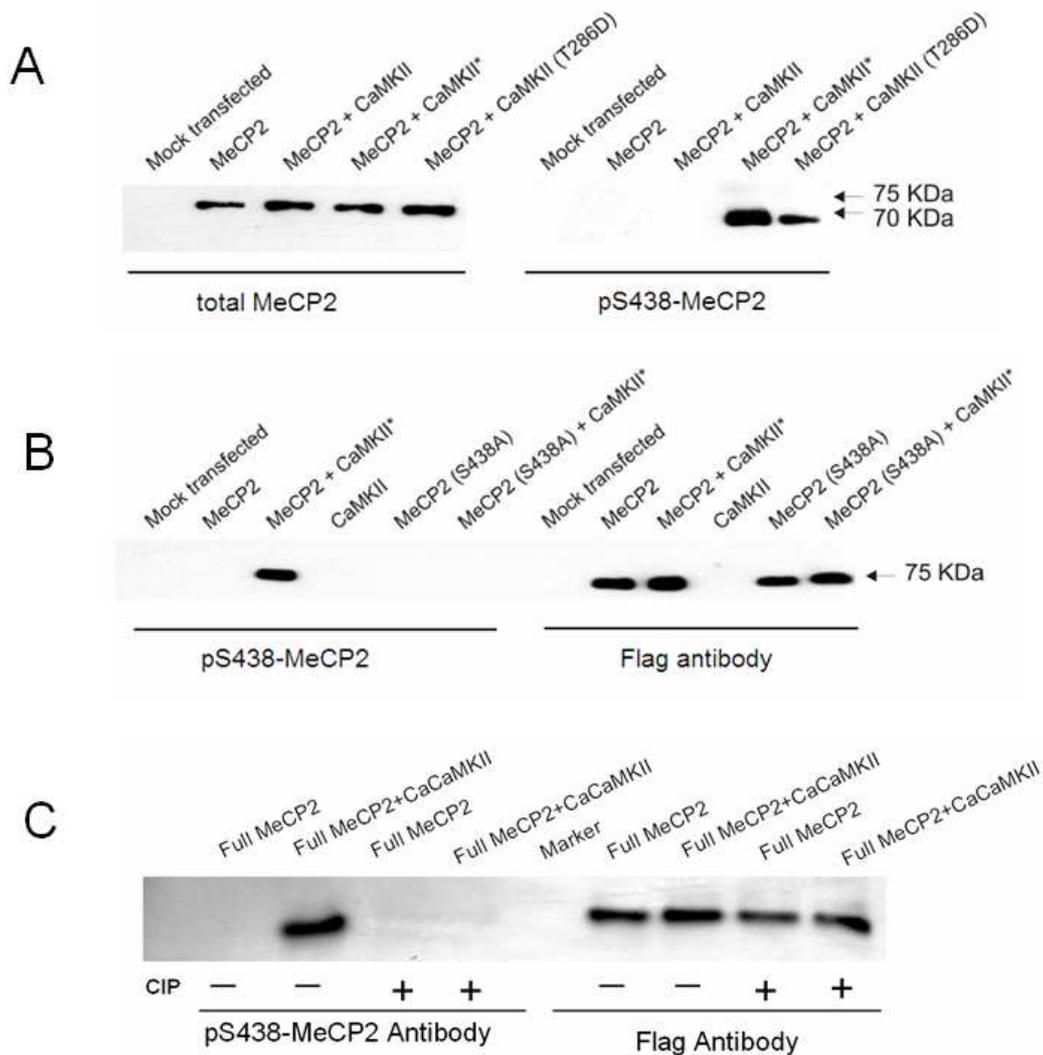
Figure 41. Characterization of the anti-phospho MeCP2-S438 antibody.

3.7.3.3 Characterization of the anti-phospho MeCP2-S97 antibody

Serine 97 phosphorylation of MeCP2 occurs under rest conditions. Wild type and mutated MeCP2 (S97A) were transfected into LLC-PK1 cells. Immunoblots were tested with either anti-total-MeCP2 or anti-MeCP2-pS97. Signals detected by MeCP2-pS97 were specific to the phosphorylated form of MeCP2. An aliquot of MeCP2-pS80 (equal to pS97 in mouse) antibody (generous gift from Jifang Tao UCLA, USA) was used as a positive control (Figure 42).
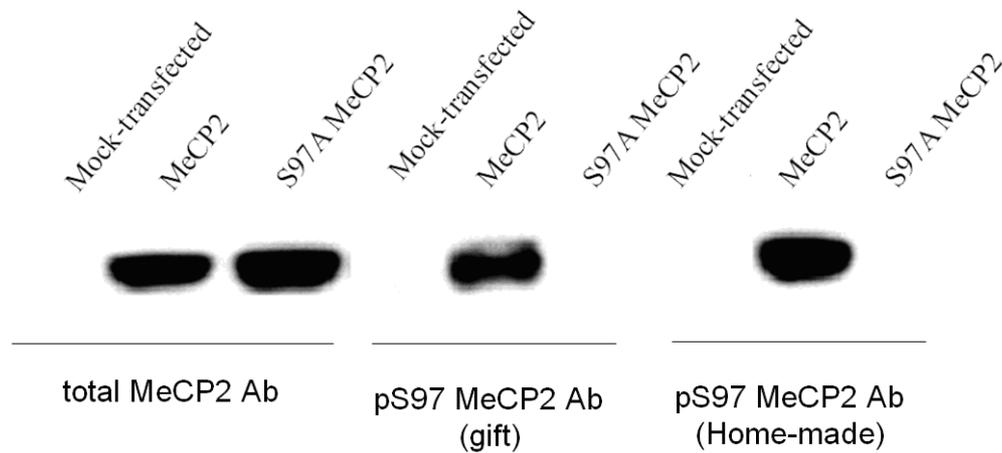
Figure 42. Characterization of the anti-phospho S97-MeCP2 antibody.

3.7.4 Antibody validation by immunocytochemistry (ICC)

Immunocytochemistry experiments were performed to validate MeCP2 antibodies. To test the C-terminal anti-total MeCP2 antibody, wild type MeCP2 and MeCP2ΔC expression constructs were transfected into LLC-PK1 cells. MeCP2 antibody from rabbit and Flag antibody from mouse were used for staining. As shown in Figure 43, the MeCP2 antibody detected expression of the wild type MeCP2 construct exclusively in the nuclei of transfected LLC-PK1 cells. By contrast, following expression of MeCP2ΔC, no signal was detected, while the Flag antibody detected both MeCP2 proteins.

In the second experiment, the specificity of MeCP2-pS97 was tested. Wild type MeCP2 and mutated MeCP2 (S97A) were separately transfected in LLC-PK1 cells. LLC-PK1 cells were fixed and incubated with anti MeCP2-pS97 and anti-flag antibodies. The anti-MeCP2-pS97 antibody detected the phosphorylated form of MeCP2 exclusively in the nuclei under resting conditions. When the residue serine 97 was mutated to alanine, the anti-MeCP2-pS97 failed to detect any signal in the cell. While the flag antibody proved the successful transfection of the MeCP2-S97A expression plasmid to the cells (Figure 44).

In the last experiment, the specificity of MeCP2-pS438 was tested (Figure 45). Wild type MeCP2 and mutated MeCP2 (S438A) were separately transfected in the absence and presence of CaMKII and immunostainings were tested with anti-total-

MeCP2, anti-MeCP2-pS438 and anti-Flag antibodies. Anti-total-MeCP2 antibody can detect the signal irrespective of the phosphorylation status of MeCP2. MeCP2-pS438 detected MeCP2 solely in the presence of transfected CaMKII and the wild type MeCP2 construct. In contrast, when the residue serine 438 was mutated to alanine, the anti-MeCP2-pS438 antibody failed to detect any signal. The flag antibody can still prove the successful transfection of MeCP2-S438A expression plasmid to the cells.
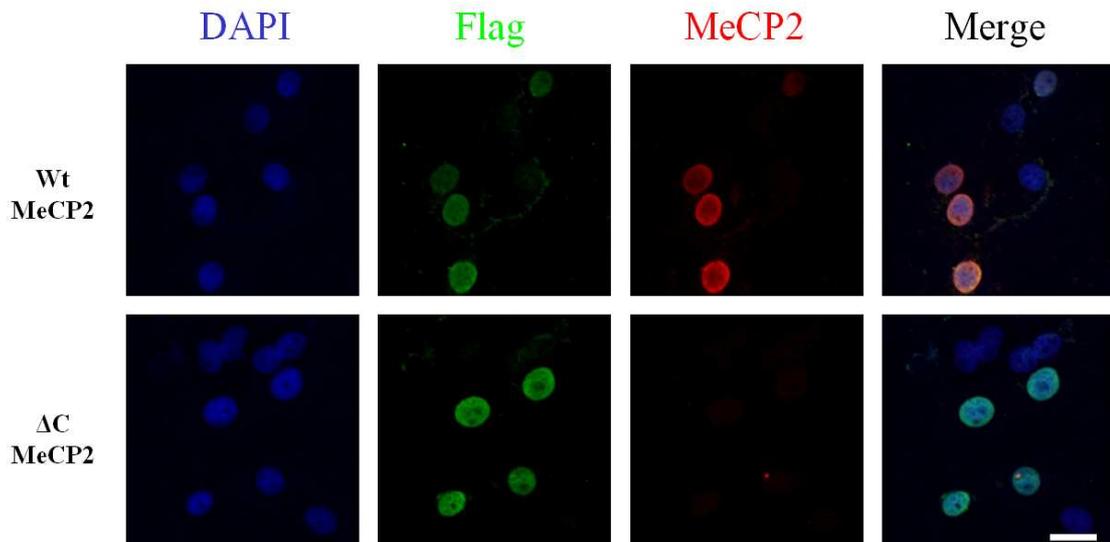
Figure 43. Total MeCP2 antibody validation using immunocytochemistry. Immunostaining of Flag-tagged wild type and C-terminal deletion MeCP2 in LLC-PK1 cells showed that total MeCP2 specifically recognized the C-terminal epitope of the MeCP2 protein. Total MeCP2 antibody failed to detect any signal from overexpression of C-terminal deletion MeCP2 (ΔC-MeCP2). The flag antibody proved the successful transfection of ΔC-MeCP2 expression plasmid into the cells. Scale bar: 10 μM
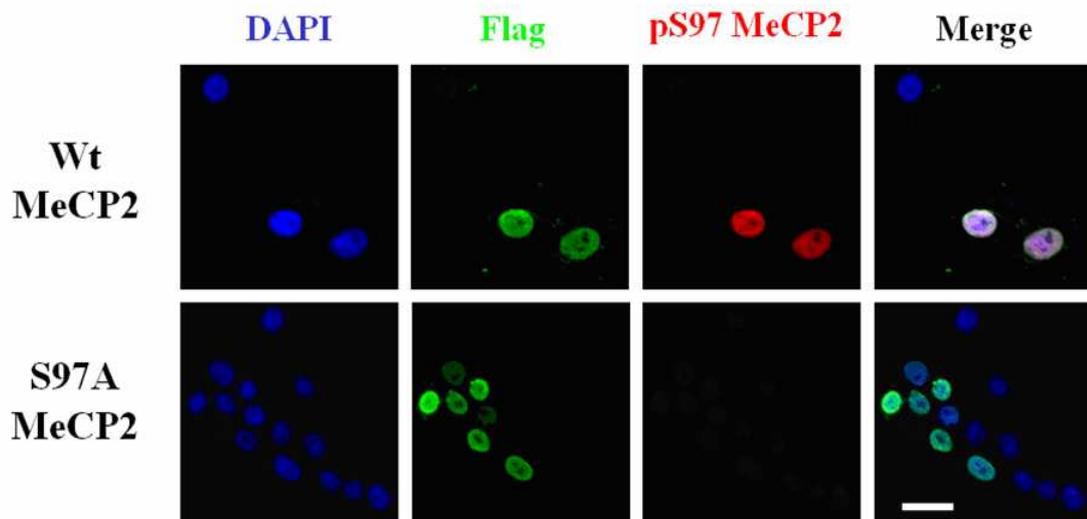
Figure 44. pS97-MeCP2 antibody validation using immunocytochemistry. Immunostaining of Flag-tagged wild type and mutated form (serine 97 to alanine) MeCP2 in LLC-PK1 cells showed pS97-MeCP2 antibody specifically recognized phosphor-serine 97 of MeCP2 protein in the cell nuclei. pS97-MeCP2 antibody failed to detect any signal from overexpression of mutated form (S97A) of MeCP2. The flag antibody proved the successful transfection of S97A-MeCP2 expression plasmid into the cells. Scale bar: 10 μM
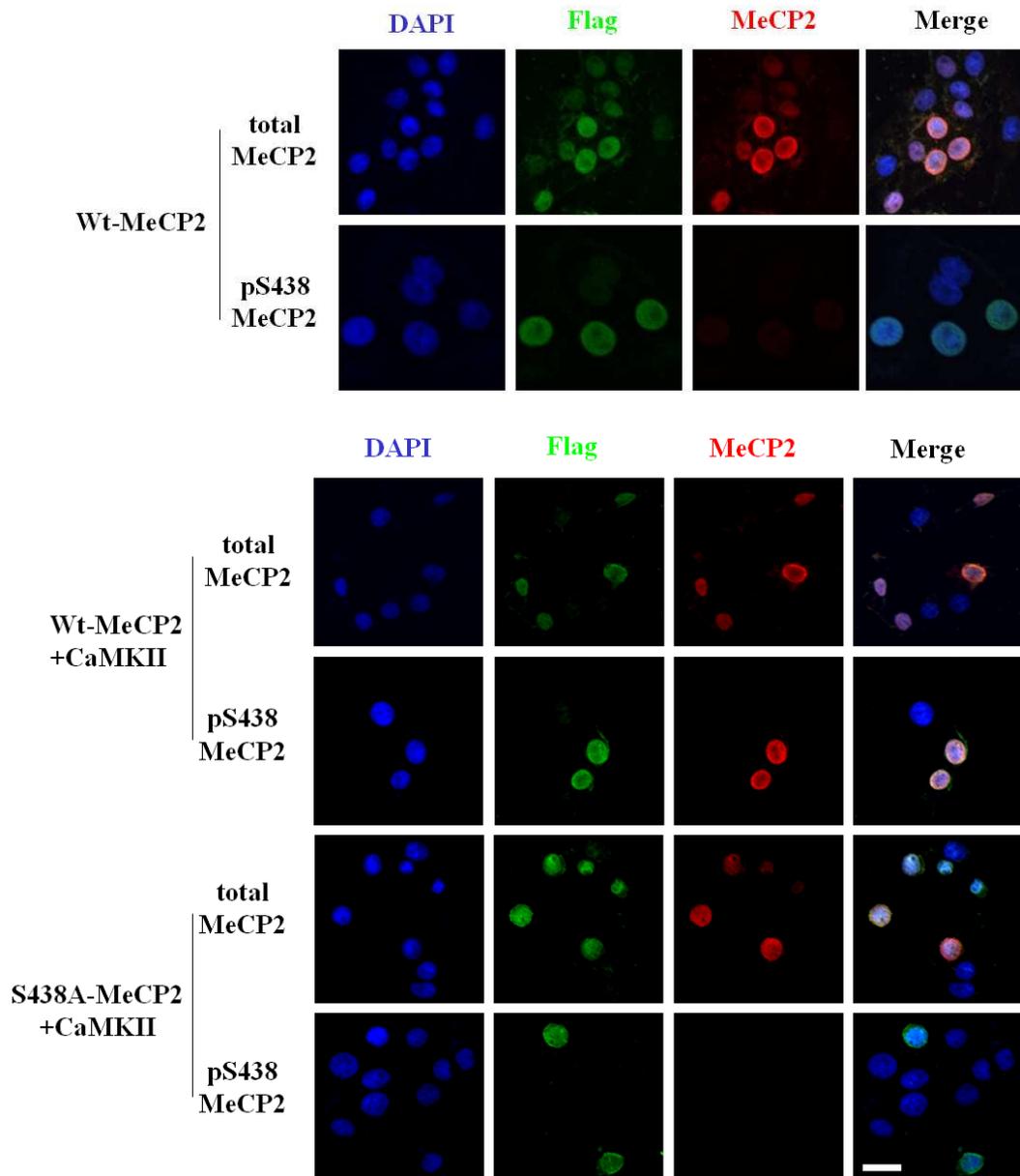
Figure 45. pS438 MeCP2 antibody validation using immunocytochemistry. Immunostaining of Flag-tagged wild type and S438A phosphorylation site MeCP2 in LLC-PK1 cells showed pS438 MeCP2 specifically recognized phosphor-serine 438 of MECP2 protein in the cell nuclei. pS97 MeCP2 antibody failed to detect any signal from overexpression of mutated form (serine 97 to alanine) of MeCP2. The Flag antibody proved the successful transfection of MeCP2 expression plasmids to the cells. Scale bar: 10 μM

4 Discussion

4.1 Early life stress programs HPA axis activity

In rodents and humans, adverse experience during early life can result in long-term changes in neuroendocrine, behavioral and cognitive functions as well as alterations in metabolism. In an attempt to find out more about the detailed mechanisms responsible for these alterations, this study used a mouse model of early life stress (ELS): 3 hours daily maternal separation. Previous research showed that the first ten days of life is very critical time window for development of the mouse brain. So, interruption of the normal maternal-pup interaction during this period is considered as a severe stressor and determinant of mouse physiology and behavior, reflected in long-lasting activation of the HPA axis in C57BL/6N mice. In this study, mouse subjected to ELS exposure were found to have larger adrenals and a smaller thymus gland, both physiological correlates of prolonged activation of the HPA axis. In addition, corticosterone secretion was significantly increased for between 6 weeks and 1 year. Further, *Pomc* mRNA levels in the pituitary were markedly increased, as shown by qRT-PCR and *in situ* hybridization.

4.2 Altered DNA methylation after ELS

Previous experiments indicated that maternal behavior can epigenetically program gene expression (Weaver et al., 2004; Murgatroyd et al., 2009). In the present study using an inbred mouse strain, all the mice were housed in the same environment with food and water *ad libitum*; thus, maternal separation was the only environmental variable imposed. The results obtained show that ELS leads to hypomethylation of a key regulatory region of the pituitary *Pomc* gene. These epigenetic events are accompanied by persistent upregulation of *Pomc* mRNA expression, and consequently, sustained hyperactivation of the HPA axis; the ELS-induced endocrine phenotype lasted for at least 1 year. In addition, previous experiments from this laboratory (Murgatroyd et al., 2009) on the same cohort of mice found that ELS mice displayed increased immobility in the forced swim test, which is an index of depression-like behavior in rodents, consistent with the well-established links between hypersecretion of adrenocorticoids and mood disturbances in humans.

Growing evidence suggests that epigenetic mechanisms, such as DNA methylation, affect gene expression in an age-dependent manner. For example, the amount of total 5-methylated cytosine was decreased in DNA extracted from uncultured peripheral blood human lymphocyte compared between young donors and old subjects (Singhal et al., 1987; Drinkwater et al., 1989), and a gradual global loss of cytosine DNA methylation was observed in various mouse, rat and human tissues (Wilson et al., 1987; Fuke et al., 2004). These observations indicate the possible importance of DNA methylation in the ageing process. Global hypomethylation has been proposed to affect genetic stability and might be a mechanism responsible for cellular senescence (Suzuki et al., 2002).

Besides global DNA hypomethylation, some specific genes display hypermethylation during ageing, probably resulting in the the inactivation of key regulatory genes in cancer (Ottaviano et al., 1994; Li et al., 2005; Esteller, 2008). In prostate cancer, hypermethylation of the pi-class glutathione S-transferase gene (GSTP1) promoter was reported as a very common genomic alteration. As a consequence, GSTP1 expression is lost even at the earliest stages of tumorigenesis (Lee et al., 1994).

In this work, DNA methylation drifts during ageing were found at the *Pomc* gene locus. In male control mice, analysis of overall DNA methylation at the distal promoter revealed a steady age-related decrease of DNA methylation: from 60% at 6 weeks to 30% at 1 year as shown in Figure 16. ELS mice also displayed age-associated DNA hypomethylation, but the effects occurred much earlier than in controls. In contrast, DNA methylation levels in females changed less during the ageing process, both in the control and ELS groups. In fact, a functional correlation between age-associated DNA hypomethylation and increased *Pomc* transcription in the pituitary was observed. These data agree with previous reports that *Pomc* mRNA levels increase with age (Nelson et al., 1988).

In addition to the observed associations of DNA methylation levels with age, there is evidence that DNA methylation levels are also influenced by gender. Several studies found higher global DNA methylation levels in males (Fuke et al., 2004; El-Maarri et al., 2007). Gender differences in DNA methylation can also occur in a gene-specific manner. For example, gender-specific DNA methylation differences have

been intensively investigated with respect to the ERα promoter and a recent report suggested that maternal behavior in rodents might regulate DNA methylation status in ERα promoter and therefore be responsible for long-lasting effects on gender-specific ERα gene expression (Champagne et al., 2006; Kurian et al., 2010). Specifically, Champagne and coworkers indicated that variations in maternal care during the early postnatal period affect ERα expression in the medial preoptic area (MPOA) by altering ERα promoter methylation and that ERα expression is higher in the offspring of high LG-ABN dams (Champagne et al., 2006). Correspondingly, the levels of cytosine methylation across the ERα promoter were decreased in the adult female offspring of high LG mothers, compared with low LG mothers. In another experiment, Kurian and colleagues showed that the natural variation in maternal care might be responsible for the gender-difference in behavior and neuronal morphology in adulthood (Kurian et al., 2010). These authors found that sex differences in DNA methylation of the ERα promoter within the developing rat preoptic area (POA), with males exhibiting more DNA methylation within ERα promoter than females. They suggested that maternal behavior plays a role in this gender-specific pattern of DNA methylation. Since the rodent mother tends to groom the anogenital region of her male offspring, it was proposed that grooming behavior may lead to increased estradiol secretion, thereby down-regulating ERα expression by increasing methylation at the ERα promoter. Together, these results suggest that maternal behavior in early life may leave stable epigenetic marks in the genome that organizes long-lasting sex differences in the brain.

Gender-specific DNA methylation differences were found at the *Pomc* gene locus in the pituitary in the present research. Males exhibited more DNA methylation within the *Pomc* distal promoter than females as revealed by bisulfite mapping of the entire promoter region and part of coding region (Figure 16). Notably, gender-specific differences were only found in the distal promoter region known to be important for *Pomc* gene expression in transfection experiments (Figure 18). Gender differences in DNA methylation were negatively correlated with *Pomc* gene expression in the pituitary, with higher levels of *Pomc* mRNA in female mice compared to male mice. Clinical reports indicate that men and women have different susceptibilities to a number of diseases. Concerning psychiatric disorders, women develop anxiety, depression, phobia, or panic disorders more often than men, whereas men more often

display antisocial behavior and substance abuse (Bebbington, 1996; Weich et al., 2001). From the present results, it would appear that increased expression of *Pomc* mRNA in female mice, resulting from hypomethylation in *Pomc* distal promoter, might contribute to differential susceptibility to psychiatric disorders between the genders.

4.3 Site-directed *in vitro* DNA methylation assay

Here, bisulfite sequencing revealed that DNA methylation decreased at the *Pomc* distal promoter after ELS. To prove a potential causal relationship between DNA methylation on *Pomc* expression, site-directed DNA methylation assays were performed. To this end, a CpG-free luciferase reporter (pCpGL-basic) was used. Since traditional luciferase vectors contain a number of CpG residues in the backbone that might repress a CpG-free promoter when the backbone DNA is methylated (Klug and Rehli, 2006), the novel pCpGL vector was designed so as to be free of CpGs in the entire sequence, and the reporter was only repressed in the presence of functionally important methylated CpG residues in the promoter fragment inserted. Results showed that if CpG 6−8 is methylated, *Pomc* luciferase activity is decreased by 40% (Figure 18). In another transfection experiment, deletion of this region (CpG 6−8) diminished reporter activity by 60%. All these results thus provide support for the functional importance of this region in the regulation of *Pomc* gene expression.

4.4 MeCP2 represses pituitary *Pomc* expression

DNA methylation is interpreted by a family of methyl-CpG-binding domain (MeCP) proteins which can recruit additional proteins (e.g. histone deacetylase (HDAC) and other chromatin remodeling complexes) to induce gene silencing. It was hypothesized that methylated DNA in the distal promoter region will recruit specific methyl-CpG-binding domain proteins to silence *Pomc* gene expression. To examine this, a series of MBD family proteins were co-transfected with methylated *Pomc* reporter constructs into the AtT20 cell line, derived from pituitary corticotropes. Our results showed that, compared with the other MBD family members, MeCP2 induced strong repression of *Pomc* expression. RT-PCR and western blot revealed that MeCP2 is strongly expressed in both, the pituitary *in vivo* and in AtT20 cells at the mRNA and protein

levels. These results with MeCP2 are the first to describe this protein's function as a repressor in the pituitary. Previous research on MeCP2 was predominantly focused on the brain, and it was not until recently that MeCP2 was reported to play a role in peripheral tissues such as cardiac and skeletal muscle (Alvarez-Saavedra et al., 2010). Since MeCP2 is widely expressed in a number of tissues, all of these new observations suggest roles of MeCP2 in non-neural tissues.

For high affinity DNA binding of MeCP2, two criteria must be met. The first one is the presence of methylated CpG dinucleotides; the second one is the presence of [AT≥4] runs close to a methylated CpG. Searching for potential binding sites in the *Pomc* DNA sequence revealed that both criteria were fulfilled in the distal promoter region; the 5' UTR region has AT runs but lacks CpG dinucleotides, whereas the coding region has CpGs but no AT runs. To test MeCP2 binding to *Pomc in vitro*, electrophoretic mobility shift assays (EMSAs) were performed, using recombinant MeCP2 and oligonucleotides that located in the distal promoter and core promoter region. Two pairs of oligonucleotides that covered the distal promoter region were designed, along with another oligonucleotide that targeted the middle region of the promoter to serve as a control. The results showed that MeCP2 preferentially binds to the methylated oligonucleotides in the distal promoter region of *Pomc*; in contrast, the control oligonucleotide did not bind, irrespective of whether it was methylated or not. Binding specificity was also tested by adding excess unlabelled oligonucleotides or by adding MeCP2 antibody. When unlabelled oligonucleotides or MeCP2 antibody was added to the reaction, MeCP2 binding was abolished. Further, a series of mutation studies showed the importance of methylated CpG and AT runs for MeCP2 binding. For example, when the wild type oligonucleotide was methylated at CpG6, about 5% of oligonucleotide was bound, whereas no binding was observed with unmethylated oligonucleotide. When one of the AT runs was mutated, binding was significantly affected, and an effect was seen when CpG7+8 were methylated. Taken together, these results indicate that the *Pomc* distal promoter (CpG6−8) contains context-specific, high-affinity MeCP2 DNA-binding sites that are important for the regulation of *Pomc* gene expression.

EMSA experiments indicated that MeCP2 binds to the *Pomc* distal promoter. In order to confirm the repressive function of MeCP2 at this locus, sequential ChIP

(seqChIP) on mouse pituitary was performed, using antibodies against either active (H3Ac) or repressive (H3K9me2) histone marks in the first round of ChIP. A second round of ChIP with anti-MeCP2 antibody showed that MeCP2 is preferentially associated with H3K9me2 at the *Pomc* promoter region. To further indentify the corepressor recuited by MeCP2 to the *Pomc* promoter, another seq-ChIP was performed on mouse pituitaries. MeCP2 antibody was used for the first round ChIP. In the second round, antibodies against either HDACs (Hdac1, Hdac2, Hdac4) or DNMTs (Dnmt1, Dnmt3a, Dnmt3b) were used. Sequential ChIP assays demonstrated that MeCP2 is associated with Hdac2 as well as Dnmt1 at the *Pomc* promoter. Previous literature indicated that HDAC2 and Brg1, the ATPase subunit of Swi/Snf complex, are involved in the GR-directed trans-repression of *Pomc* in the rat pituitary (Bilodeau et al., 2006). *In vivo*, Brg1 is required to stabilize the interaction between GR and Nur77 (also called NGFI-B) as well as between HDAC2 and Nur77. Nur77 residues in the NurRE site in the *Pomc* distal promoter region, where MeCP2 binds with high affinity. It should be noted that a number of reports have indicated an interaction between MeCP2 and HDACs (Nan et al., 1998; Suzuki et al., 2003); thus, it is possible that MeCP2 is also involved in GR-mediated trans-repression in the *Pomc* promoter and that Hdac2 mediates this event.

4.5 Experience-dependent phosphorylation of MeCP2

In the brain, neuronal activity can dynamically regulate gene transcription through phosphorylation of MeCP2 in response to diverse extracellular stimuli. For example, previous studies showed that phosphorylation of MeCP2 at serine 421 in cultured rat neurons precedes the release of MeCP2 from the Bdnf promoter, resulting in an increase in BDNF expression (Chen et al., 2003). It was shown that MeCP2 phosphorylation is controlled by neuron activity-dependent calcium influx and a CaMKII mediated mechanism. In spite of the ubiquitous expression of MeCP2 (Shahbazian et al., 2002b), its functions have so far only been studied in the context of the brain. Previous research pointed out that altered MeCP2 expression in cardiac and skeletal tissues has detrimental effects during normal development (Alvarez-Saavedra et al., 2010). Phospho-MeCP2(438) (homolous to rat phospho-421 MeCP2) antibody recognizes MeCP2 in the mouse heart isolated as early as E12.5 days, whereas MeCP2 cannot be detected in heart from adult mice or *Mecp2$^{-/Y}$* null mice. This

finding suggests that MeCP2 phosphorylation is not brain specific, and supports a functional role for MeCP2 in tissues besides brain. In the present study, it was found that MeCP2 is ubiquitously expressed in pituitary cells, with high expression in corticotrope cells. Moreover, MeCP2 was found to be phosphorylated at serine 438 in cultured mouse primary pituitary cells upon membrane depolarization by KCl (Figure 26B); the latter was associated with an increase in the expression of *Pomc* mRNA (Figure 29B). Notably, membrane depolarization induced phosphorylation of MeCP2 was not confined to corticotrope cells, as evidenced by the presence of phospho-438 MeCP2 in ACTH- positive and -negative cells (Figure 26B). The idea that MeCP2 phosphorylation is required for activity-dependent activation of the *Pomc* gene was supported by overexpression of a non-phosphorylatable mutant form of MeCP2 (S438A), which inhibits *Pomc* induction in response to active CaMKII; it was also shown that the latter inhibition is dependent on DNA binding (Figure 29). Thus, MeCP2 phosphorylation at serine 438 results in a decreased binding of MeCP2 to *Pomc* promoter.

MeCP2 phosphorylation occurs in response to physiological stimuli such as light exposure during the subjective night or cocaine administration (Mao et al., ; Zhou et al., 2006). It was therefore asked whether MeCP2 phosphorylation could be triggered in a psychological context in the pituitary. As we know, MeCP2 phosphorylation is driven by calcium influx and CaMKII activity. Previous research showed that AVP activates *Pomc* expression through binding to the V1b receptor at the corticotrope cell membrane; this event initiated calcium influx. Results shown in Figure 30 demonstrate that increased calcium levels stimulate CaMKII enzymatic activity, resulting in phosphorylation of MeCP2 in pituitary cells upon AVP stimulation. Interestingly, MeCP2 phosphorylation occurs predominantly in corticotrope cells expressing the AVP V1b receptor (Figure 30B). Supporting this, it was found that AVP-induced MeCP2 phosphorylation can be blocked by pre-treatment with the AVP V1b receptor antagonist---SSRI 149415 (Figure 30B). Specificity of the effect was further demonstrated in an experiment in corticotrope AtT20 cells which had been stably transfected with an AVP V1b receptor since they lack expression of this receptor (Figure 31).

Previous research in our laboratory has shown that ELS produces long-lasting elevations of the levels of AVP mRNA and peptide in the hypothalamus. The present results show that MeCP2 phosphorylation status can be dynamically regulated by AVP in pituitary cells (Figure 30). Taken together, these findings suggest that ELS can trigger the dynamic modification of MeCP2 via AVP stimulation. Our results demonstrate that early life adversity can lead to epigenetic marking of the genome by reducing MeCP2 occupancy at the *Pomc* promoter in ELS mice (Figure 34, 35).

During mammalian cell division, DNA methylation patterns can be faithfully copied to the newly synthesized daughter strand. This process depends on the maintenance of DNA methyltransferase activity. Pituitary cells proliferate postnatally, especially during the first postnatal days. During this process, a co-repressor complex, comprising MeCP2, Hdac2 and Dnmt1, appears to contribute to maintaining DNA methylation in dividing pituitary cells. Maternal separation induces AVP expression in the hypothalamic PVN which, in turn, leads to higher levels of MeCP2 phosphorylation. As a consequence, MeCP2 dissociates from the *Pomc* promoter, resulting in a loss of binding of co-repressors such as Hdac2 and Dnmt1. Dnmt1 is a methyltransferase which is responsible for maintenance of DNA methylation patterns during cell replication. Due to the loss of Dnmt1 binding at the *Pomc* promoter, when pituitary cells experienced mitosis, the DNA methylation pattern cannot be faithfully maintained, leading to passive DNA demethylation. On the other hand, the DNA methylation pattern is well preserved during pituitary cell mitosis in control animals due to the relatively higher levels of MeCP2 as well as Dnmt1 at the *Pomc* promoter.

4.6 Model

Early life stress produced long-lasting alterations of the HPA axis characterized by elevated corticosterone level, increased *Pomc* mRNA levels in the pituitary as well as hypersecretion of ACTH into the blood. Epigenetic mechanisms, especially DNA methylation, appear to be responsible for controlling *Pomc* gene expression by recruiting MeCP2 to silence the gene. We showed that ELS mice displayed reduced occupancy of MeCP2 at the *Pomc* promoter both in early postnatal days (PND10) and in adulthood (6 weeks). As shown previously, MeCP2 preferentially binds to methylated CpG residues. This decreased occupancy of MeCP2 in ELS mice at the

Pomc locus could result from hypo-methylation of multiple CpG residues (CpG 6–8) at the *Pomc* distal promoter region. As a consequence, reduced CpG methylation level weakened the MeCP2 binding affinity to its recognition sites. However, there seems to be a distinct MeCP2 binding pattern in early postnatal days. We observed a reduced MeCP2 occupancy in *Pomc* promoter region, which correlated with higher *Pomc* mRNA level in ELS mice, while this differential binding could not be explained by methylation alterations since there was no difference in DNA methylation between ELS mice and controls. This paradoxical finding implied that MeCP2 binding could be regulated by other mechanisms besides DNA methylation, such as phosphorylation.

Immunostaining of primary pituitary cells showed that MeCP2 is phosphorylated at serine 438 by membrane depolarization after KCl treatment. Interestingly, treatment of primary pituitary cells with hypothalamic peptide AVP could also induce MeCP2 phosphorylation at serine 438 by activation of CaMKII activity. MeCP2 serves as a platform, to which Hdac2 and Dnmt1 can bind, to repress *Pomc* gene activity. Pituitary cells proliferate postnatally, especially during the early postnal days. During this process, this co-repressor complex (MeCP2, Hdac2 and Dnmt1) could help the pituitary cells to maintain DNA methylation during pituitary cell mitosis. Maternal separation induced higher levels of AVP expression in the PVN of the hypothalamus which in turn leads to higher level of MeCP2 phosphorylation. As a consequence, MeCP2 becomes phosphorylated and dissociated from the *Pomc* promoter resulting in loss binding of co-repressor complex such as Hdac2 and Dnmt1. Dnmt1 is a methyltransferase which is responsible for maintenance of DNA methylation pattern during cell replication. Due to the loss of Dnmt1 binding at the Pomc promoter during mitosis, DNA methylation pattern could not be faithfully maintained, probably promoting passive DNA demethylation. On the contrary, in the control animals DNA methylation pattern is well preserved during pituitary cell mitosis since relatively higher level of MeCP2 as well as Dnmt1 are present at the *Pomc* promoter.
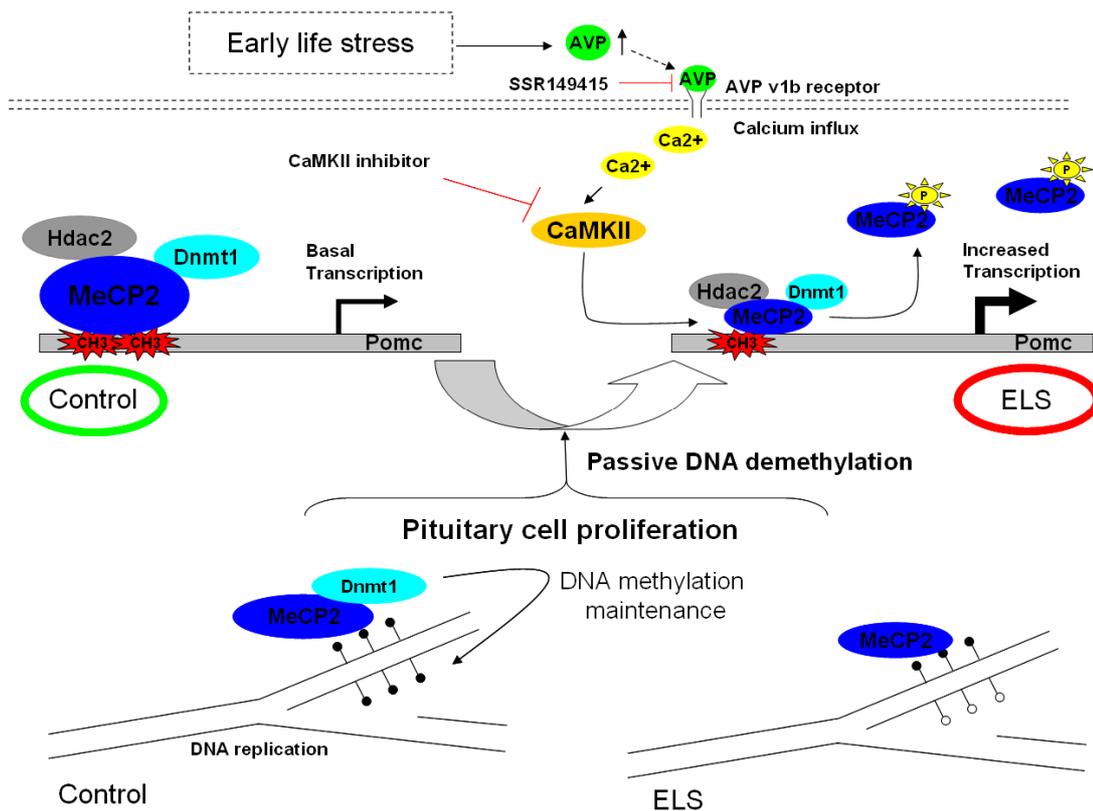
Figure 46. Model of how early life stress (ELS) leads to epigenetic upregulation of *Pomc* gene expression. Early life stress produces long-lasting increases in the activity of the HPA axis, characterized by increased pituitary *Pomc* mRNA expression, ACTH secretion and elevated levels of corticosterone. Epigenetic mechanisms, especially DNA methylation, appear to be responsible for controlling *Pomc* gene expression by recruiting MeCP2 to silence the gene under baseline (control) conditions. ELS mice display reduced occupancy of MeCP2 at the *Pomc* promoter, resulting from hypomethylation of multiple CpG residues (CpG 6−8) in the distal promoter region of *Pomc*. In addition, MeCP2 binding affinity is also regulated by phosphorylation at serine 438. When MeCP2 is phosphorylated at serine 438, the configuration of MeCP2 protein might change and MeCP2 dissociates from the *Pomc* promoter, leading to loss of binding of co-repressor complexes such as Hdac2 and Dnmt1. Pituitary cells proliferate postnatally. During this mitosis, co-repressor complexes (MeCP2, Hdac2 and Dnmt1) may facilitate maintenance of DNA methylation. The maternal separation (ELS) paradigm induces higher levels of AVP expression in the hypothalamic PVN (Murgatroyd et al., 2009) which, in turn, leads to higher levels of MeCP2 phosphorylation. As a consequence, MeCP2 proteins, together with co-repressor complexes, dissociate from the *Pomc* promoter, resulting in increased *Pomc* expression. Dnmt1 is a methyltransferase involved in maintenance of DNA methylation patterns during cell replication. It is hypothesized that loss of Dnmt1 binding at the *Pomc* promoter during mitosis, does not allow faithful duplication of the parental DNA methylation pattern and results in passive DNA demethylation. On the contrary, the DNA methylation pattern is well preserved during pituitary cell mitosis in control animals because of the relatively higher levels of MeCP2 and Dnmt1 at the *Pomc* promoter.

5 Summary

Early-life stress (ELS) can lead to enduring changes in the structure and function of neural circuits and endocrine pathways, resulting in altered vulnerability thresholds for stress-related disorders such as depression and anxiety.

The question addressed in this work was whether epigenetic mechanisms contribute to the long-term programming of altered hypothalamus-pituitary-adrenal axis activity in ELS (maternal separated on postnatal days 1-10) mice.

Adrenocorticotropic hormone (ACTH), a key pituitary mediator of the adrenocortical response to stress, is encoded by the proopiomelanocortin (*Pomc*) gene. Corticotropin releasing hormone (CRH) and arginine vasopressin (AVP) are the main upstream neural regulators of *Pomc* gene expression and the post-translational processing of its peptidergic products, whereas glucocorticoids, secreted by the adrenals in response to stress, exert negative feedback actions on Pomc synthesis and ACTH secretion. It was shown that *Pomc* mRNA level is persistently increased in ELS mice and leads to sustained hypersecretion of glucocorticoids. Interestingly, ELS causes a reduction in DNA methylation at a critical regulatory region of the *Pomc* gene; this occurs with some delay after onset of the stress and persists for up to 1 year. A series of experiments (including reporter-, EMSA-, IHC- and ChIP-assays) supported the concept that the adverse early-life event induces changes in *Pomc* gene methylation and results in persistently upregulated expression of the *Pomc* gene. Interestingly, stress-induced changes in DNA-methylation were found to be more pronounced in males than in females, raising the possibility that epigenetic encoding occurs in a sex-specific manner; this may help to explain sex differences in susceptibility to stress-related disorders.

Collectively, the results of this study indicate that epigenetic mechanisms can serve to translate environmental cues into stable changes ("cellular memory") in gene expression in post-mitotic tissues, without the need for alterations in the genetic code.

Keywords: early life stress (ELS), proopiomelanocortin (*Pomc*), epigenetics, DNA methylation, MeCP2

6 References

Aguilera G, Harwood JP, Wilson JX, Morell J, Brown JH, Catt KJ (1983) Mechanisms of action of corticotropin-releasing factor and other regulators of corticotropin release in rat pituitary cells. J Biol Chem 258:8039-8045.

Aisa B, Elizalde N, Tordera R, Lasheras B, Del Rio J, Ramirez MJ (2009) Effects of neonatal stress on markers of synaptic plasticity in the hippocampus: implications for spatial memory. Hippocampus 19:1222-1231.

Alvarez-Saavedra M, Carrasco L, Sura-Trueba S, Demarchi Aiello V, Walz K, Neto JX, Young JI (2010) Elevated expression of MeCP2 in cardiac and skeletal tissues is detrimental for normal development. Hum Mol Genet 19:2177-2190.

Amir RE, Van den Veyver IB, Wan M, Tran CQ, Francke U, Zoghbi HY (1999) Rett syndrome is caused by mutations in X-linked MECP2, encoding methyl-CpG-binding protein 2. Nat Genet 23:185-188.

Anisman H, Zaharia MD, Meaney MJ, Merali Z (1998) Do early-life events permanently alter behavioral and hormonal responses to stressors Int J Dev Neurosci 16:149-164.

Arborelius L, Owens MJ, Plotsky PM, Nemeroff CB (1999) The role of corticotropin-releasing factor in depression and anxiety disorders. J Endocrinol 160:1-12.

Ariani F, Mari F, Pescucci C, Longo I, Bruttini M, Meloni I, Hayek G, Rocchi R, Zappella M, Renieri A (2004) Real-time quantitative PCR as a routine method for screening large rearrangements in Rett syndrome: Report of one case of MECP2 deletion and one case of MECP2 duplication. Hum Mutat 24:172-177.

Barres R, Osler ME, Yan J, Rune A, Fritz T, Caidahl K, Krook A, Zierath JR (2009) Non-CpG methylation of the PGC-1alpha promoter through DNMT3B controls mitochondrial density. Cell Metab 10:189-198.

Bebbington P (1996) The origin of sex differences in depressive disorder: bridging the gap. Int Rev Psychiatry 8:295-332.

Bilodeau S, Vallette-Kasic S, Gauthier Y, Figarella-Branger D, Brue T, Berthelet F, Lacroix A, Batista D, Stratakis C, Hanson J, Meij B, Drouin J (2006) Role of Brg1 and HDAC2 in GR trans-repression of the pituitary POMC gene and misexpression in Cushing disease. Genes Dev 20:2871-2886.

Bird A (2002) DNA methylation patterns and epigenetic memory. Genes Dev 16:6-21.

Bird A (2007) Perceptions of epigenetics. Nature 447:396-398.

Bird AP (1986) CpG-rich islands and the function of DNA methylation. Nature 321:209-213.

Bourc'his D, Xu GL, Lin CS, Bollman B, Bestor TH (2001) Dnmt3L and the establishment of maternal genomic imprints. Science 294:2536-2539.

Buonassisi V, Sato G, Cohen AI (1962) Hormone-producing cultures of adrenal and pituitary tumor origin. Proc Natl Acad Sci U S A 48:1184-1190.

Caldji C, Francis D, Sharma S, Plotsky PM, Meaney MJ (2000) The effects of early rearing environment on the development of GABAA and central benzodiazepine receptor levels and novelty-induced fearfulness in the rat. Neuropsychopharmacology 22:219-229.

Campanero MR, Armstrong MI, Flemington EK (2000) CpG methylation as a mechanism for the regulation of E2F activity. Proc Natl Acad Sci U S A 97:6481-6486.

Chahrour M, Jung SY, Shaw C, Zhou X, Wong ST, Qin J, Zoghbi HY (2008) MeCP2, a key contributor to neurological disease, activates and represses transcription. Science 320:1224-1229.

Champagne FA, Weaver IC, Diorio J, Dymov S, Szyf M, Meaney MJ (2006) Maternal care associated with methylation of the estrogen receptor-alpha1b promoter and estrogen receptor-alpha expression in the medial preoptic area of female offspring. Endocrinology 147:2909-2915.

Chandler SP, Guschin D, Landsberger N, Wolffe AP (1999) The methyl-CpG binding transcriptional repressor MeCP2 stably associates with nucleosomal DNA. Biochemistry 38:7008-7018.

Chen CL, Mather JP, Morris PL, Bardin CW (1984) Expression of pro-opiomelanocortin-like gene in the testis and epididymis. Proc Natl Acad Sci U S A 81:5672-5675.

Chen CL, Chang CC, Krieger DT, Bardin CW (1986) Expression and regulation of proopiomelanocortin-like gene in the ovary and placenta: comparison with the testis. Endocrinology 118:2382-2389.

Chen RZ, Akbarian S, Tudor M, Jaenisch R (2001) Deficiency of methyl-CpG binding protein-2 in CNS neurons results in a Rett-like phenotype in mice. Nat Genet 27:327-331.

Chen WG, Chang Q, Lin Y, Meissner A, West AE, Griffith EC, Jaenisch R, Greenberg ME (2003) Derepression of BDNF transcription involves calcium-dependent phosphorylation of MeCP2. Science 302:885-889.

Cirulli F, Santucci D, Laviola G, Alleva E, Levine S (1994) Behavioral and hormonal responses to stress in the newborn mouse: effects of maternal deprivation and chlordiazepoxide. Dev Psychobiol 27:301-316.

Clark AJ, Lavender PM, Coates P, Johnson MR, Rees LH (1990) In vitro and in vivo analysis of the processing and fate of the peptide products of the short proopiomelanocortin mRNA. Mol Endocrinol 4:1737-1743.

Collins AL, Levenson JM, Vilaythong AP, Richman R, Armstrong DL, Noebels JL, David Sweatt J, Zoghbi HY (2004) Mild overexpression of MeCP2 causes a progressive neurological disorder in mice. Hum Mol Genet 13:2679-2689.

de Wilde EJ, Kienhorst IC, Diekstra RF, Wolters WH (1992) The relationship between adolescent suicidal behavior and life events in childhood and adolescence. Am J Psychiatry 149:45-51.

DeBold CR, Mufson EE, Menefee JK, Orth DN (1988) Proopiomelanocortin gene expression in a pheochromocytoma using upstream transcription initiation sites. Biochem Biophys Res Commun 155:895-900.

Dragich JM, Kim YH, Arnold AP, Schanen NC (2007) Differential distribution of the MeCP2 splice variants in the postnatal mouse brain. J Comp Neurol 501:526-542.

Drinkwater RD, Blake TJ, Morley AA, Turner DR (1989) Human lymphocytes aged in vivo have reduced levels of methylation in transcriptionally active and inactive DNA. Mutat Res 219:29-37.

Dube SR, Anda RF, Felitti VJ, Chapman DP, Williamson DF, Giles WH (2001) Childhood abuse, household dysfunction, and the risk of attempted suicide throughout the life span: findings from the Adverse Childhood Experiences Study. Jama 286:3089-3096.

Eden S, Constancia M, Hashimshony T, Dean W, Goldstein B, Johnson AC, Keshet I, Reik W, Cedar H (2001) An upstream repressor element plays a role in Igf2 imprinting. Embo J 20:3518-3525.

Ehrlich M, Gama-Sosa MA, Huang LH, Midgett RM, Kuo KC, McCune RA, Gehrke C (1982) Amount and distribution of 5-methylcytosine in human DNA from different types of tissues of cells. Nucleic Acids Res 10:2709-2721.

El-Maarri O, Becker T, Junen J, Manzoor SS, Diaz-Lacava A, Schwaab R, Wienker T, Oldenburg J (2007) Gender specific differences in levels of DNA methylation at selected loci from human total blood: a tendency toward higher methylation levels in males. Hum Genet 122:505-514.

Esteller M (2008) Epigenetics in cancer. N Engl J Med 358:1148-1159.

Evans CJ, Erdelyi E, Weber E, Barchas JD (1983) Identification of pro-opiomelanocortin-derived peptides in the human adrenal medulla. Science 221:957-960.

Filion GJ, Zhenilo S, Salozhin S, Yamada D, Prokhortchouk E, Defossez PA (2006) A family of human zinc finger proteins that bind methylated DNA and repress transcription. Mol Cell Biol 26:169-181.

Fraga MF, Ballestar E, Montoya G, Taysavang P, Wade PA, Esteller M (2003) The affinity of different MBD proteins for a specific methylated locus depends on their intrinsic binding properties. Nucleic Acids Res 31:1765-1774.

Friend JP (1979) Cell size and cell division of the anterior pituitary: time course in the growing rat. Experientia 35:1577-1578.

Fuke C, Shimabukuro M, Petronis A, Sugimoto J, Oda T, Miura K, Miyazaki T, Ogura C, Okazaki Y, Jinno Y (2004) Age related changes in 5-methylcytosine content in human peripheral leukocytes and placentas: an HPLC-based study. Ann Hum Genet 68:196-204.

Fuks F, Hurd PJ, Deplus R, Kouzarides T (2003a) The DNA methyltransferases associate with HP1 and the SUV39H1 histone methyltransferase. Nucleic Acids Res 31:2305-2312.

Fuks F, Hurd PJ, Wolf D, Nan X, Bird AP, Kouzarides T (2003b) The methyl-CpG-binding protein MeCP2 links DNA methylation to histone methylation. J Biol Chem 278:4035-4040.

Gardiner-Garden M, Frommer M (1987) CpG islands in vertebrate genomes. J Mol Biol 196:261-282.

Gardiner-Garden M, Frommer M (1994) Transcripts and CpG islands associated with the pro-opiomelanocortin gene and other neurally expressed genes. J Mol Endocrinol 12:365-382.

Gee CE, Chen CL, Roberts JL, Thompson R, Watson SJ (1983) Identification of proopiomelanocortin neurones in rat hypothalamus by in situ cDNA-mRNA hybridization. Nature 306:374-376.

Ghoshal K, Majumder S, Datta J, Motiwala T, Bai S, Sharma SM, Frankel W, Jacob ST (2004) Role of human ribosomal RNA (rRNA) promoter methylation and of

methyl-CpG-binding protein MBD2 in the suppression of rRNA gene expression. J Biol Chem 279:6783-6793.

Giguere V, Labrie F, Cote J, Coy DH, Sueiras-Diaz J, Schally AV (1982) Stimulation of cyclic AMP accumulation and corticotropin release by synthetic ovine corticotropin-releasing factor in rat anterior pituitary cells: site of glucocorticoid action. Proc Natl Acad Sci U S A 79:3466-3469.

Goll MG, Kirpekar F, Maggert KA, Yoder JA, Hsieh CL, Zhang X, Golic KG, Jacobsen SE, Bestor TH (2006) Methylation of tRNAAsp by the DNA methyltransferase homolog Dnmt2. Science 311:395-398.

Grammatopoulos DK, Chrousos GP (2002) Functional characteristics of CRH receptors and potential clinical applications of CRH-receptor antagonists. Trends Endocrinol Metab 13:436-444.

Guy J, Hendrich B, Holmes M, Martin JE, Bird A (2001) A mouse Mecp2-null mutation causes neurological symptoms that mimic Rett syndrome. Nat Genet 27:322-326.

Hagberg B, Aicardi J, Dias K, Ramos O (1983) A progressive syndrome of autism, dementia, ataxia, and loss of purposeful hand use in girls: Rett's syndrome: report of 35 cases. Ann Neurol 14:471-479.

Hardwick SA, Reuter K, Williamson SL, Vasudevan V, Donald J, Slater K, Bennetts B, Bebbington A, Leonard H, Williams SR, Smith RL, Cloosterman D, Christodoulou J (2007) Delineation of large deletions of the MECP2 gene in Rett syndrome patients, including a familial case with a male proband. Eur J Hum Genet 15:1218-1229.

Hermann A, Schmitt S, Jeltsch A (2003) The human Dnmt2 has residual DNA-(cytosine-C5) methyltransferase activity. J Biol Chem 278:31717-31721.

Hoffmann A, Spengler D (2008) A new coactivator function for Zac1's C2H2 zinc finger DNA-binding domain in selectively controlling PCAF activity. Mol Cell Biol 28:6078-6093.

Hoffmann A, Barz T, Spengler D (2006) Multitasking C2H2 zinc fingers link Zac DNA binding to coordinated regulation of p300-histone acetyltransferase activity. Mol Cell Biol 26:5544-5557.

Hoffmann A, Ciani E, Boeckardt J, Holsboer F, Journot L, Spengler D (2003) Transcriptional activities of the zinc finger protein Zac are differentially controlled by DNA binding. Mol Cell Biol 23:988-1003.

Holsboer F (2000) The corticosteroid receptor hypothesis of depression. Neuropsychopharmacology 23:477-501.

Horike S, Cai S, Miyano M, Cheng JF, Kohwi-Shigematsu T (2005) Loss of silent-chromatin looping and impaired imprinting of DLX5 in Rett syndrome. Nat Genet 37:31-40.

Horvath E, Kovacs K (1988) Pituitary gland. Pathol Res Pract 183:129-142.

Iguchi-Ariga SM, Schaffner W (1989) CpG methylation of the cAMP-responsive enhancer/promoter sequence TGACGTCA abolishes specific factor binding as well as transcriptional activation. Genes Dev 3:612-619.

Iversen AC, Fear NT, Simonoff E, Hull L, Horn O, Greenberg N, Hotopf M, Rona R, Wessely S (2007) Influence of childhood adversity on health among male UK military personnel. Br J Psychiatry 191:506-511.

Jaffee SR, Moffitt TE, Caspi A, Fombonne E, Poulton R, Martin J (2002) Differences in early childhood risk factors for juvenile-onset and adult-onset depression. Arch Gen Psychiatry 59:215-222.

Jeannotte L, Burbach JP, Drouin J (1987) Unusual proopiomelanocortin ribonucleic acids in extrapituitary tissues: intronless transcripts in testes and long poly(A) tails in hypothalamus. Mol Endocrinol 1:749-757.

Johnson JG, Cohen P, Gould MS, Kasen S, Brown J, Brook JS (2002) Childhood adversities, interpersonal difficulties, and risk for suicide attempts during late adolescence and early adulthood. Arch Gen Psychiatry 59:741-749.

Jones PL, Veenstra GJ, Wade PA, Vermaak D, Kass SU, Landsberger N, Strouboulis J, Wolffe AP (1998) Methylated DNA and MeCP2 recruit histone deacetylase to repress transcription. Nat Genet 19:187-191.

Jordan C, Li HH, Kwan HC, Francke U (2007) Cerebellar gene expression profiles of mouse models for Rett syndrome reveal novel MeCP2 targets. BMC Med Genet 8:36.

Kendler KS, Kessler RC, Walters EE, MacLean C, Neale MC, Heath AC, Eaves LJ (1995) Stressful life events, genetic liability, and onset of an episode of major depression in women. Am J Psychiatry 152:833-842.

Kimura H, Shiota K (2003) Methyl-CpG-binding protein, MeCP2, is a target molecule for maintenance DNA methyltransferase, Dnmt1. J Biol Chem 278:4806-4812.

Klebe RR (1969) Neuroblastoma: cell culture analysis of a differentiating stem cell system. . J Cell Biol 43:69A.

Klose RJ, Sarraf SA, Schmiedeberg L, McDermott SM, Stancheva I, Bird AP (2005) DNA binding selectivity of MeCP2 due to a requirement for A/T sequences adjacent to methyl-CpG. Mol Cell 19:667-678.

Klug M, Rehli M (2006) Functional analysis of promoter CpG methylation using a CpG-free luciferase reporter vector. Epigenetics 1:127-130.

Kokura K, Kaul SC, Wadhwa R, Nomura T, Khan MM, Shinagawa T, Yasukawa T, Colmenares C, Ishii S (2001) The Ski protein family is required for MeCP2-mediated transcriptional repression. J Biol Chem 276:34115-34121.

Kovalovsky D, Refojo D, Liberman AC, Hochbaum D, Pereda MP, Coso OA, Stalla GK, Holsboer F, Arzt E (2002) Activation and induction of NUR77/NURR1 in corticotrophs by CRH/cAMP: involvement of calcium, protein kinase A, and MAPK pathways. Mol Endocrinol 16:1638-1651.

Kriaucionis S, Bird A (2004) The major form of MeCP2 has a novel N-terminus generated by alternative splicing. Nucleic Acids Res 32:1818-1823.

Kurian JR, Olesen KM, Auger AP (2010) Sex differences in epigenetic regulation of the estrogen receptor-alpha promoter within the developing preoptic area. Endocrinology 151:2297-2305.

Kuryshev YA, Childs GV, Ritchie AK (1996) Corticotropin-releasing hormone stimulates Ca2+ entry through L- and P-type Ca2+ channels in rat corticotropes. Endocrinology 137:2269-2277.

Lacaze-Masmonteil T, de Keyzer Y, Luton JP, Kahn A, Bertagna X (1987) Characterization of proopiomelanocortin transcripts in human nonpituitary tissues. Proc Natl Acad Sci U S A 84:7261-7265.

Lee WH, Morton RA, Epstein JI, Brooks JD, Campbell PA, Bova GS, Hsieh WS, Isaacs WB, Nelson WG (1994) Cytidine methylation of regulatory sequences near

the pi-class glutathione S-transferase gene accompanies human prostatic carcinogenesis. Proc Natl Acad Sci U S A 91:11733-11737.

Levine S (1994) The ontogeny of the hypothalamic-pituitary-adrenal axis. The influence of maternal factors. Ann N Y Acad Sci 746:275-288; discussion 289-293.

Levine S (2001) Primary social relationships influence the development of the hypothalamic--pituitary--adrenal axis in the rat. Physiol Behav 73:255-260.

Lewis JD, Meehan RR, Henzel WJ, Maurer-Fogy I, Jeppesen P, Klein F, Bird A (1992) Purification, sequence, and cellular localization of a novel chromosomal protein that binds to methylated DNA. Cell 69:905-914.

Li E, Bestor TH, Jaenisch R (1992) Targeted mutation of the DNA methyltransferase gene results in embryonic lethality. Cell 69:915-926.

Li LC, Carroll PR, Dahiya R (2005) Epigenetic changes in prostate cancer: implication for diagnosis and treatment. J Natl Cancer Inst 97:103-115.

Lippmann M, Bress A, Nemeroff CB, Plotsky PM, Monteggia LM (2007) Long-term behavioural and molecular alterations associated with maternal separation in rats. Eur J Neurosci 25:3091-3098.

Lister R, Pelizzola M, Dowen RH, Hawkins RD, Hon G, Tonti-Filippini J, Nery JR, Lee L, Ye Z, Ngo QM, Edsall L, Antosiewicz-Bourget J, Stewart R, Ruotti V, Millar AH, Thomson JA, Ren B, Ecker JR (2009) Human DNA methylomes at base resolution show widespread epigenomic differences. Nature 462:315-322.

Litvin Y, PasMantier R, Fleischer N, Erlichman J (1984) Hormonal activation of the cAMP-dependent protein kinases in AtT20 cells. Preferential activation of protein kinase I by corticotropin releasing factor, isoproterenol, and forskolin. J Biol Chem 259:10296-10302.

Liu D, Diorio J, Tannenbaum B, Caldji C, Francis D, Freedman A, Sharma S, Pearson D, Plotsky PM, Meaney MJ (1997) Maternal care, hippocampal glucocorticoid receptors, and hypothalamic-pituitary-adrenal responses to stress. Science 277:1659-1662.

Lolait SJ, Clements JA, Markwick AJ, Cheng C, McNally M, Smith AI, Funder JW (1986) Pro-opiomelanocortin messenger ribonucleic acid and posttranslational processing of beta endorphin in spleen macrophages. J Clin Invest 77:1776-1779.

Luikenhuis S, Giacometti E, Beard CF, Jaenisch R (2004) Expression of MeCP2 in postmitotic neurons rescues Rett syndrome in mice. Proc Natl Acad Sci U S A 101:6033-6038.

Majumder S, Ghoshal K, Datta J, Smith DS, Bai S, Jacob ST (2006) Role of DNA methyltransferases in regulation of human ribosomal RNA gene transcription. J Biol Chem 281:22062-22072.

Makedonski K, Abuhatzira L, Kaufman Y, Razin A, Shemer R (2005) MeCP2 deficiency in Rett syndrome causes epigenetic aberrations at the PWS/AS imprinting center that affects UBE3A expression. Hum Mol Genet 14:1049-1058.

Mao LM, Horton E, Guo ML, Xue B, Jin DZ, Fibuch EE, Wang JQ Cocaine increases phosphorylation of MeCP2 in the rat striatum in vivo: A differential role of NMDA receptors. Neurochem Int 59:610-617.

Margot JB, Ehrenhofer-Murray AE, Leonhardt H (2003) Interactions within the mammalian DNA methyltransferase family. BMC Mol Biol 4:7.

Martinowich K, Hattori D, Wu H, Fouse S, He F, Hu Y, Fan G, Sun YE (2003) DNA methylation-related chromatin remodeling in activity-dependent BDNF gene regulation. Science 302:890-893.

Matthews K, Robbins TW (2003) Early experience as a determinant of adult behavioural responses to reward: the effects of repeated maternal separation in the rat. Neurosci Biobehav Rev 27:45-55.

McGowan PO, Sasaki A, D'Alessio AC, Dymov S, Labonte B, Szyf M, Turecki G, Meaney MJ (2009) Epigenetic regulation of the glucocorticoid receptor in human brain associates with childhood abuse. Nat Neurosci 12:342-348.

Meins M, Lehmann J, Gerresheim F, Herchenbach J, Hagedorn M, Hameister K, Epplen JT (2005) Submicroscopic duplication in Xq28 causes increased expression of the MECP2 gene in a boy with severe mental retardation and features of Rett syndrome. J Med Genet 42:e12.

Mnatzakanian GN, Lohi H, Munteanu I, Alfred SE, Yamada T, MacLeod PJ, Jones JR, Scherer SW, Schanen NC, Friez MJ, Vincent JB, Minassian BA (2004) A previously unidentified MECP2 open reading frame defines a new protein isoform relevant to Rett syndrome. Nat Genet 36:339-341.

Moore HP, Gumbiner B, Kelly RB (1983a) A subclass of proteins and sulfated macromolecules secreted by AtT-20 (mouse pituitary tumor) cells is sorted with adrenocorticotropin into dense secretory granules. J Cell Biol 97:810-817.

Moore HP, Gumbiner B, Kelly RB (1983b) Chloroquine diverts ACTH from a regulated to a constitutive secretory pathway in AtT-20 cells. Nature 302:434-436.

Murgatroyd C, Wu Y, Bockmuhl Y, Spengler D (2010) Genes learn from stress: How infantile trauma programs us for depression. Epigenetics 5.

Murgatroyd C, Patchev AV, Wu Y, Micale V, Bockmuhl Y, Fischer D, Holsboer F, Wotjak CT, Almeida OF, Spengler D (2009) Dynamic DNA methylation programs persistent adverse effects of early-life stress. Nat Neurosci 12:1559-1566.

Nan X, Ng HH, Johnson CA, Laherty CD, Turner BM, Eisenman RN, Bird A (1998) Transcriptional repression by the methyl-CpG-binding protein MeCP2 involves a histone deacetylase complex. Nature 393:386-389.

Nelson JF, Bender M, Schachter BS (1988) Age-related changes in proopiomelanocortin messenger ribonucleic acid levels in hypothalamus and pituitary of female C57BL/6J mice. Endocrinology 123:340-344.

Newell-Price J, King P, Clark AJ (2001) The CpG island promoter of the human proopiomelanocortin gene is methylated in nonexpressing normal tissue and tumors and represses expression. Mol Endocrinol 15:338-348.

Newport DJ, Stowe ZN, Nemeroff CB (2002) Parental depression: animal models of an adverse life event. Am J Psychiatry 159:1265-1283.

Okano M, Xie S, Li E (1998a) Cloning and characterization of a family of novel mammalian DNA (cytosine-5) methyltransferases. Nat Genet 19:219-220.

Okano M, Xie S, Li E (1998b) Dnmt2 is not required for de novo and maintenance methylation of viral DNA in embryonic stem cells. Nucleic Acids Res 26:2536-2540.

Okano M, Bell DW, Haber DA, Li E (1999) DNA methyltransferases Dnmt3a and Dnmt3b are essential for de novo methylation and mammalian development. Cell 99:247-257.

Olmsted JB, Carlson K, Klebe R, Ruddle F, Rosenbaum J (1970) Isolation of microtubule protein from cultured mouse neuroblastoma cells. Proc Natl Acad Sci U S A 65:129-136.

Ottaviano YL, Issa JP, Parl FF, Smith HS, Baylin SB, Davidson NE (1994) Methylation of the estrogen receptor gene CpG island marks loss of estrogen receptor expression in human breast cancer cells. Cancer Res 54:2552-2555.

Perantoni A, Berman JJ (1979) Properties of Wilms' tumor line (TuWi) and pig kidney line (LLC-PK1) typical of normal kidney tubular epithelium. In Vitro 15:446-454.

Percy AK (2002) Rett syndrome. Current status and new vistas. Neurol Clin 20:1125-1141.

Plagemann A, Harder T, Brunn M, Harder A, Roepke K, Wittrock-Staar M, Ziska T, Schellong K, Rodekamp E, Melchior K, Dudenhausen JW (2009) Hypothalamic proopiomelanocortin promoter methylation becomes altered by early overfeeding: an epigenetic model of obesity and the metabolic syndrome. J Physiol 587:4963-4976.

Planas-Silva MD, Means AR (1992) Expression of a constitutive form of calcium/calmodulin dependent protein kinase II leads to arrest of the cell cycle in G2. Embo J 11:507-517.

Plotsky PM, Kjaer A, Sutton SW, Sawchenko PE, Vale W (1991) Central activin administration modulates corticotropin-releasing hormone and adrenocorticotropin secretion. Endocrinology 128:2520-2525.

Pohorecky LA (1981) The interaction of alcohol and stress. A review. Neurosci Biobehav Rev 5:209-229.

Pohorecky LA (2006) Housing and rank status of male Long-Evans rats modify ethanol's effect on open-field behaviors. Psychopharmacology (Berl) 185:289-297.

Pratt KG, Watt AJ, Griffith LC, Nelson SB, Turrigiano GG (2003) Activity-dependent remodeling of presynaptic inputs by postsynaptic expression of activated CaMKII. Neuron 39:269-281.

Prokhortchouk A, Hendrich B, Jorgensen H, Ruzov A, Wilm M, Georgiev G, Bird A, Prokhortchouk E (2001) The p120 catenin partner Kaiso is a DNA methylation-dependent transcriptional repressor. Genes Dev 15:1613-1618.

Quaderi NA, Meehan RR, Tate PH, Cross SH, Bird AP, Chatterjee A, Herman GE, Brown SD (1994) Genetic and physical mapping of a gene encoding a methyl CpG binding protein, Mecp2, to the mouse X chromosome. Genomics 22:648-651.

Reisine T, Rougon G, Barbet J, Affolter HU (1985) Corticotropin-releasing factor-induced adrenocorticotropin hormone release and synthesis is blocked by incorporation of the inhibitor of cyclic AMP-dependent protein kinase into anterior pituitary tumor cells by liposomes. Proc Natl Acad Sci U S A 82:8261-8265.

Rice P, Longden I, Bleasby A (2000) EMBOSS: the European Molecular Biology Open Software Suite. Trends Genet 16:276-277.

Richards EJ (2006) Inherited epigenetic variation--revisiting soft inheritance. Nat Rev Genet 7:395-401.

Rikhye K, Tyrka AR, Kelly MM, Gagne GG, Jr., Mello AF, Mello MF, Price LH, Carpenter LL (2008) Interplay between childhood maltreatment, parental bonding, and gender effects: impact on quality of life. Child Abuse Negl 32:19-34.

Robertson KD, Uzvolgyi E, Liang G, Talmadge C, Sumegi J, Gonzales FA, Jones PA (1999) The human DNA methyltransferases (DNMTs) 1, 3a and 3b: coordinate mRNA expression in normal tissues and overexpression in tumors. Nucleic Acids Res 27:2291-2298.

Romeo RD, Mueller A, Sisti HM, Ogawa S, McEwen BS, Brake WG (2003) Anxiety and fear behaviors in adult male and female C57BL/6 mice are modulated by maternal separation. Horm Behav 43:561-567.

Rosenfeld P, Gutierrez YA, Martin AM, Mallett HA, Alleva E, Levine S (1991) Maternal regulation of the adrenocortical response in preweanling rats. Physiol Behav 50:661-671.

Russo VEA, Martienssen, R. A. & Riggs, A. D. (eds) (1996) Epigenetic Mechanisms of Gene Regulation. Cold Spring Harbor Laboratory Press, Woodbury.

Saito M, Ishikawa F (2002) The mCpG-binding domain of human MBD3 does not bind to mCpG but interacts with NuRD/Mi2 components HDAC1 and MTA2. J Biol Chem 277:35434-35439.

Samaco RC, Hogart A, LaSalle JM (2005) Epigenetic overlap in autism-spectrum neurodevelopmental disorders: MECP2 deficiency causes reduced expression of UBE3A and GABRB3. Hum Mol Genet 14:483-492.

Sapolsky RM, Meaney MJ (1986) Maturation of the adrenocortical stress response: neuroendocrine control mechanisms and the stress hyporesponsive period. Brain Res 396:64-76.

Sawchenko PE, Imaki T, Potter E, Kovacs K, Imaki J, Vale W (1993) The functional neuroanatomy of corticotropin-releasing factor. Ciba Found Symp 172:5-21; discussion 21-29.

Schapiro S, Geller E, Eiduson S (1962) Neonatal adrenal cortical response to stress and vasopressin. Proc Soc Exp Biol Med 109:937-941.

Schmidt MV, Oitzl MS, Levine S, de Kloet ER (2002) The HPA system during the postnatal development of CD1 mice and the effects of maternal deprivation. Brain Res Dev Brain Res 139:39-49.

Schmidt MV, Enthoven L, van der Mark M, Levine S, de Kloet ER, Oitzl MS (2003) The postnatal development of the hypothalamic-pituitary-adrenal axis in the mouse. Int J Dev Neurosci 21:125-132.

Serradeil-Le Gal C, Raufaste D, Derick S, Blankenstein J, Allen J, Pouzet B, Pascal M, Wagnon J, Ventura MA (2007) Biological characterization of rodent and human vasopressin V1b receptors using SSR-149415, a nonpeptide V1b receptor ligand. Am J Physiol Regul Integr Comp Physiol 293:R938-949.

Shahbazian M, Young J, Yuva-Paylor L, Spencer C, Antalffy B, Noebels J, Armstrong D, Paylor R, Zoghbi H (2002a) Mice with truncated MeCP2 recapitulate many Rett syndrome features and display hyperacetylation of histone H3. Neuron 35:243-254.

Shahbazian MD, Zoghbi HY (2001) Molecular genetics of Rett syndrome and clinical spectrum of MECP2 mutations. Curr Opin Neurol 14:171-176.

Shahbazian MD, Antalffy B, Armstrong DL, Zoghbi HY (2002b) Insight into Rett syndrome: MeCP2 levels display tissue- and cell-specific differences and correlate with neuronal maturation. Hum Mol Genet 11:115-124.

Singhal RP, Mays-Hoopes LL, Eichhorn GL (1987) DNA methylation in aging of mice. Mech Ageing Dev 41:199-210.

Slotten HA, Kalinichev M, Hagan JJ, Marsden CA, Fone KC (2006) Long-lasting changes in behavioural and neuroendocrine indices in the rat following neonatal maternal separation: gender-dependent effects. Brain Res 1097:123-132.

Spengler D, Waeber C, Pantaloni C, Holsboer F, Bockaert J, Seeburg PH, Journot L (1993) Differential signal transduction by five splice variants of the PACAP receptor. Nature 365:170-175.

Stanton ME, Gutierrez YR, Levine S (1988) Maternal deprivation potentiates pituitary-adrenal stress responses in infant rats. Behav Neurosci 102:692-700.

Suzuki M, Yamada T, Kihara-Negishi F, Sakurai T, Oikawa T (2003) Direct association between PU.1 and MeCP2 that recruits mSin3A-HDAC complex for PU.1-mediated transcriptional repression. Oncogene 22:8688-8698.

Suzuki T, Fujii M, Ayusawa D (2002) Demethylation of classical satellite 2 and 3 DNA with chromosomal instability in senescent human fibroblasts. Exp Gerontol 37:1005-1014.

Takai D, Jones PA (2002) Comprehensive analysis of CpG islands in human chromosomes 21 and 22. Proc Natl Acad Sci U S A 99:3740-3745.

Taniguchi Y, Kominami R, Yasutaka S, Kawarai Y (2000) Proliferation and differentiation of pituitary corticotrophs during the fetal and postnatal period: a quantitative immunocytochemical study. Anat Embryol (Berl) 201:229-234.

Taniguchi Y, Yasutaka S, Kominami R, Shinohara H (2002) Proliferation and differentiation of rat anterior pituitary cells. Anat Embryol (Berl) 206:1-11.

Tao J, Hu K, Chang Q, Wu H, Sherman NE, Martinowich K, Klose RJ, Schanen C, Jaenisch R, Wang W, Sun YE (2009) Phosphorylation of MeCP2 at Serine 80 regulates its chromatin association and neurological function. Proc Natl Acad Sci U S A 106:4882-4887.

Tatematsu KI, Yamazaki T, Ishikawa F (2000) MBD2-MBD3 complex binds to hemi-methylated DNA and forms a complex containing DNMT1 at the replication foci in late S phase. Genes Cells 5:677-688.

Timpl P, Spanagel R, Sillaber I, Kresse A, Reul JM, Stalla GK, Blanquet V, Steckler T, Holsboer F, Wurst W (1998) Impaired stress response and reduced anxiety in mice lacking a functional corticotropin-releasing hormone receptor 1. Nat Genet 19:162-166.

Tudor M, Akbarian S, Chen RZ, Jaenisch R (2002) Transcriptional profiling of a mouse model for Rett syndrome reveals subtle transcriptional changes in the brain. Proc Natl Acad Sci U S A 99:15536-15541.

Van Esch H, Bauters M, Ignatius J, Jansen M, Raynaud M, Hollanders K, Lugtenberg D, Bienvenu T, Jensen LR, Gecz J, Moraine C, Marynen P, Fryns JP, Froyen G (2005) Duplication of the MECP2 region is a frequent cause of severe mental retardation and progressive neurological symptoms in males. Am J Hum Genet 77:442-453.

Van Speybroeck L (2002) From epigenesis to epigenetics: the case of C. H. Waddington. Ann N Y Acad Sci 981:61-81.

Ventura MA, Rene P, de Keyzer Y, Bertagna X, Clauser E (1999) Gene and cDNA cloning and characterization of the mouse V3/V1b pituitary vasopressin receptor. J Mol Endocrinol 22:251-260.

Vita N, Laurent P, Lefort S, Chalon P, Lelias JM, Kaghad M, Le Fur G, Caput D, Ferrara P (1993) Primary structure and functional expression of mouse pituitary and human brain corticotrophin releasing factor receptors. FEBS Lett 335:1-5.

von Dreden G, Loeffler JP, Grimm C, Hollt V (1988) Influence of calcium ions on proopiomelanocortin mRNA levels in clonal anterior pituitary cells. Neuroendocrinology 47:32-37.

Waddington CH (1942) The epigenotype. Endeavour 1:18-20.

Wade PA, Gegonne A, Jones PL, Ballestar E, Aubry F, Wolffe AP (1999) Mi-2 complex couples DNA methylation to chromatin remodelling and histone deacetylation. Nat Genet 23:62-66.

Walker CD, Perrin M, Vale W, Rivier C (1986) Ontogeny of the stress response in the rat: role of the pituitary and the hypothalamus. Endocrinology 118:1445-1451.

Weaver IC, Cervoni N, Champagne FA, D'Alessio AC, Sharma S, Seckl JR, Dymov S, Szyf M, Meaney MJ (2004) Epigenetic programming by maternal behavior. Nat Neurosci 7:847-854.

Weber M, Hellmann I, Stadler MB, Ramos L, Paabo S, Rebhan M, Schubeler D (2007) Distribution, silencing potential and evolutionary impact of promoter DNA methylation in the human genome. Nat Genet 39:457-466.

Weich S, Sloggett A, Lewis G (2001) Social roles and the gender difference in rates of the common mental disorders in Britain: a 7-year, population-based cohort study. Psychol Med 31:1055-1064.

Wilson VL, Smith RA, Ma S, Cutler RG (1987) Genomic 5-methyldeoxycytidine decreases with age. J Biol Chem 262:9948-9951.

Xie S, Wang Z, Okano M, Nogami M, Li Y, He WW, Okumura K, Li E (1999) Cloning, expression and chromosome locations of the human DNMT3 gene family. Gene 236:87-95.

Ye L, Li X, Kong X, Wang W, Bi Y, Hu L, Cui B, Li X, Ning G (2005) Hypomethylation in the promoter region of POMC gene correlates with ectopic overexpression in thymic carcinoids. J Endocrinol 185:337-343.

Young JI, Hong EP, Castle JC, Crespo-Barreto J, Bowman AB, Rose MF, Kang D, Richman R, Johnson JM, Berget S, Zoghbi HY (2005) Regulation of RNA splicing by the methylation-dependent transcriptional repressor methyl-CpG binding protein 2. Proc Natl Acad Sci U S A 102:17551-17558.

Zhang LX, Levine S, Dent G, Zhan Y, Xing G, Okimoto D, Kathleen Gordon M, Post RM, Smith MA (2002) Maternal deprivation increases cell death in the infant rat brain. Brain Res Dev Brain Res 133:1-11.

Zhou Z, Hong EJ, Cohen S, Zhao WN, Ho HY, Schmidt L, Chen WG, Lin Y, Savner E, Griffith EC, Hu L, Steen JA, Weitz CJ, Greenberg ME (2006) Brain-specific phosphorylation of MeCP2 regulates activity-dependent Bdnf transcription, dendritic growth, and spine maturation. Neuron 52:255-269.

7 Abbreviations

7.1 Standard

^{35}S	Sulphor-isotope 35	5'UTR	5' Untranslated region
5hmC	5' Hydroxymethyl cytosine	5mC	5' Methyl cytosine
aa	Amino acids	A	Adenine
C	Cytosine	cDNA	Complementary DNA
cm,mm	Centimeter, Millimeter	cpm	Counts per Minute
DNA	Deoxyribonucleic acid	EMSA	Electrophoretic mobility shift assay
G	Guanine	g	Gram
h, min, sec	Hour, Minute, Second	kb	Kilobase
kDa	Kilodalton	l	Litre
μ	Micro	m	Milli
M	Molar	mRNA	Messenger RNA
n	Nano	OD	Optical density
PCR	Polymerase chain reaction	RNA	Ribonucleic acid
rRNA	Ribosomal RNA	RT	Room temperature
RT-PCR	Reverse transcription PCR	T	Thymine
Tm	Melting temperature	U	Uracil
Vol	Volume	W	Watt

7.2 Buffers and substances

Ac	Acetate	ATP	Adenosine-5'-triphosphate
BSA	Bovine serum albumin	ddH$_2$O	di-distilled water
DEPC	Diethylpyrocarbonate	DMEM	Dulbecco's Modified Eagle Medium
DMSO	Dimethyl sulfoxide	dNTP	Deoxyribonucleotide
DTT	Dithiothreitol	EDTA	Ethylendiamintetraacetate
FCS	Fetal calf serum	GST	Glutathione-S-transferase
HEPES	4-(2-hydroxyethyl)-1-piperazineethanesulfonic acid	IPTG	Isopropyl β-D-1-thiogalactopyranoside
PAGE	Polyacrylamid gel electrophoresis	PBS	Phosphate buffered saline
SDS	Sodium dodecyl sulfate	TBS	Tris-buffered saline

| TE | Tris-EDTA buffer | TEMED | Tetramethylethylenediamine |
| Tris | Tris-(hydroxymethyl)-aminomethane | X-Gal | Bromo-chloro-indolyl-galactopyranoside |

7.3 Non-standard

ACTH	Adrenocorticotropic hormone	AP-1	Activator protein 1
AVP	Arginine vasopressin	AVP v1bR	AVP v1b receptor
CaMKII	Calcium/calmodulin kinase II	cAMP	Cyclic adenosine monophosphate
CGI	CpG island	ChIP	Chromatin immunoprecipitation
CpG	Cytosine-phosphate- guanine	CRH	Corticotropin-releasing hormone
DEX	Dexamethasone	Dnmt	DNA-methyl-transferase
E.coli	*Escherichia coli*	ELS	Early-life stress
FLAG	DYKDDDDK	GAPDH	Glyceraldehyde-3-phosphate dehydrogenase
GR	Glucocorticoid receptor	H3Ac	Histone 3 acetylation
H3K9me2	Histone 3 lysine 9 dimethylation	HAT	Histone acetyltransferase
HDAC	Histone deacetylase	His	Histone
HPA	Hypothalamic-pituitary-adrenal	HPRT	Hypoxanthine guanine phosphoribosyl transferase
MeCP2	Methyl CpG binding protein 2	NGFI-B	Nerve growth factor-induced protein B
Nur77	Orphan receptor family nuclear protein	RNA Pol II	RNA polymerase II
POMC	Proopiomelanocortin	PVN	Paraventricular nucleus
SP1	Transcription factor SP1	SSRI	Selective serotonin re-uptake inhibitors

8 Acknowledgments

This work was performed at the Max Planck Institute of Psychiatry, in the laboratory of molecular endocrinology under the supervision of Dr. Dietmar Spengler.

First of all, I would also like to thank institute's head, Prof. Dr. Dr. Dr. h. c. Florian Holsboer for giving me the opportunity to work in this institute.

I would like to thank Prof. Dr. Rainer Landgraf for accepting me as his registered PhD student in Ludwig-Maximilians-Universität München. His help, support and encouragement have been indispensable for me to pursue the doctor's degree.

I would like to express my gratitude to Dr. Spenlger for offering me the chance to join his group and work on the scientific field of epigenetics. Thanks to Dr. Spengler for his supervision, his in-depth knowledge and valuable suggestions.

I am grateful to Dr. Osborne Almeida for his continuous help, support, patience, understanding, friendship, encouragement and concern during my stay. He has always been available to discuss all kinds of questions during my work, and has generously shared his knowledge and support.

I would like to thank Professor Dr. Günter K. Stalla and Dr. Ulrich Renner for their substantial support and encouragement to help me finish my PhD work and for giving me more perspective for my career.

I would like to thank Guillaume Daniel, Yannick Menger and Dr. Alexandre Patchev for their enthusiastic help with the experiments and also for their substantial support during my PhD life.

I would like to thank all my colleagues in the lab for the friendly, cooperative environment they have provided me and also for their selfless and enthusiastic help. I would like to give many thanks to Anke Hoffmann, Dr. Christopher Murgatroyd, Dr. Yvonne Bockmühl, Dieter Fischer, Marc Bettscheider, Udo Schmidt, Dr. Thomas Arztberger, Dr. Bing Shan, Johanna Stalla, Bärbel Wölfel, Dr. Marily Theodoropoulou and Jose Luis Monteserin Garcia. I have spent a lot of joyful time with all of them and this wonderful memory will never fade away.

To all my friends, who contributed in this and that way to my working and private success, I think of you and thank you a lot.

Last but not least, I want to deliver my deepest gratitude to my beloved parents and my sister in China, my girlfriend Yanan Yin in Munich. They have showed enormous love and support to me, which have been the greatest inspiration to my work.

9 Curriculum Vitae

Yonghe Wu

Kraepelinstrasse 12

80804 München

+49-17652706857

yonghe@mpipsykl.mpg.de

Born on 5th August 1977 in Heilongjiang, P.R.China

EDUCATION

Aug 2005 –	**Max Planck Institute of Psychiatry, Munich, Germany** AG Molecular Neuroendocrinology Doctoral thesis submitted "Epigenetic programming of POMC by early life stress"
Sep 2002 – Jun 2005	**Chinese Academy of Medical Sciences & Peking Union Medical College, Beijing, China** Dept. Human Genetics; Master of Science Research: Screening human breast cancer type1 susceptibility gene (BRCA1) mutations by DHPLC in Chinese population
Sep 1997 – Jun 2001	**Central University for Nationalities, Beijing, China** Dept. Chemistry Engineering, Bachelor of Technology Research: Extracting ginkgo flavone and ginkolide from ginkgo folium

WORKING EXPERIENCE

Mar 2002 – Jun 2002	**Beijing Genomics Institute, Chinese Academy of Science, Beijing, China** Staff member in the institute director office